DISSERTATION

ASSESSING THE IMPACTS OF INTERMITTENT FASTING ON ARTERIAL STIFFNESS AND SARS-CoV-2 INFECTION IN MICE

Submitted by

Elliot Lempert Graham

Department of Food Science & Human Nutrition

In partial fulfillment of the requirements

For the Degree of Doctor of Philosophy

Colorado State University

Fort Collins, Colorado

Summer 2025

Doctoral Committee:

Advisor: Christopher L. Gentile
Co-Advisor: Tiffany L. Weir

Christopher Melby
Alan Schenkel

ABSTRACT

ASSESSING THE IMPACTS OF INTERMITTENT FASTING ON ARTERIAL STIFFNESS AND SARS-CoV-2 INFECTION IN MICE

Intermittent fasting (IF), regulated periods of caloric abstinence followed by *ad libitum* energy intake, has emerged as one of the most popular dietary strategies globally. Although there are many factors facilitating IF's growing popularity, a primary reason could be its purported health benefits. Notably, an extensive amount of research has shown that IF reduces cardiovascular disease (CVD), the leading cause of death worldwide, by reducing prominent CVD risk factors including hypertension, hypercholesterolemia, and hypertriglyceridemia. Obesity-related arterial stiffness is another independent cardiovascular disease risk factor, yet whether IF impedes arterial stiffening in obesity is poorly understood.

Our lab has shown that the gut microbiota is a key determinant of obesity-related arterial stiffness. Mechanistically, obesity broadly perturbs gut microbial composition and function, which can lead to systemic inflammation. This overactive inflammatory response provokes vascular injury and arterial stiffness. Interestingly, by impeding aberrant gut-immune signaling, IF has been shown to reduce blood pressure and improve endothelial function in overweight and obese individuals. Therefore, IF may be leveraged to impede obesity-related arterial stiffness through similar mechanisms, yet this has not been explored. Moreover, there are other pertinent questions on IF and arterial stiffness that have yet to be answered; including 1) how many bouts of IF are needed to reduce arterial stiffness, and 2) once arterial de-stiffening occurs, how long after the fasting period is it maintained?

While IF may have benefits on the cardiovascular system, it might also have some drawbacks. One potential concern is IF's immunosuppressive effect, which may be beneficial for long-term vascular health, but might increase the risk of acute infections. SARS-CoV-2 (SC2), the culprit of the COVID-19 pandemic, is still a prominent virus that can lead to mild-to-severe health complications. Furthermore,

data suggest that a robust immune response and changes to the gut microbiota at the onset of SC2 infection predict infection severity and long-term sequelae. Thus, understanding whether IF-induced modifications to the gut microbiota and immune system lead to worse SC2 infection is essential, but has not yet been studied.

Chapter 3 of this dissertation investigated differences in arterial de-stiffening between a single fasting-refeeding cycle and a multi-week, once-weekly, 24-hour IF protocol. Surprisingly, we found that a single 24-hour fast acutely increased arterial stiffness in lean, but not obese mice. However, this was not due to acute changes within the gut microbiota or immune system and may be the result of other acute factors (i.e., blood pressure, nitric oxide signaling, vascular smooth muscle cell function). Furthermore, the elevated arterial stiffness was diminished after refeeding, suggesting no long-term vascular effects. In contrast, a prolonged period of once-weekly, 24-hour IF only impacted (reduced) arterial stiffness in obese mice. These vascular improvements occurred without changes in body weight or food intake, and we also show that the arterial de-stiffening effects of multi-week IF lasted for at least 5 days after fasting. Mechanistically, reductions in obesity-related arterial stiffness were associated with compositional and functional changes to the gut microbiota, reduced circulating chemokines, and reduced perivascular adipose tissue lymphocyte accumulation.

In the second study (**Chapter 4**), we investigated whether there is a discordant impact of multi-week, once-weekly, 24-hour IF on arterial stiffness and SC2 infection in mice. After 10 weeks of IF, we once again observed arterial de-stiffening in obese mice. After 12 weeks of IF, we infected mice with a mouse-adapted SC2 strain. We found that IF before SC2 infection did not substantially impact SC2 burden in the lungs, circulating SC2-specific antibodies, gut microbial ecology, or lung and spleen immune cell populations in either lean or obese mice. Overall, these findings reveal that once-weekly 24-hour fasting could be a safe and feasible dietary strategy that improves a putative determinant of cardiovascular health with minimal impacts on acute SC2 infection severity. Future studies should uncover how the “gut-immune axis” modulates obesity-related arterial stiffness, as well as translate the arterial de-stiffening effects of IF to human vascular health.

ACKNOWLEDGEMENTS

This dissertation was supported by the National Heart, Lung, and Blood Institute (R01HL144611) awarded to Co-Advisors Dr. Christopher L. Gentile and Dr. Tiffany L. Gentile. Apart from funding, it is hard to describe the roles Dr. Gentile and Dr. Weir have played in my life during the past half decade in just one sentence. Their scientific expertise and rigor, kind and patient attitude, and genuine love for advising undergraduate and graduate students is unmatched. Their guidance has helped mold me into the biomedical researcher and person I am today. Moreover, I sincerely thank Dr. Christopher Melby not only for his mentorship as a committee member, but for his kind and approachable demeanor, and helping to foster and develop my teaching and critical thinking skills. Lastly, I would like to thank Dr. Alan Schenkel, who has been a crucial part of my PhD as a committee member and my professor in Immunobiology, the very first immunology class I ever took. Without taking this class, my dissertation would have taken a drastically different turn, and I'm not sure if I would be pursuing a career in cardiovascular immunology.

Aside from my committee members, I would like to express my sincere gratitude to those who have helped and supported me, both inside and outside the lab, during my tenure at Colorado State University. Starting with the Integrative Cardiovascular Physiology and Intestinal Health Laboratories, I would like to thank Satya Raj John Trikha, Dr. Briana D. Risk, Scott D. Wrigley, Yuren Wei, Mingyue Zhang, Lance Poehlein, Phoenix Espinoza, Ryan Bayer, Rania Hart, Kayla Hinkle, Gabriele D. Brown, and Grace C. Stark for their invaluable contributions to my dissertation and my growth as an aspiring independent researcher. Within the department of Microbiology, Immunology, and Pathology at Colorado State University, I would like to thank Dr. Marcela Henao-Tamayo, Dr. Taru Dutt, Dr. Pablo Maldonado, and Amanda Hitpas for their work on **Chapter 4** of this dissertation as well as inviting me into their laboratory with open arms. Dr. Taru Dutt, along with the Flow Cytometry Core at Colorado State University (Dr. Bradly Burke and Elizabeth Creissen) were indispensable for all immunological aspects of this dissertation, including but not limited to antibody panel design, flow cytometry, and gating strategies. Likewise, Dr.

Janet Siebert was instrumental in **Chapter 3**, as her Visualization of LineAr Regression Elements (VOLARE) pipeline helped uncover many of the novel gut-immune axes identified within this dissertation.

To my Fort Collins and Cheyenne tennis family, thank you for rekindling my love for tennis and always putting a smile on my face. To my Skidmore professor Dr. Denise Smith, I would not be obtaining my PhD if it wasn't for you, and I am thankful for the close friendship we share to this day. Finally, to Jessica Ampel, thank you for being one of my best friends for the last 7 years. I am forever grateful for your love and kindness, especially during this particularly crazy year.

DEDICATION

I would like to dedicate this dissertation my mom, Debby Graham, and my dad, Russell Graham. They are my two biggest supporters, mentors, and constructive critics when need be. I could not have asked for two better parents, as their love and security are never-ending. I love you both very much.

TABLE OF CONTENTS

CHAPTER 1: INTRODUCTION

Intermittent Fasting as a Potential Combatant Against Obesity-Related Arterial Stiffness

Intermittent fasting (IF) is one of the most popular dietary strategies globally [1–3]. Recent reports show that IF has become more popular than many diets and nutritional strategies aimed at improving health, including Mediterranean-style, Dietary Approaches to Stop Hypertension (DASH), low-carbohydrate, and ketogenic diets, as well as calorie counting[4]. Several factors might explain the recent surge in IF popularity. First, IF focuses on *when* to eat rather than *what* to eat [5], making it more accessible and straightforward than diets that control food preferences and daily calorie intake. Second, there are many forms of IF, making it a flexible dietary strategy suitable for individuals from all walks of life. For example, alternate-day fasting, once-weekly 24-hour fasting, the 5:2 diet, time-restricted-eating, and modified fasting are all different forms of IF **(Table 1.1)** that can be integrated into many different lifestyles. Finally, and potentially most importantly, habitual IF tends to be associated with improved health, including weight loss and cardiometabolic benefits.

Due to its popularity and supposed health benefits, studies have investigated IF's potential as a dietary therapeutic for cardiovascular disease, the leading cause of death globally [6]. IF has been shown to alleviate traditional cardiovascular disease risk factors, including hypertension, hypercholesterolemia, hypertriglyceridemia, and insulin resistance [7]. Arterial stiffness is another independent risk factor for cardiovascular disease onset and mortality [8,9]. Furthermore, excess adiposity (obesity) contributes to elevated arterial stiffness [10], and those with obesity are twice as likely to die from cardiovascular disease compared to non-obese individuals [11]. Although data are scarce, IF can reduce obesity-related arterial stiffness [12,13]. However, the mechanisms by which IF promotes arterial de-stiffening during obesity remain unclear.

The Gut Microbiota and Immune System Contribute to Obesity-Related Arterial Stiffness

One factor that is impacted by IF is the gut microbiota[14,15], the trillions of microbes that inhabit

Table 1.1. Definition and Examples of Intermittent Fasting.

Regimen	Definition
Intermittent Fasting	Repetitive periods of voluntary abstinence from some or all foods or foods and beverages for up to 48 hours.
Alternate-Day Fasting (ADF)	Alternating between a day of eating *ad libitum* and a day of water-only fasting.
Once-Weekly 24-Hour Fasting	Fasting for 24 consecutive hours once per week. The time at which the 24-hour fast starts and ends does not need to be consistent each week. For example, one week, you could fast from 8 am Monday morning to 8 am Tuesday morning. Another week, you could fast from 8 pm Thursday night to 8 pm Friday night.
The 5:2 Diet	Fasting for a total of 48 hours (2 days) per week while eating *ad libitum* for the remaining 5 days of the week. The 48 hour fast can be done at once or split up between two 24-hour fasts. For instance, you could fast from 8 am Monday morning to 8 am Wednesday morning (consecutive) or fast from 8 am Monday morning to 8 am Tuesday morning as well as 8 am Thursday morning to 8 am Friday morning (2x non-consecutive 24-hour fasts). As with the once-weekly 24-hour fasting, the time(s) at which the consecutive or non-consecutive fast(s) start and end does not need to be consistent each week.
Time-Restricted-Eating/Feeding (TRE/TRF)	Food intake and the consumption of caloric beverages is restricted to a specific period during the day, resulting in a daily fasting window of at least 14 hours. There is no explicit limit on energy intake during eating hours. In animal studies, time-restricted eating is called time-restricted feeding.
Modified Fasting (MFD)	Limiting energy intake to typically up to 25% of energy needs on modified fasting days. Common modified fasting regimens are alternate-day modified fasting (alternating between a day of ad *libitum* eating and a day of 25% energy intake), once-weekly 24-hour modified fasting (one day per week of eating 25% of energy intake), or 5:2 modified fasting (25% energy intake for the consecutive or non-consecutive 48 hours of fasting).

Definitions adapted from Koppold et al. [1]

the gastrointestinal tract. IF's ability to alter the gut microbiota is crucial, as it regulates host health. Indeed, the gut microbiota has a wide range of functions vital to host health, including but not limited to nutrient availability and absorption[16], vitamin production[16], drug efficacy [17], mucus production and gut barrier integrity [18,19], pathogen resistance[20,21], and glucose metabolism[22]. However, large-scale compositional and metabolic perturbations to the gut microbiota, as seen during obesity, can negatively impact host health and exacerbate disease. This relationship between obesity and gut microbiota perturbations is now considered a crucial step in the pathogenesis of obesity-related cardiovascular dysfunction, and our lab has been at the forefront of this research for nearly a decade. For example, our previous data show that obese mice harbored a distinct gut microbial profile associated with arterial stiffness [23–25]. We have also demonstrated that the transplantation of an "obese" human or mouse microbiota exacerbated arterial stiffness in mice[24,26]. In contrast, antibiotic-induced suppression of an obese gut microbiota reduced arterial stiffness in mice[23]. These results indicate that modulations of the gut microbiota impact arterial stiffness.

The immune system is a key biological factor linking the obese gut microbiota with elevated arterial stiffness. It is well-accepted that the obese gut microbiota increases inflammation, highlighted by the overabundance of circulating and tissue-resident leukocytes and cytokines. This resulting inflammation is a notorious predecessor of vascular dysfunction and cardiovascular disease [27–36]. Our lab has provided some evidence for this aberrant gut-immune signaling to impact cardiovascular health, particularly arterial stiffness. Specifically, we showed that diet-induced obese mice incapable of lipopolysaccharide (LPS) toll-like receptor 4 (TLR4) signaling (TLR4 knockout mice) were partially protected from elevated arterial stiffness [37]. However, since all Gram-negative microbes produce LPS, and TLR4 is expressed on an array of innate immune cells, we could not reveal the specific gut microbe-immune interactions implicated in arterial stiffness. Furthermore, we only observed partial arterial de-stiffening in obese mice, suggesting that other gut microbe-immune interactions are likely involved in obesity-related arterial stiffness. Thus, much about gut microbe-immune signaling during obesity and its relationship with arterial stiffness remains unresolved.

Furthermore, although the mechanisms linking IF to reduced Obesity-Related arterial stiffness have been largely unexplored, recent data show that IF reduced other risk factors for CVD (blood pressure and endothelial dysfunction) in overweight/obese individuals by altering the gut microbiota and decreasing inflammation [38,39]. These results highlight the potential for IF to reduce Obesity-Related arterial stiffness through altering aberrant gut-immune signaling. Furthermore, directly testing this hypothesis could help further uncover the specific gut microbes and components of the immune system (immune cells or cytokines) that influence arterial stiffness during obesity.

A Potential Detriment of Intermittent Fasting

Despite IF's potential arterial de-stiffening effects, the gut microbiota impacts pathogen resistance through priming and training of the host immune system [20,21]. Thus, any alterations to the gut microbiota and immune system could potentially affect the host's susceptibility to invading pathogens.

As a diet practiced by millions, it is crucial to understand whether IF could impact infection. The recent COVID-19 pandemic, caused by the SARS-CoV-2 (SC2) virus, highlights the potential importance of IF on infection. Although the peak of COVID-19 seems to be behind us, SC2 is still a common respiratory pathogen that can impact health in the short and long term. Moreover, obesity is a well-established risk factor for SC2 infection severity [24,40–42] and directly suppresses the immune response towards infections [43]. Therefore, the potential suppression of inflammation via IF might lead to improved cardiovascular health but worsen infection during obesity. Similarly, since the gut microbiota can impact infection severity and symptom resolution [44–47], IF might also exacerbate SC2 infection through its profound impact on the gut microbiota. Lastly, although reviews have hypothesized how IF could impact SC2 infection [48–50], there is little direct evidence. Some of the only available data relating to IF and SC2 are observational studies which showed that periodic fasting in humans was associated with lower SC2 severity and less heart-failure hospitalization in COVID-19-positive patients. Yet, these data could be confounded by the fact that the non-fasting cohort included a significantly higher proportion of smokers (prior or current) and higher levels of COPD and asthma [51,52].

Hypotheses and Specific Aims

Identifying the potential discordant effects of IF on Obesity-Related arterial stiffness and SC2 infection severity has large-scale, translational implications as IF has a reputation as an all-encompassing beneficial dietary strategy. Therefore, the overarching objectives of this dissertation were to (1) investigate whether IF reduces arterial stiffness in obese mice by modifying aberrant gut microbe-immune interactions during obesity and (2) determine if these modifications predispose mice to exacerbated SC2 infection. We hypothesized that IF would attenuate arterial stiffness in obese mice in correspondence with changes to gut microbial composition and function as well as reduce systemic and vascular-resident inflammation **(Figure 1.1)**. However, we predicted that IF would leave mice susceptible to worse acute SC2 infection **(Figure 1.1)**, highlighted by a greater lung viral burden, greater weight loss, reduced food intake, and reduced circulating SC2-specific antibody titers. First, this dissertation reviews the existing literature relating IF with improved vascular function (i.e., reduced arterial stiffness) **(Chapter 2)**. At the same time, Chapter 2 highlights how the immune system is a key mediator of IF's effects on vascular function and proposes that an emerging concept in the field of immunology, fasting-induced immune cell could augment vascular function. This dissertation then directly investigates the impact of IF on arterial stiffness **(Chapter 3)** and acute SC2 infection **(Chapter 4)** in conjunction with gut microbiota and immune system changes. More specifically, in **Chapter 3**, we explored the effects of a single fasting-refeeding cycle (acute IF) and a multi-week, once-weekly, 24-hour IF paradigm (chronic IF) on Obesity-Related arterial stiffness, gut microbial compositional and functional changes, splenocyte counts, and circulating cytokine levels. We then ran robust statistical models to identify what relationships between the gut microbiota and immune system predict arterial stiffness during acute and chronic IF. In **Chapter 4**, we tested whether once-weekly 24-hour IF exacerbated SC2 infection in lean and obese mice. We also investigated whether IF-induced alterations to the gut microbiota and immune system were differentially impacted by SC2 infection compared to controls.

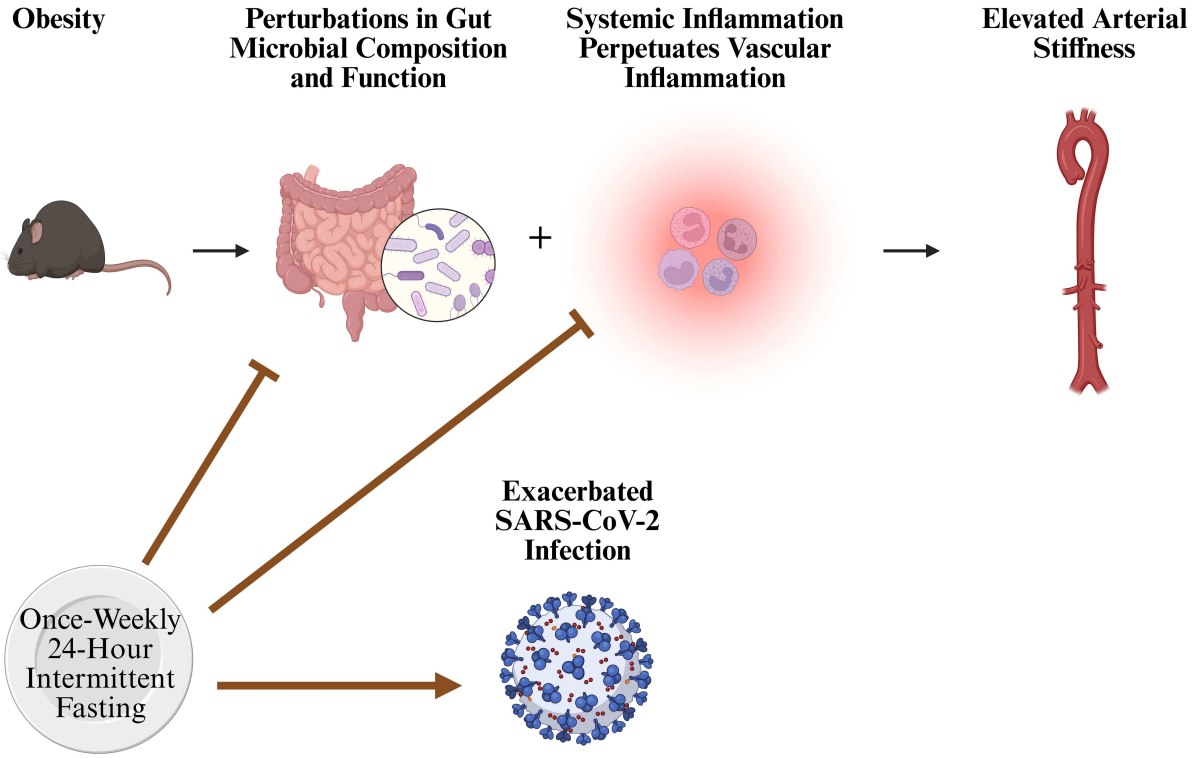

Figure 1.1. Overall Working Hypothesis. Image created at Biorender.com.

REFERENCES

1. Koppold DA, Breinlinger C, Hanslian E, et al. International consensus on fasting terminology. *Cell Metab*. 2024;36(8):1779-1794.e4. doi:10.1016/j.cmet.2024.06.013

2. Persynaki A, Karras S, Pichard C. Unraveling the metabolic health benefits of fasting related to religious beliefs: A narrative review. *Nutrition*. 2017;35:14-20. doi:10.1016/j.nut.2016.10.005

3. Gonzalez JE, Cooke WH. Influence of an acute fast on ambulatory blood pressure and autonomic cardiovascular control. *Am J Physiol-Regul Integr Comp Physiol*. 2022;322(6):R542-R550. doi:10.1152/ajpregu.00283.2021

4. *2024 Food and Health Survey: International Food Information Council.*; 2024. https://foodinsight.org/2024-food-health-survey/

5. Catterson JH, Khericha M, Dyson MC, et al. Short-Term, Intermittent Fasting Induces Long-Lasting Gut Health and TOR-Independent Lifespan Extension. *Curr Biol*. 2018;28(11):1714-1724.e4. doi:10.1016/j.cub.2018.04.015

6. Martin SS, Aday AW, Almarzooq ZI, et al. 2024 Heart Disease and Stroke Statistics: A Report of US and Global Data From the American Heart Association. *Circulation*. 2024;149(8). doi:10.1161/CIR.0000000000001209

7. de Cabo R, Mattson MP. Effects of Intermittent Fasting on Health, Aging, and Disease. Longo DL, ed. *N Engl J Med*. 2019;381(26):2541-2551. doi:10.1056/NEJMra1905136

8. Mitchell GF, Hwang SJ, Vasan RS, et al. Arterial Stiffness and Cardiovascular Events: The Framingham Heart Study. *Circulation*. 2010;121(4):505-511. doi:10.1161/CIRCULATIONAHA.109.886655

9. Vasan RS, Pan S, Xanthakis V, et al. Arterial Stiffness and Long-Term Risk of Health Outcomes: The Framingham Heart Study. *Hypertension*. 2022;79(5):1045-1056. doi:10.1161/HYPERTENSIONAHA.121.18776

10. Safar ME, Czernichow SAA, Blacher J. Obesity, Arterial Stiffness, and Cardiovascular Risk. *J Am Soc Nephrol*. 2006;17(4_suppl_2):S109-S111. doi:10.1681/ASN.2005121321

11. Krauss RM, Winston M, Fletcher BJ, Grundy SM. Obesity: Impact on Cardiovascular Disease. *Circulation*. 1998;98(14):1472-1476. doi:10.1161/01.CIR.98.14.1472

12. Alinezhad-Namaghi M, Eslami S, Nematy M, et al. Association of time-restricted feeding, arterial age, and arterial stiffness in adults with metabolic syndrome. *Health Sci Rep*. 2023;6(7):e1385. doi:10.1002/hsr2.1385

13. Eldeeb A, Mahmoud M, Ibrahim A, Yousef E, Sabry A. Effect of Ramadan fasting on arterial stiffness parameters among Egyptian hypertensive patients with and without chronic kidney disease. *Saudi J Kidney Dis Transplant*. 2020;31(3):582. doi:10.4103/1319-2442.289444

14. Paukkonen I, Törrönen EN, Lok J, Schwab U, El-Nezami H. The impact of intermittent fasting on gut microbiota: a systematic review of human studies. *Front Nutr*. 2024;11:1342787. doi:10.3389/fnut.2024.1342787

15. Li L, Su Y, Li F, et al. The effects of daily fasting hours on shaping gut microbiota in mice. *BMC Microbiol*. 2020;20(1):65. doi:10.1186/s12866-020-01754-2

16. Gentile CL, Weir TL. The gut microbiota at the intersection of diet and human health. *Science*. 2018;362(6416):776-780. doi:10.1126/science.aau5812

17. Yang T, Mei X, Tackie-Yarboi E, et al. Identification of a Gut Commensal That Compromises the Blood Pressure-Lowering Effect of Ester Angiotensin-Converting Enzyme Inhibitors. *Hypertension*. 2022;79(8):1591-1601. doi:10.1161/HYPERTENSIONAHA.121.18711

18. Paone P, Cani PD. Mucus barrier, mucins and gut microbiota: the expected slimy partners? *Gut*. 2020;69(12):2232-2243. doi:10.1136/gutjnl-2020-322260

19. Kelly CJ, Zheng L, Campbell EL, et al. Crosstalk between Microbiota-Derived Short-Chain Fatty Acids and Intestinal Epithelial HIF Augments Tissue Barrier Function. *Cell Host Microbe*. 2015;17(5):662-671. doi:10.1016/j.chom.2015.03.005

20. Kamada N, Chen GY, Inohara N, Núñez G. Control of pathogens and pathobionts by the gut microbiota. *Nat Immunol*. 2013;14(7):685-690. doi:10.1038/ni.2608

21. Zheng D, Liwinski T, Elinav E. Interaction between microbiota and immunity in health and disease. *Cell Res*. 2020;30(6):492-506. doi:10.1038/s41422-020-0332-7

22. Wang K, Zhang Z, Hang J, et al. Microbial-host-isozyme analyses reveal microbial DPP4 as a potential antidiabetic target. *Science*. 2023;381(6657):eadd5787. doi:10.1126/science.add5787

23. Battson ML, Lee DM, Jarrell DK, et al. Suppression of gut dysbiosis reverses Western diet-induced vascular dysfunction. *Am J Physiol-Endocrinol Metab*. 2018;314(5):E468-E477. doi:10.1152/ajpendo.00187.2017

24. Battson ML, Lee DM, Li Puma LC, et al. Gut microbiota regulates cardiac ischemic tolerance and aortic stiffness in obesity. *Am J Physiol-Heart Circ Physiol*. 2019;317(6):H1210-H1220. doi:10.1152/ajpheart.00346.2019

25. Lee DM, Ecton KE, Trikha SRJ, et al. Microbial metabolite indole-3-propionic acid supplementation does not protect mice from the cardiometabolic consequences of a Western diet. *Am J Physiol-Gastrointest Liver Physiol*. 2020;319(1):G51-G62. doi:10.1152/ajpgi.00375.2019

26. Trikha SRJ, Lee DM, Ecton KE, et al. Transplantation of an obesity-associated human gut microbiota to mice induces vascular dysfunction and glucose intolerance. *Gut Microbes*. 2021;13(1):1940791. doi:10.1080/19490976.2021.1940791

27. Majeed BA, Eberson LS, Tawinwung S, Larmonier N, Secomb TW, Larson DF. Functional aortic stiffness: role of CD4+ T lymphocytes. *Front Physiol*. 2015;6. doi:10.3389/fphys.2015.00235

28. Lintermans LL, Stegeman CA, Heeringa P, Abdulahad WH. T Cells in Vascular Inflammatory Diseases. *Front Immunol*. 2014;5. doi:10.3389/fimmu.2014.00504

29. Silvestre-Roig C, Braster Q, Ortega-Gomez A, Soehnlein O. Neutrophils as regulators of cardiovascular inflammation. *Nat Rev Cardiol*. 2020;17(6):327-340. doi:10.1038/s41569-019-0326-7

30. Fang P, Li X, Shan H, et al. Ly6C $^{+}$ Inflammatory Monocyte Differentiation Partially Mediates Hyperhomocysteinemia-Induced Vascular Dysfunction in Type 2 Diabetic db/db Mice. *Arterioscler Thromb Vasc Biol*. 2019;39(10):2097-2119. doi:10.1161/ATVBAHA.119.313138

31. Williams JW, Zaitsev K, Kim KW, et al. Limited proliferation capacity of aortic intima resident macrophages requires monocyte recruitment for atherosclerotic plaque progression. *Nat Immunol*. 2020;21(10):1194-1204. doi:10.1038/s41590-020-0768-4

32. Guzik TJ, Hoch NE, Brown KA, et al. Role of the T cell in the genesis of angiotensin II–induced hypertension and vascular dysfunction. *J Exp Med*. 2007;204(10):2449-2460. doi:10.1084/jem.20070657

33. Liu C, Yalavarthi S, Tambralli A, et al. Inhibition of neutrophil extracellular trap formation alleviates vascular dysfunction in type 1 diabetic mice. *Sci Adv*. 2023;9(43):eadj1019. doi:10.1126/sciadv.adj1019

34. Chan CT, Sobey CG, Lieu M, et al. Obligatory Role for B Cells in the Development of Angiotensin II–Dependent Hypertension. *Hypertension*. 2015;66(5):1023-1033. doi:10.1161/HYPERTENSIONAHA.115.05779

35. Moore JP, Vinh A, Tuck KL, et al. M2 macrophage accumulation in the aortic wall during angiotensin II infusion in mice is associated with fibrosis, elastin loss, and elevated blood pressure. *Am J Physiol-Heart Circ Physiol*. 2015;309(5):H906-H917. doi:10.1152/ajpheart.00821.2014

36. Williams H, Mack CD, Li SCH, Fletcher JP, Medbury HJ. Nature versus Number: Monocytes in Cardiovascular Disease. *Int J Mol Sci*. 2021;22(17):9119. doi:10.3390/ijms22179119

37. Ecton KE, Graham EL, Risk BD, et al. Toll-like receptor 4 deletion partially protects mice from high fat diet-induced arterial stiffness despite perturbation to the gut microbiota. *Front Microbiomes*. 2023;2:1095997. doi:10.3389/frmbi.2023.1095997

38. Guo Y, Luo S, Ye Y, Yin S, Fan J, Xia M. Intermittent Fasting Improves Cardiometabolic Risk Factors and Alters Gut Microbiota in Metabolic Syndrome Patients. *J Clin Endocrinol Metab*. 2021;106(1):64-79. doi:10.1210/clinem/dgaa644

39. Maifeld A, Bartolomaeus H, Löber U, et al. Fasting alters the gut microbiome reducing blood pressure and body weight in metabolic syndrome patients. *Nat Commun*. 2021;12(1):1970. doi:10.1038/s41467-021-22097-0

40. Kass DA, Duggal P, Cingolani O. Obesity could shift severe COVID-19 disease to younger ages. *The Lancet*. 2020;395(10236):1544-1545. doi:10.1016/S0140-6736(20)31024-2

41. Gao M, Piernas C, Astbury NM, et al. Associations between body-mass index and COVID-19 severity in 6·9 million people in England: a prospective, community-based, cohort study. *Lancet Diabetes Endocrinol*. 2021;9(6):350-359. doi:10.1016/S2213-8587(21)00089-9

42. Singh R, Rathore SS, Khan H, et al. Association of Obesity With COVID-19 Severity and Mortality: An Updated Systemic Review, Meta-Analysis, and Meta-Regression. *Front Endocrinol*. 2022;13:780872. doi:10.3389/fendo.2022.780872

43. Milner JJ, Beck MA. The impact of obesity on the immune response to infection. *Proc Nutr Soc*. 2012;71(2):298-306. doi:10.1017/S0029665112000158

44. Sencio V, Machelart A, Robil C, et al. Alteration of the gut microbiota following SARS-CoV-2 infection correlates with disease severity in hamsters. *Gut Microbes*. 2022;14(1):2018900. doi:10.1080/19490976.2021.2018900

45. Zuo T, Zhang F, Lui GCY, et al. Alterations in Gut Microbiota of Patients With COVID-19 During Time of Hospitalization. *Gastroenterology*. 2020;159(3):944-955.e8. doi:10.1053/j.gastro.2020.05.048

46. Yeoh YK, Zuo T, Lui GCY, et al. Gut microbiota composition reflects disease severity and dysfunctional immune responses in patients with COVID-19. *Gut*. 2021;70(4):698-706. doi:10.1136/gutjnl-2020-323020

47. Li Z, Chen J, Li Y, et al. Impact of SARS-CoV-2 infection on respiratory and gut microbiome stability: a metagenomic investigation in long-term-hospitalized COVID-19 patients. *Npj Biofilms Microbiomes*. 2024;10(1):126. doi:10.1038/s41522-024-00596-4

48. Ealey KN, Phillips J, Sung HK. COVID-19 and obesity: fighting two pandemics with intermittent fasting. *Trends Endocrinol Metab*. 2021;32(9):706-720. doi:10.1016/j.tem.2021.06.004

49. Wang Y, Chi H. Fasting as key tone for COVID immunity. *Nat Metab*. 2022;4(10):1229-1231. doi:10.1038/s42255-022-00646-1

50. Faris MAIslamE, Salem M, Jahrami H, Madkour M, BaHammam A. Ramadan intermittent fasting and immunity: An important topic in the era of COVID-19. *Ann Thorac Med*. 2020;15(3):125. doi:10.4103/atm.ATM_151_20

51. Horne BD, May HT, Muhlestein JB, et al. Association of periodic fasting with lower severity of COVID-19 outcomes in the SARS-CoV-2 prevaccine era: an observational cohort from the INSPIRE registry. *BMJ Nutr Prev Health*. Published online July 1, 2022:e000462. doi:10.1136/bmjnph-2022-000462

52. Horne BD, Anderson JL, Haddad F, et al. Periodic Fasting and Acute Cardiac Events in Patients Evaluated for COVID-19: An Observational Prospective Cohort Study. *Nutrients*. 2024;16(13):2075. doi:10.3390/nu16132075

CHAPTER 2: EXPLORING THE IMPACT OF INTERMITTENT FASTING ON VASCULAR FUNCTION AND THE IMMUNE SYSTEM: A NARRATIVE REVIEW AND NOVEL PERSPECTIVE[1]

SUMMARY

Vascular function is a critical determinant of cardiovascular health and all-cause mortality. Recent studies have suggested that intermittent fasting, a popular dietary strategy, elicits beneficial effects on vascular function. These studies also suggest that fasting-mediated improvements in vascular function coincide with reductions in systemic inflammation. However, the mechanisms that connect fasting, the immune system, and vascular function remain largely underexplored. The current review summarizes the effects of different intermittent fasting modalities on vascular health, focusing on endothelial dysfunction and arterial stiffness, 2 critical indices of vascular function. Improvements in vascular function are associated with reduced inflammation and are mechanistically linked to decreased circulating immune cells and their accumulation within the vascular wall and perivascular tissue. Recent data show that fasting redistributes circulating and tissue-resident immune cells to the bone marrow, affecting their inflammatory actions. However, there is no direct evidence relating immune cell redistribution to cardiovascular health. By relating fasting-induced immune cell redistribution to reduced inflammation and improved vascular function, we propose an exciting avenue of further exploration is determining whether fasting-induced immune cell redistribution impacts cardiovascular health.

[1] This research is published in the journal *Arteriosclerosis, Thrombosis, and Vascular Biology*. To adhere to CSU Graduate School dissertation formatting, the following changes were made: 1) keywords and journal ending statements (i.e., funding, acknowledgments, nonstandard abbreviations and acronyms) are not displayed; 2) spacing has been adjusted to match CSU formatting. Citation information: **Graham EL**, Weir TL, Gentile CL. Exploring the Impact of Intermittent Fasting on Vascular Function and the Immune System: A Narrative Review and Novel Perspective. *Arterioscler Thromb Vasc Biol*. Published online April 3, 2025:ATVBAHA.125.322692. doi:10.1161/ATVBAHA.125.322692

INTRODUCTION

Intermittent fasting (IF) is one of the most popular dietary strategies globally.[1–3] The International Food Information Council survey recently reported that IF was more popular than Mediterranean-style, DASH (Dietary Approaches to Stop Hypertension), low-carbohydrate, and ketogenic diets, as well as dietary strategies aimed at weight loss, such as calorie counting.[4] The widespread popularity and enhanced compliance of IF compared with other diets is likely due to its focus on when to eat rather than what to eat,[5] along with emerging evidence of health benefits from fasting that are independent of caloric restriction and weight loss.[6]

There are various forms of IF, including once-weekly 24-hour fasting, alternate-day fasting (ADF), and the 5:2 diet, during which individuals fast for 2 (consecutive or nonconsecutive) days per week. Time-restricted eating (TRE; time-restricted-feeding [TRF] in preclinical animal models) is another form of IF that limits calorie consumption to a specific period, resulting in a daily fasting window of at least 14 hours.[1] A typical form of TRE is the 16:8 protocol (16-hour fasting/8-hour *ad libitum* [Ad-Lib] eating). Ramadan fasting is a religious form of TRE during which Muslims abstain from eating or drinking food from dawn to dusk during the ninth month of the Islamic calendar, a diet pattern that closely resembles a 16:8 protocol. In modified fasting (MFD), calories are limited to ≈25% of energy intake on fasting days.[1]

Concomitant with IF's increasing popularity, a growing number of studies have investigated its potential as a dietary therapeutic for the prevention of cardiovascular disease (CVD). Currently, the effects of IF on atherosclerosis, the leading cause of CVD, are equivocal.[7–13] However, IF has been shown to alleviate traditional CVD risk factors, including obesity, hypertension, hypercholesterolemia, hypertriglyceridemia, and insulin resistance,[6] as well as improve measures of cardiac function.[14–16] These findings suggest that IF might be well suited to prevent CVD by reducing prominent CVD risk factors. Vascular dysfunction, which clinically manifests as arterial stiffness and endothelial dysfunction, is a significant risk factor and strong determinant of CVD.[17–20] Compared with traditional CVD risk factors, studies investigating the effects of IF on vascular dysfunction are scarce. Moreover, although several

studies suggest that certain forms of IF improve vascular function,[21–31] the mechanistic underpinnings of these interactions remain poorly understood.

The immune system is a key biological factor that mediates vascular health. Improved vascular function via IF coincides with reduced inflammation,[23,28] suggesting a mechanistic link between IF, the immune system, and improved vascular function. The blood, vascular wall, and perivascular tissue are populated with a vast array of immune cells that, depending on the specific cell type, can positively or negatively impact vascular structure and function.[32–40] Many of these immune cells can exacerbate systemic inflammation by producing an array of cytokines/chemokines, leading to an influx of even more inflammatory immune cells and the perpetuation of vascular inflammation.[41–43] Thus, although there are putative links between IF, reduced inflammation, and improved vascular function, it is unknown whether IF improves vascular function by reducing immune cell recruitment into the vascular wall and perivascular tissue.

Recent studies have shown that fasting profoundly impacts circulating and tissue-resident immune cells.[44–47] Indeed, in response to fasting, immune cells can traverse from one part of the body to another while markedly altering their phenotype. Following refeeding, the cells can then move back to their prefasting location. This fasting-induced immune cell redistribution has also been shown to impact health. For instance, a recent study by Delconte et al determined that IF redistributes peripheral and tissue-resident (splenic) natural killer (NK) cells into the bone marrow. While in the bone marrow, these NK cells are primed by IL (interleukin)-12–expressing myeloid cells to produce IFN-γ (interferon-γ) and improve anti-tumor immunity.[47] In another recent study by Wang et al,[48] redistribution of T cells into the bone marrow via 24-hour fasting was related to suppressed T-cell activation, differentiation, cytokine production, and autoimmune disease development in mice. Fasting also influenced monocyte redistribution to the bone marrow, reducing inflammation and improving disease incidence (clinical course) compared with controls in a mouse model of multiple sclerosis.[44] The potential for fasting-induced immune cell redistribution impacting CVD has only been proposed once,[45] and thus, its prospect as a mechanism contributing to improved cardiovascular health is largely unexplored. Given that vascular

dysfunction is a hallmark of CVD progression, it is intriguing to speculate whether fasting-induced redistribution of immune cells could have a lasting impact on vascular function by impeding immune cell accumulation within the vascular wall and perivascular tissue.

In this narrative review, we highlight the potential of various forms of IF to improve vascular function and discuss how these improvements are linked to reduced inflammation, decreased circulating immune cells, and less immune cell accumulation in vascular tissues. We aim to relate IF to vascular dysfunction, as other available reviews focus on general cardiovascular health, with relatively little discussion of the impacts of IF on vascular function.[13,49–53] We also cover recent findings on immune cell redistribution to the bone marrow during fasting and propose that this redistribution warrants future consideration as a putative mediator of IF-induced improvements in vascular function.

EFFECT OF IF ON ATHEROSCLEROSIS

Several studies have investigated the impact of IF on atherosclerosis. Chen et al[7] displayed that 7 and 14 weeks of IF (3 days of high-fat diet feeding and 1-day fasting) reduced CCL2 (C-C motif chemokine ligand 2) expression and monocyte-endothelium adhesion, macrophage accumulation, atherosclerotic lesion size, and necrotic core area, as well as increased fibrous cap area and plaque stabilization in *Ldlr*$^{-/-}$ mice. Twelve weeks of 14:10 TRE reduced atherogenic lipids (total cholesterol, low-density lipoprotein cholesterol, and non–high-density lipoprotein cholesterol) in patients with metabolic syndrome.[12] Furthermore, Dorighello et al displayed that 12 weeks of ADF reduced cholesterolemia by 28% in wild-type mice. Surprisingly, in the same study, 12 weeks of ADF increased atherogenic lipids (total cholesterol by 37%, low-density lipoprotein cholesterol by 50%, and very-low-density lipoprotein cholesterol by 195%) and atherosclerotic lesion area in *Ldlr*$^{-/-}$ mice.[8] Similarly, Mérian et al[9] reported that 4 months of ADF reduced hypertriglyceridemia and atherosclerotic lesion area in *Apoe*$^{-/-}$ mice fed a control diet but exacerbated dyslipidemia when fed a high-fat, high-cholesterol diet. These latter findings suggest that the impact of IF on atherosclerosis could be due to genetic differences, the level of accrued plaque before starting IF, or complementary diets during IF. Collectively, the effects

of IF on atherosclerosis remain inconclusive, yet most available data suggest that IF improves cardiovascular health by mitigating CVD risk factors.[6]

EFFECT OF IF ON VASCULAR FUNCTION

Of the available studies investigating the impact of IF on human vascular function, many are observational studies that collected data pre- and post-Ramadan. Although observational studies suffer from methodological limitations, these Ramadan fasting studies have helped highlight a potential relationship between TRE and improved vascular function. Alinezhad-Namaghi et al[21] observed significant reductions in arterial stiffness (reduced pulse wave velocity [PWV]) after Ramadan in individuals with metabolic syndrome. Furthermore, Demirci et al[23] showed that brachial artery flow-mediated dilation (FMD), the gold standard measurement of endothelial function in humans, improved in older patients with hypertension following Ramadan fasting. In contrast, 2 studies show no significant effect of Ramadan fasting on arterial stiffness. Sezen et al[54] reported only modest reductions in arterial stiffness in overweight and obese men, and Eldeeb et al[22] showed no significant differences in PWV following Ramadan in patients with hypertension either with chronic kidney disease (CKD) or without CKD. Interestingly, Eldeeb et al[22] found that fasting during Ramadan decreased the augmentation index (an indirect measure of arterial stiffness) in patients with hypertension without CKD, suggesting that measures of arterial stiffness other than PWV were attenuated.

The discrepant findings among these studies may be explained by the techniques used to determine arterial stiffness. For example, Alinezhad-Namaghi et al[21] measured arterial stiffness via carotid-femoral PWV,[55,56] while Sezen et al[54] and Eldeeb et al[22] utilized arteriography and the brachial oscillometric method via Mobil-O-Graph, respectively. It is possible that the latter 2 methods may lack the sensitivity needed to detect the modest vascular benefits following Ramadan fasting.[57,58] One reason Ramadan fasting could more readily affect endothelial function than arterial stiffness is because the former is more sensitive to acute stimuli. That is, various stimuli can acutely regulate endothelial function, including NO (nitric oxide), cytokines, reactive oxygen species, and endothelial-derived

hyperpolarizing factors,[43,59–61] whereas arterial stiffness, although moderately sensitive to acute stimuli such as blood pressure fluctuations,[62–66] is governed in large part by long-term structural changes to the vascular wall.[67–70] In this regard, since Ramadan is only 1 month per year, this time frame may be sufficient to impact endothelial function but insufficient to reduce long-term structural changes associated with arterial stiffness.

Interventional trials in rodents and humans have also sought to uncover the effects of TRE on vascular function. Azemi et al[24] found that 6 weeks of Ad-Lib high-fat feeding followed by another 6 weeks of either 16:8 high-fat–fed or standard diet–fed TRF significantly improved thoracic aorta endothelial function in experimental rats. These results suggest that 6 weeks of 16:8 TRF can reduce diet-induced endothelial dysfunction regardless of macronutrient composition. However, in humans, 5 weeks of TRE did not significantly reduce arterial stiffness in prediabetic men,[71] and 6 weeks of 16:8 TRE did not affect carotid-femoral PWV, carotid intima-media thickness, or FMD in healthy midlife and older adults.[72]Another study also found no benefit of 16:8 TRF on vascular function.[73] Ultimately, these results suggest that reducing the feeding window down to 8 hours may not be a strong enough stimulus to improve vascular function.

In contrast to TRE, other IF regimens could improve vascular function by emphasizing extended fasting periods (MFD) or more frequent fasts per week (ADF). In Wistar albino rats, 2 months of ADF improved abdominal aorta vasoreactivity to acetylcholine, which suggests enhanced endothelial function.[26] A more extended ADF protocol (12-week ADF) improved mesenteric artery endothelial function in diabetic mice ($Lepr^{db}$).[27] These improvements were accompanied by significantly reduced mesenteric artery nitrotyrosine, an oxidative stress biomarker. Moreover, 12-week ADF increased plasma adiponectin, which can activate eNOS (endothelial NO synthase) via AMPK (AMP-activated protein kinase) and potentiate NO production.[74,75] Adiponectin can also reduce endothelial adhesion molecule expression, NF-κB (nuclear factor-κB)–mediated macrophage cytokine production, and TNF (tumor necrosis factor)-mediated monocyte-endothelial cell interactions.[76] Thus, increased adiponectin via IF may suppress systemic and vascular inflammation, improving vascular function **(Figure 2.1)**.

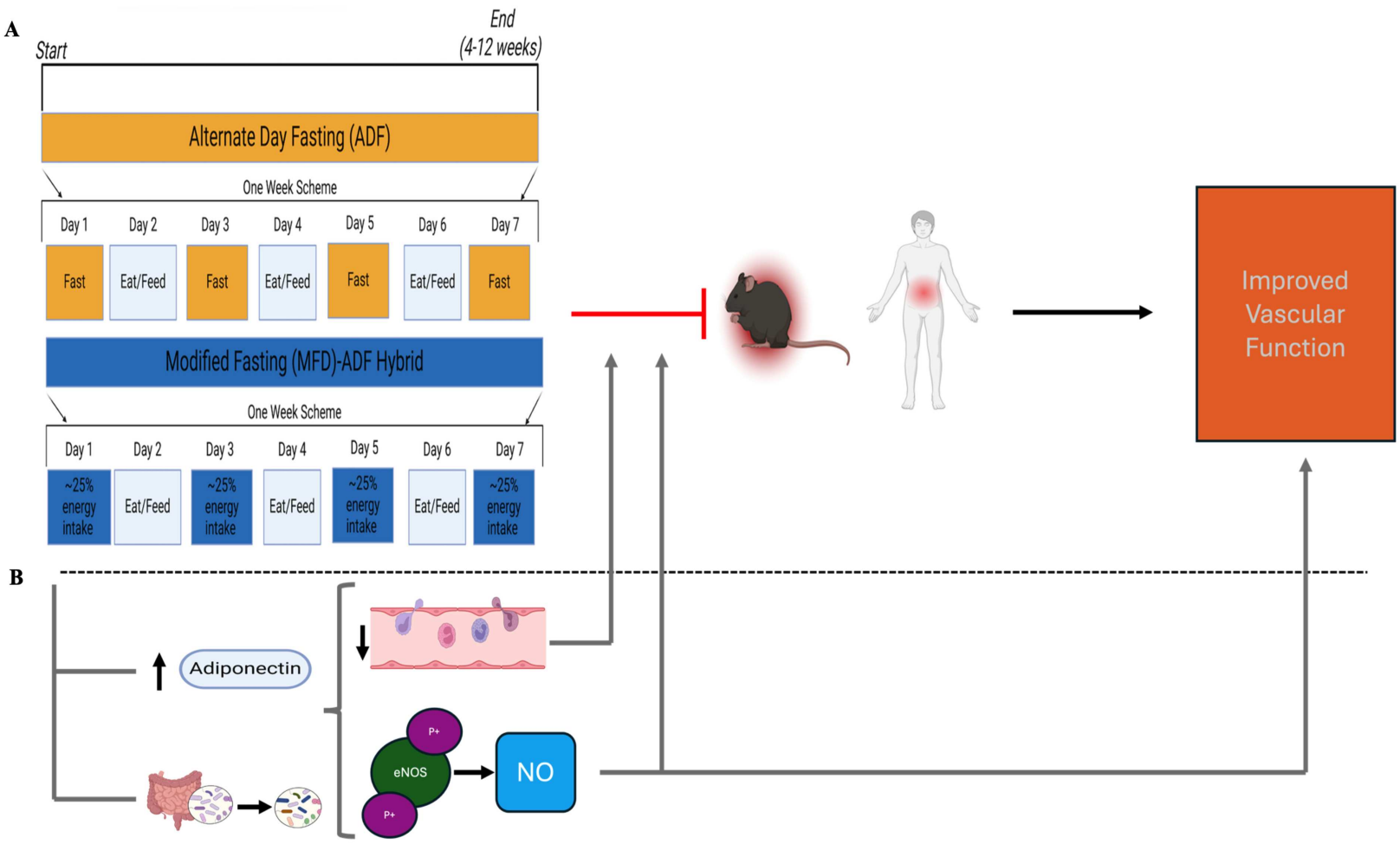

Figure 2.1. The immune system is a critical biological factor relating intermittent fasting to improved vascular function. A) In rodents and humans, alternate-day fasting (ADF) and modified fasting (MFD)-ADF hybrids seem to be the most vascular protective forms of intermittent fasting. Improved vascular function via ADF or MFD-ADF concurs with reduced inflammation. **B**) Intermittent fasting–induced increases in adiponectin and changes to the gut microbiota impact vascular function by affecting the immune system. Both adiponectin and the altered gut microbiota attenuate the movement of inflammatory immune cells into the vascular wall, leading to reduced vascular inflammation and injury. Adiponectin and the altered gut microbiota also activate eNOS (endothelial NO synthase) to produce NO, which could lead to reduced reactive oxygen species (ie, superoxide) formation and less inflammation. Furthermore, NO directly improves vascular function by reducing arterial stiffness and increasing endothelial function. Created at BioRender.com

In humans, 4 weeks of ADF reduced PWV in healthy, middle-aged adults.[25] Furthermore, 8 weeks of an ADF-MFD hybrid diet (25% energy intake on the fast day followed by Ad-Lib on the feast day) increased brachial artery FMD and plasma adiponectin in insulin-sensitive subjects.[29] In the study by Klempel et al,[30] participants were asked to participate in an ADF-MFD protocol but were also randomized to low-fat or high-fat eating. After 8 weeks, brachial artery FMD increased in the low-fat group but not in the high-fat group. Moreover, increases in adiponectin were only significantly associated with improved FMD in the low-fat group, again suggesting adiponectin to be a particular adipokine implicated in endothelial function. Although higher adiponectin levels correspond with improved vascular function in rodents and humans, ADF-MFD can improve brachial artery FMD without affecting adiponectin levels.[31] Thus, improved vascular function via IF does not seem entirely dependent upon increased adiponectin, and other fasting-mediated mechanisms are likely involved.

The gut microbiota has emerged as a crucial regulator of vascular function,[77–80] and studies have shown that IF can affect gut microbial composition. In turn, the gut microbiome has been shown to impact vascular function[78,79] through modulation of signaling molecules (ie, NO) and their precursors or by altering systemic inflammation. In patients with metabolic syndrome, 8 weeks of MFD (≈30% energy intake for 2 nonconsecutive days per week) altered gut microbial composition and function (increased carbohydrate metabolism), increased plasma short-chain fatty acids, and decreased circulating lipopolysaccharide levels. These changes to the gut microbiota occurred in conjunction with significantly increased total nitrate levels (NO donor) and reduced asymmetric dimethylarginine (endogenous eNOS competitive inhibitor) compared with Ad-Lib controls.[28] In addition, Shi et al[81] determined that 10 weeks of ADF reduced blood pressure in spontaneous hypertensive stroke-prone rats. These reductions in blood pressure were dependent upon alterations to the gut microbiome and resulted in increased circulating bile acids. Because the vascular endothelium expresses bile acid receptors (ie, TGR5 [Takeda G-protein–coupled receptor 5]), further analyses showed that supplementation with a TGR5 agonist (oleanolic acid) improved mesenteric artery endothelial function in spontaneous hypertensive stroke-prone rats. Overall,

these results suggest that changes to the gut microbiota via MFD and ADF improve vascular function in rodents and humans.

In summary, Ramadan and TRE have minimal effects on vascular function, whereas ADF and MFD improve arterial stiffness and vascular function in various populations **(Table 2.1)**. Furthermore, because the studies had similar experimental designs, study durations, and participants/subjects **(Table 2.1)**, the vascular benefits of ADF and MFD are likely due to their extended fasting periods.

CHANGES TO THE IMMUNE SYSTEM FOLLOWING IF CORRELATE WITH IMPROVED VASCULAR FUNCTION

There is a strong link between increased inflammation and the development of vascular dysfunction,[42,82] suggesting the immune system is an important mediator of vascular health. For instance, inflammatory mediators (ie, cytokines) can modify endothelial cell–derived vasodilator and vasoconstrictor production, activate voltage-gated ion channels in vascular smooth muscle cells to facilitate vasoconstriction, increase vascular remodeling and smooth muscle cell migration, recruit proinflammatory immune cells to the vascular wall, and induce endothelial cell apoptosis.[42,82] An increasing number of studies have demonstrated that IF reduces inflammation[52] **(Figure 2.1)**. Interestingly, those who have examined this demonstrate that alterations to the immune system tend to occur concomitantly with improvements in vascular function. For example, improved endothelial function observed after Ramadan fasting in older patients with hypertension was associated with reduced plasma levels of the acute-phase reactant CRP (C-reactive protein),[23] which can directly impair vascular function via reduced NO production and eNOS inhibition.[83] CRP can also impact monocyte and T-cell recruitment to the vascular wall and impact expression of potent inflammatory molecules important for immune cell adhesion (E-selectin and CCL2).[83,84] Guo et al[28] found that markers of vascular function improved following MFD and were accompanied by reductions in soluble CD (cluster of differentiation) 40 ligand (CD40L), which can bind to CD40 expressed on endothelial cells, activating them and facilitating their

Table 2.1. Studies Examining the Effects of Intermittent Fasting on Vascular Function

Regimen	Author	Species	Subjects	Study duration	Vascular outcomes	Main results
Ramadan	Alinezhad-Namaghi et al*[21]	Human	Individuals with metabolic syndrome	Fasting for 10 d was considered the minimum acceptable number for the Ramadan fasting group (average of 26.5±6 d of fasting) Individuals who fasted for <10 d were considered the control group (average of 2.7±3 d of fasting)	cfPWV	Reduced cfPWV in the fasting group (8.5±1.2 m/s pre-Ramadan vs 8.2±1.1 m/s post-Ramadan; *P*=0.01)† No change in cfPWV in the control group (8.0±1.2 m/s pre-Ramadan vs 8.2±1.0 m/s post-Ramadan; *P*=0.51)
	Sezen et al[54]	Human	Overweight and obese males	29 d	PWV (TensioMed Arteriograph)	No change in PWV (8.9±1.9 m/s pre-Ramadan vs 8.6±1.8 m/s post-Ramadan; *P*=0.19)
	Eldeeb et al*[22]	Human	Patients with hypertension either with or without chronic kidney disease	29 d	PWV (Mobil-O-Graph) Augmentation index (Mobil-O-Graph)	No change in PWV in those with CKD (9.0±1.8 m/s pre-Ramadan vs 8.5±2.0 m/s post-Ramadan; *P*=0.17) No change in PWV in those without CKD (8.7±1.9 m/s pre-Ramadan vs 8.4±1.6 m/s post-Ramadan; *P*=0.31) No change in augmentation index in those with CKD

Regimen	Author	Species	Subjects	Study duration	Vascular outcomes	Main results
						(25.9±9.7% pre-Ramadan vs 25.0±9.0% post-Ramadan; *P*=0.38) Reduced augmentation index in those without CKD (36.2±13.6% pre-Ramadan vs 26.2±9.0% post-Ramadan; *P*<0.01)†
	Demirci et al*[23]	Human	Individuals with hypertension	30 d	Brachial artery FMD	Increased FMD (8.7±3.8% pre-Ramadan vs 10.8±3.7% post-Ramadan; *P*<0.01)†
TRE/TRF	Sutton et al[71]	Human	Overweight and obese adult males aged 35 to 70 y with prediabetes	5 wk of 18:6 TRE	PWV (radial artery applanation tonometry)	No change in PWV (Δ=−0.5±0.4 m/s; *P*=0.23)
	Martens et al[72]	Human	Healthy midlife and older adults	6 wk of 16:8 TRE	cfPWV Carotid intima-media thickness (ultrasound) Brachial artery FMD	No change in cfPWV No change in carotid intima-media thickness No change in FMD
	Azemi et al*[24]	Rat	Sprague Dawley rats	Group 1: 6 wk of a standard diet followed by 6 wk of standard diet 16:8 TRF Group 2: 6 wk of a high-fat diet followed	Thoracic aorta force myography	Group 1: increased FMD compared with high-fat control (acetylcholine E_{max}: 95.3±6.8% vs 69.2±1.8%)†

Regimen	Author	Species	Subjects	Study duration	Vascular outcomes	Main results
				by 6 wk of high-fat diet 16:8 TRF Group 3: 6 wk of a high-fat diet followed by 6 wk of standard diet 16:8 TRF		Group 2: increased FMD compared with high-fat control (acetylcholine E_{max}: 107.5±4.7% vs 69.2±1.8%)† Group 3: increased FMD compared with high-fat control (acetylcholine E_{max}: 92.3±3.0% vs 69.2±1.8%)†
ADF	Stekovic et al*[25]	Human	Healthy nonobese individuals	4 wk of ADF	PWV (Mobil-O-Graph)	Reduced PWV in the ADF group (Δ=−0.1 [−0.225 to 0] m/s; *P*=0.02)† No change in the control group (Δ=0 [−0.15 to 0.2] m/s; *P*=47)
	Razzak et al*[26]	Rat	Wistar albino rats	2 mo of ADF	Abdominal aorta wire myography	Increased abdominal aorta vasoreactivity to acetylcholine†
	Cui et al*[27]	Mouse	Diabetic mice (*Lepr*^{db})	12 wk of ADF	Mesenteric artery wire myography	Increased mesenteric artery endothelial function†
Hybrid protocols	Guo et al*[28]	Human	Individuals with metabolic syndrome	8 wk of ≈30% energy intake for 2 nonconsecutive days per week (average energy intake on	ADMA and VCAM-1 (ELISA)	Reduced total nitrate and ADMA in the MFD group compared with controls (q=0.062, q=0.068)†

Regimen	Author	Species	Subjects	Study duration	Vascular outcomes	Main results
				fasting days: 31.0% [95% CI, 27.8%–34.2%])	Nitrate (calorimetry)	No change in VCAM-1 compared with controls
	Hoddy et al*[29]	Human	Obese adults	8 wk of an ADF-MFD hybrid (25% energy intake on the fast day followed by normal eating on the feast day)	Brachial artery FMD	Increased FMD between insulin-sensitive (3±0%) and insulin-resistant (−3±0%) obese individuals (P<0.05)†
	Klempel et al*[30]	Human	Obese adults	8 wk of an ADF-MFD hybrid (25% energy intake needs on the fast day followed by 125% on the feast day) Subjects participated in either low- or high-fat eating throughout the ADF-MFD hybrid protocol	Brachial artery FMD	Increased FMD in the low-fat group (Δ=2.1±1.0% [−4.7% to 8.2%])† No change in the high-fat group (Δ=−1.8±1.7% [−8.6% to 6.8%])
	Bhutani et al*[31]	Human	Obese adults	12 wk of an ADF-MFD hybrid (25% energy intake on the fast day followed by normal eating on the feast day)	Brachial artery FMD	Increased FMD compared with baseline measures (5±1% to 10±2%; P<0.05)†

ADF indicates alternate-day fasting; ADMA, asymmetric dimethylarginine; cfPWV, carotid-femoral pulse wave velocity; CKD, chronic kidney disease; FMD, flow-mediated dilation; MFD, modified fasting; PWV, pulse wave velocity; TRE, time-restricted eating; TRF, time-restricted feeding; and VCAM-1, vascular cell adhesion molecule-1.

*An experiment in which significant improvements in vascular function were found.

†Significant finding.

production of inflammatory cytokines and reactive oxygen species. In addition, soluble CD40L-CD40 interactions induce endothelial cell E-selectin, VCAM-1 (vascular cell adhesion molecule-1), and ICAM-1 (intercellular adhesion molecule-1) expression.[85] These adhesion molecules can recruit immune cells into the vascular wall, further augmenting vascular inflammation and injury. CD40L can also destabilize eNOS mRNA,[85] reducing NO production and endothelial function.

Finally, the gut microbiota is a potent modulator of the immune system, and changes to the gut microbiota via IF may impact both immune and vascular function. Shi et al[81] showed that 10 weeks of ADF altered gut microbial composition and circulating bile acids in spontaneously hypertensive stroke-prone rats, which may improve endothelial function via TGR5-dependent pathways.[81] Endothelial TGR5 signaling induces $eNOS^{ser1177}$ and Akt^{ser473} phosphorylation, as well as reduces TNF-mediated monocyte adhesion, NF-κB activation, and lipopolysaccharide-induced monocyte adhesion.[86] In addition, Guo et al[28] reported relative increases in *Rumonococcaceae* and *Roseburia*, as well as short-chain fatty acids, in conjunction with improved endothelial health. A high relative abundance of *Rumonococcaceae* and *Roseburia* is associated with a reduced prevalence of inflammatory-mediated diseases, including Crohn's disease and irritable bowel disease.[87] Furthermore, *Roseburia* is an avid butyrate (short-chain fatty acid) producer, which can reduce inflammation by inducing regulatory T-cell differentiation.[87] Nevertheless, regardless of the distinct mechanisms, this evidence suggests a gut-immune-vascular axis, whereby IF-induced changes to the gut microbiota can reduce inflammation, leading to improved vascular function **(Figure 2.1)**.

VASCULAR-ASSOCIATED IMMUNE CELLS CONTRIBUTE TO VASCULAR DYSFUNCTION

The vascular wall and perivascular tissue contain a depot of immune cells that impact vascular structure and function, and this niche can be maintained by self-renewal (proliferation of existing resident immune cells), repopulation (influx of circulating immune cells), or polarization from circulating precursors once deposited into the vascular wall. Indeed, inflammatory signals from endothelial cells,

vascular smooth muscle cells, fibroblasts, resident immune cells, and perivascular cells can exacerbate the recruitment and accumulation of circulating immune cells into the vascular wall or perivascular tissue.[41–43] Once these cells infiltrate the vascular wall or perivascular tissue, they can become polarized and exert effector functions. Furthermore, circulating immune cells can directly impact vascular inflammation and vascular function without moving into the vascular wall by signaling to the endothelium, adventitia, or perivascular tissue. Because not all immune cells that impact vascular function reside within the vascular wall, the term vascular-associated immune cells is a more accurate description of the various immune cell subsets that impact vascular health.

Many different types of vascular-associated immune cells contribute to vascular inflammation and dysfunction.[32–34,36–40,88,89] For example, circulating Ly6C^{hi} (lymphocyte antigen 6 C1 high) monocytes can infiltrate the vascular wall via CCR2 expression and differentiate into M2-like macrophages, exacerbating hypertension and ECM (extracellular matrix) remodeling, both putative determinants of arterial stiffness.[88] Furthermore, peripheral and aortic accumulation of Ly6C^{hi}monocytes, M1-polarized macrophages, and inflammatory cytokines increased endothelial dysfunction in a mouse model of hyperhomocysteinemia and type 2 diabetes.[36] TNF and IFN-γ–producing CD4$^+$ and CD8$^+$ T-cell accumulation in the aorta and mesenteric arteries has been shown to exacerbate age-related vascular dysfunction.[90] T cells can also mediate Ang II (angiotensin II)–induced hypertension and vascular dysfunction.[32,38] Specifically, Majeed et al[32] found that *Rag1* (recombination activating gene 1)$^{-/-}$ mice devoid of functional lymphocytes were not susceptible to Ang II–mediated arterial stiffness. However, the adoptive transfer of CD4$^+$ T cells into *Rag1*$^{-/-}$ mice facilitated Ang II–induced stiffening. Furthermore, Guzik et al[38] showed that Ang II increased T cells in the perivascular adipose tissue and adventitia via CD44 and CCR5, which increased hypertension and vascular dysfunction. Another study corroborates that increased accumulation of macrophages and T cells in the vascular wall and perivascular adipose tissue is associated with vascular dysfunction.[91]

Other immune cells, such as neutrophils, B cells, and NK cells, have also been associated with vascular dysfunction. Liu et al[39] showed that knocking out neutrophil elastase (*Elane*$^{-/-}$)

or peptidylarginine deiminase 4 (*Pad4*$^{-/-}$), drivers of neutrophil extracellular trap formation, improved endothelial function and reduced ICAM-1 levels in type 1 diabetic Akita mice. Furthermore, enhanced endothelial function was observed in mice supplemented with the neutrophil elastase inhibitor GW311616A compared with vehicle-supplemented controls. The adoptive transfer of Akita neutrophils into young, wild-type mice increased vascular dysfunction, while the transfer of Akita-*Elane*$^{-/-}$ or Akita-*Pad4*$^{-/-}$neutrophils did not. Mechanistically, the authors suggest that knockout Akita mice had improved vascular function by inhibiting neutrophil extracellular trap formation and thromboxane production.

Chan et al[40] demonstrated reduced collagen deposition and PWV after Ang II infusion in BAFF-R KO (knockout) mice (defective splenic B-cell maturation). BAFF-R KO mice also displayed reduced aortic IgG accumulation, transitional (CD206^{+} MHCII^{hi} or CD206^{-} MHCII^{lo}) and M2-polarized (CD206^{+} MHCII^{lo}) macrophages, and TGF-β (transforming growth factor-β) expression compared with wild-type mice. Finally, Kossmann et al[92] showed that IFN-γ production by NK cells in the aortic wall augmented vascular oxidative stress, inflammatory immune cell recruitment and activation, and endothelial dysfunction.

These data support the notion that the accumulation of many different immune cell subsets in the vascular wall or perivascular tissue can exacerbate vascular dysfunction. In contrast, IF appears to reduce systemic inflammation, which is mechanistically linked to decreased circulating immune cells and their recruitment into the vascular wall and perivascular tissue. Thus, determining whether IF improves vascular function by reducing the accumulation of immune cells in the blood, vascular wall, and perivascular tissue is an exciting area of future investigation.

EVIDENCE OF FASTING-INDUCED IMMUNE CELL REDISTRIBUTION

Although the direct effects of IF on vascular-associated immune cells are unknown, evidence of fasting-induced immune cell redistribution has been prevalent since the early 1950s[93] and was further validated in the 1980s.[94] Wing et al[94]showed that 72 hours of fasting reduced thymus cellularity to 5% of baseline, and after 7 days of refeeding, cellularity recovered to >50% of baseline. Similar changes were

observed in the spleen, as cellularity dropped to 18% of baseline after 72 hours of fasting and returned to normal after 7 days of refeeding. In a separate experiment, thymus, spleen, and blood cellularity were significantly reduced after 48 hours of fasting compared with 24 hours of refeeding. These data suggest a cyclical disappearance and repopulation of the thymus, spleen, and blood immune cells in response to fasting and refeeding. These changes in cellularity were diminished in adrenalectomized mice, suggesting that the acute stress response to fasting (i.e., increased corticosteroids) mediates organ cellularity **(Figure 2.2A)**.[94]

More recent studies have expanded upon these original findings and provide further evidence of fasting-induced immune cell redistribution. In 2023, Janssen et al[45] reported in experimental mice that 24-hour fasting significantly reduced immune cell counts in circulation, as well as in the spleen, lung, pancreas, brown adipose tissue, white adipose tissue, heart, peritoneum, and tissues of the gastrointestinal tract (small intestine, Peyer's patches, mesenteric lymph nodes, and mesenteric adipose tissue). When limiting their focus to circulating monocytes, the authors showed that fasting facilitated the redistribution of transcriptionally unique proinflammatory ($Ly6C^{hi}$) monocytes[95] from circulation to the bone marrow. Specifically, Janssen et al show that adoptively transferred GFP^+ (green fluorescent protein) monocytes appeared in the circulation of fed mice but were absent in the blood of 24-hour fasted mice. Instead, GFP^+ monocytes were identified in higher numbers in the bone marrow of fasted mice. Further experiments, including parabiosis of GFP^+ mice with wild-type mice, showed more GFP^+ $Ly6C^{hi}$ monocytes in the blood and less in the bone marrow of fasted-refed mice compared with fasted mice, suggesting that the cells that accumulated in the bone marrow during fasting reappeared in circulation following refeeding. Next, the authors used a double-pulse-chase strategy that utilized the sequential injection of 5-ethynyl-2′-deoxyuridine (EdU) and 5-bromodeoxyuridin (BrdU), 2 nucleotide analogs. EdU was injected 24 hours before fasting, and BrdU was injected halfway through the fast. Thus, Edu^+ $Ly6C^{hi}$ monocytes were considered old (originated prefast), and $BrdU^+$ $Ly6C^{hi}$ monocytes were considered young (originated during fasting). Importantly, although similar rates of EdU were incorporated in bone marrow monocytes, higher numbers of bone marrow Edu^+ monocytes were identified in fasted and fasted-refed mice. BrdU

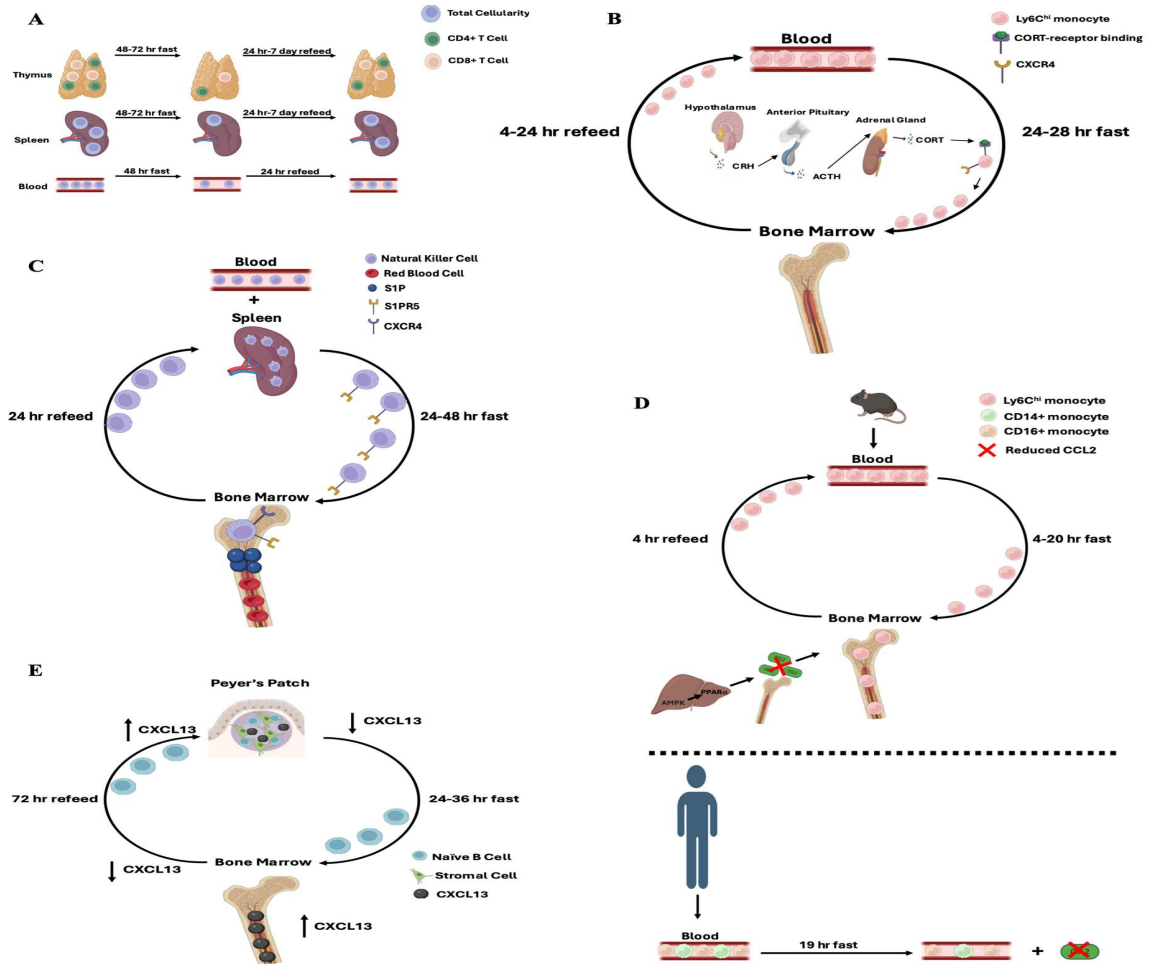

Figure 2.2. Examples of fasting-induced immune cell redistribution. A) In the study by Wing et al, fasting for 48 to 72 hours in mice significantly reduced thymus, spleen, and blood cellularity and decreased thymus CD (cluster of differentiation) 4^+ and $CD8^+$ T cells. Cellularity in all tissues was partially restored within 1 to 7 days. These results did not occur in adrenalectomized mice. **B**) Janssen et al showed that transcriptionally unique circulating $Ly6C^{hi}$ (lymphocyte antigen 6 C1 high) monocytes traverse to and from the bone marrow in response to fasting and refeeding, respectively. Fasting-mediated redistribution to the bone marrow was regulated by stress-induced corticosteroid production, which augmented CXCR4 (C-X-C chemokine receptor type 4) expression on $Ly6C^{hi}$ monocytes. **C**) A recent article by Delconte et al showed that spleen and circulating natural killer (NK) cells were redistributed to the bone marrow during a 48-hour fast and then were restored in the circulation and spleen within 24 hours after feeding. NK cell redistribution depended on red blood cell S1P (sphingosine-1-phosphate) production in the bone marrow, allowing S1PR (S1P receptor)-expressing NK cells to accumulate in the bone marrow during fasting. CXCR4 on NK cells facilitated bone marrow retention. **D**) Jordan et al found that 4 to 20 hours of fasting in mice redistributed circulating $Ly6C^{hi}$ monocytes to the bone marrow, while monocytes reappeared in circulation in as little as 4 hours after refeeding. The accumulation of $Ly6C^{hi}$ monocytes in the bone marrow was regulated by a hepatic AMPK (AMP-activated protein kinase)-PPARα (peroxisome proliferator-activated receptor-α) pathway, which reduced bone marrow CCL2 (C-C motif chemokine ligand 2) production and monocyte egress. Extended fasting periods seemed to impact monocyte metabolism and phenotype more potently. In humans, fasting reduced circulating CCL2 and $CD14^+$(phagocytic) and $CD16^+$ (patrolling) monocytes. **E**) Nagai et al showed that fasting redistributed naive B cells from Peyer's patches to the bone marrow via reduced Peyer's patch stromal cell CXCL13 (chemokine [C-X-C motif] ligand 13) expression and increased bone marrow CXCL13 expression. In contrast, refeeding increased Peyer's patch CXCL13 expression and recruited naive B cells back to the intestine. Created at BioRender.com. ACTH indicates adrenocorticotropic hormone; CORT, corticosterone; and CRH, corticotropin-releasing hormone.

incorporation was lower in bone marrow monocytes from fasted and fasted-refed mice than in controls, suggesting the reduced production of new monocytes in the bone marrow during fasting. Finally, there were significantly higher numbers of circulating Edu^+ monocytes in fasted-refed mice compared with fed and fasted mice. Yet, there were no differences in circulating $BrdU^+$ monocyte levels between the groups. These results indicate that $Ly6C^{hi}$ monocytes are redistributed to the bone marrow during fasting and reappear in circulation after refeeding. Mechanistically, this redistribution was mediated by a corticosteroid-CXCR4 (C-X-C chemokine receptor type 4) axis, whereby heightened corticosterone production during fasting augmented monocyte CXCR4 expression, a chemokine receptor implicated in immune cell redistribution. Upon activation of the corticosteroid-CXCR4 axis, monocytes were redistributed to the bone marrow **(Figure 2.2B)**.

NK cells also seem to depend on CXCR4 for redistribution into the bone marrow during fasting. A recent article by Delconte et al[47] showed that a 48-hour fast reduced splenic and circulating NK cells but increased NK cells in the bone marrow. After refeeding, NK cells were reduced in the bone marrow but increased in circulation and spleen. Interestingly, fasting did not impact the number of dead splenic and blood NK cells. The authors transferred mature splenic NK cells from CD45.1 mice into CD45.2-expressing recipient mice to validate the redistribution theory. Again, fasting reduced $CD45.1^+$ splenic and circulating NK cells while increasing their appearance in the bone marrow. Similar results were found when using the i$Nkp46^{tdTomato}$ mouse model to trace NK cell location, suggesting that circulating and splenic NK cells are redistributed to the bone marrow in response to fasting and then reappear in the spleen and circulation following refeeding. Utilization of AMD3100, a CXCR4 antagonist, confirmed that fasting-induced redistribution of NK cells to the bone marrow was at least partially regulated by CXCR4-mediated NK cell retention. Another process implicated in NK cell redistribution was bone marrow red blood cell accumulation, as Delconte et al showed increased red blood cells in the bone marrow in fasting mice compared with controls. Red blood cells constitute a significant source of S1P (sphingosine-1-phosphate), which induces immune cell trafficking through interactions with S1PRs (S1P receptors). By

utilizing *S1pr5*$^{-/-}$ mice and *S1pr5*$^{-/-}$ NK cells, the authors validated that the S1P-S1PR axis was instrumental in fasting-mediated NK cell redistribution to the bone marrow **(Figure 2.2C)**.

Two other studies have found that CXCR4 is an important chemokine contributing to fasting-induced immune cell redistribution. Wang et al found that a 24-hour fast increased T cells in the bone marrow and reduced counts in the blood, spleen, and inguinal lymph nodes. These changes were likely not caused by cell death or proliferation, as fasting did not alter the percentage of FVD^{+} (fixable viability dye positive) and Ki67^{+} T cells in the blood and bone marrow. Further analyses determined that catecholaminergic neuron activation during fasting increased glucocorticoid release from adrenal glands, likely via corticotropin-releasing hormone neurons in the hypothalamic paraventricular nucleus. This neuronal circuit drove T-cell redistribution from the circulation to bone marrow via the CXCR4-CXCL12 axis while having a marked immunosuppressive effect on redistributed T cells.[48] Additionally, 14:10 TRF in mice affected the rhythmic movement of neutrophils, as circulating neutrophil CXCR4 expression and neutrophil abundance in the lung were reduced in TRF but not in Ad-Lib mice at the beginning of the inactive phase.[96] Thus, TRF may affect neutrophil redistribution by reducing chemokine receptor expression, increasing their blood latency.

Data have shown that fasting induces immune cell redistribution independently of CXCR4. Jordan et al[44] showed that 4 and 20 hours of fasting promoted circulating Ly6C^{hi} monocyte accumulation in the bone marrow. There was no difference in activated caspase-positive monocytes in the blood or CXCR4^{+} monocyte precursors in the bone marrow, so this accumulation was likely not due to cell death or proliferation. Mechanistically, bone marrow Ly6C^{hi} monocyte accumulation depended on hepatic AMPK-PPARα signaling, which resulted in reduced bone marrow CCL2 production and monocyte egress. These data also suggest that more extended fasting periods (i.e., 20 versus 4 hours) produce more substantial effects on bone marrow monocyte metabolism and phenotype. Surprisingly, just 4 hours after refeeding, Ly6C^{hi} monocytes were restored in circulation. Furthermore, Jordan et al reported that fasting reduced CCL2, as well as CD14^{+} (phagocytic) and CD16^{+} (patrolling) monocytes, in healthy humans

(Figure 2.2D). These data suggest a translatable mechanism in which fasting regulates monocyte redistribution in both mice and humans by reducing CCL2.

In another recent study, Nagai et al[46] reported that fasting promoted the redistribution of naive IgM^+ IgD^+ B cells from Peyer's patches to the bone marrow. Importantly, the accumulation of bone marrow B cells did not result from enhanced B-cell proliferation within the bone marrow, as both immature and $Ki67^+$ B cells decreased in the bone marrow during fasting. Mechanistically, the redistribution of B cells was regulated through the expression of CXCL13 (chemokine [C-X-C motif] ligand 13) by stromal cells in Peyer's patches. During fasting, the expression of CXCL13 in Peyer's patches was reduced, while it was increased in the bone marrow. In contrast, refeeding skewed metabolism of Peyer's patches toward aerobic glycolysis, increasing CXCL13 expression and recruiting naive B cells back to the intestine **(Figure 2.2E)**.

In summary, during fasting, many different immune cells within several tissues are redistributed to the bone marrow, which likely affects their metabolism and phenotype. These cells reappear in their prefasting location upon refeeding.

NOVEL PERSPECTIVE: COULD FASTING-INDUCED IMMUNE CELL REDISTRIBUTION BE LEVERAGED TO IMPROVE VASCULAR FUNCTION?

As stated in the previous section, a direct link between IF and the vascular-associated immune system remains unproven. Yet, these data propose that an area of new and novel research in vascular biology could be whether fasting-induced immune cell redistribution impacts vascular health **(Figure 2.3)**.

There are several examples of how fasting-induced immune cell redistribution could improve vascular function. For instance, fasting facilitates the movement of many circulating immune cells related to vascular dysfunction ($Ly6C^{hi}$monocytes, NK cells, and T cells). The large-scale redistribution of these immune cells to the bone marrow could impede their accumulation into the vascular wall and perivascular tissue. Furthermore, spleen-resident and Peyer's patch–resident immune cells traverse to the bone marrow

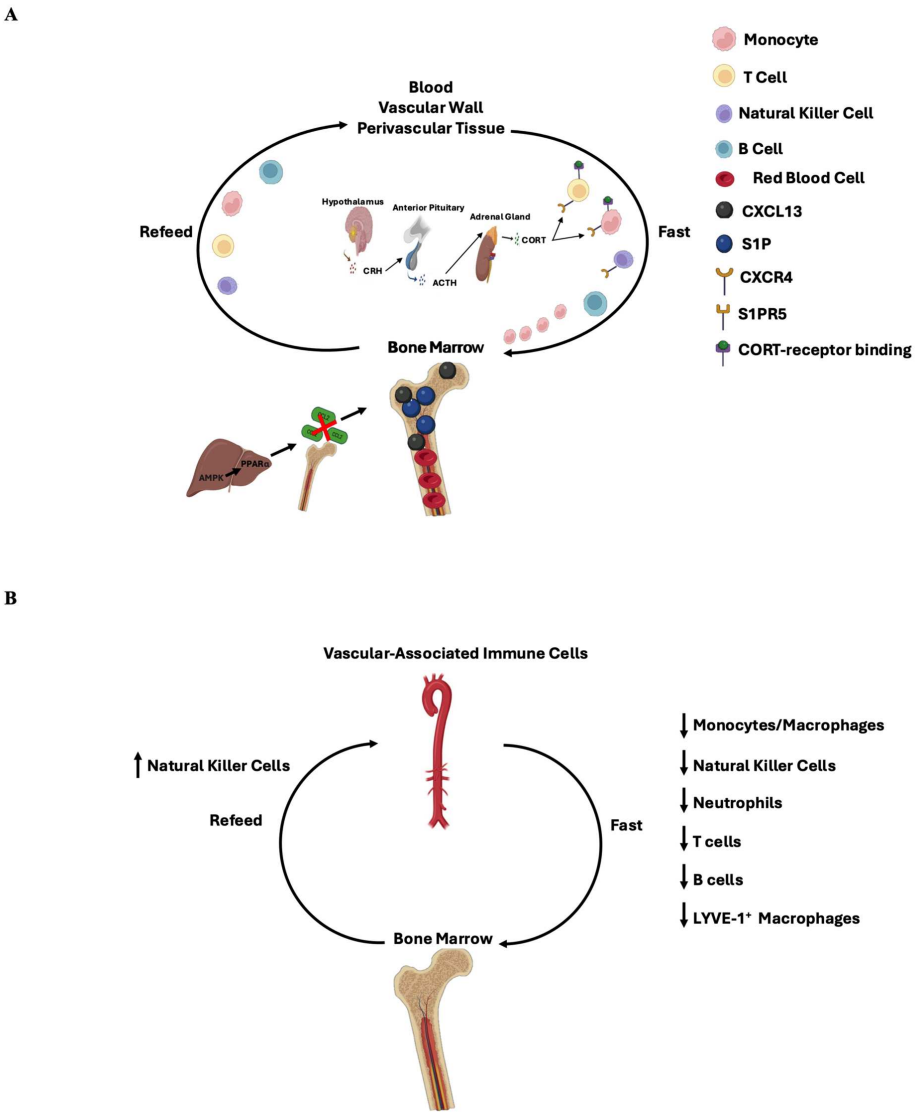

Figure 2.3. Could fasting-induced immune cell redistribution affect vascular function? A) Proposed mechanisms of immune cell redistribution in vascular-associated immune cells. By adapting the available fasting-redistribution data to vascular-associated immune cells, we propose that during fasting, increased glucocorticoid production via the hypothalamic-pituitary-adrenal axis could augment CXCR4 (C-X-C chemokine receptor type 4) expression on circulating and possibly vascular wall–resident and perivascular tissue–resident monocytes and T cells. Heightened CXCR4 expression facilitates the movement of these cells to the bone marrow. In conjunction with increased red blood cell and sphingosine-1-phosphate production in the bone marrow, CXCR4 expression on vascular-associated natural killer (NK) cells could also influence their redistribution to the bone marrow. Furthermore, reduced CCL2 production by the bone marrow could minimize monocyte egress during fasting. Finally, increased CXCL13 (chemokine [C-X-C motif] ligand 13) expression from the bone marrow could increase vascular-associated B-cell movement into the bone marrow. Once in the bone marrow, immune cells might undergo stark phenotypic changes, affecting their phenotype in the bone marrow and upon restoration to their prefasting location (ie, blood, vascular wall, and perivascular tissue) following refeeding. **B**) Consequences of multiweek intermittent fasting on vascular function. Repeated movement of inflammatory and vascular-associated monocytes/macrophages, NK cells, neutrophils, T cells, and B cells could reduce vascular inflammation, oxidative stress, and compounding immune cell influx into the vascular wall and perivascular tissue, which could lead to improved vascular function over time. It is essential to consider that constant redistribution of IFN-γ (interferon-γ)–producing NK cells and LYVE-1^{+} (lymphatic vessel endothelial hyaluronan receptor 1) macrophages might not improve vascular function. Created at BioRender.com

during fasting. These data suggest that other tissue-resident immune cell subsets, such as cells resident to the vascular wall and perivascular tissue, could also traverse to the bone marrow in response to fasting.

Additionally, metabolic reprogramming of immune cells via fasting-induced immune cell redistribution has already been shown to attenuate progression of various pathologies. Jordan et al demonstrated that 4 weeks of ADF reduced monocyte accumulation in circulation and in the spinal cord of mice with experimental autoimmune encephalomyelitis (model for multiple sclerosis). The spinal cord monocytes also had downregulated inflammatory genes, such as *Tnf*, *Cxcl2*, *Cxcl10*, and downregulated gene modules associated with inflammation compared with monocytes from Ad-Lib mice. Consequentially, IF mice had significant improvement in experimental autoimmune encephalomyelitis clinical course.[44] Wang et al[48] found that the redistribution of T cells via IF (ADF) was associated with reduced plasma and spinal cord proinflammatory cytokines, as well as reduced monocyte, $CD4^+$ T cell (Th1 (type 1 helper T cells) and Th17 (type 17 helper T cells)), $CD8^+$ T cell, and neutrophil infiltration in the spinal cord of experimental autoimmune encephalomyelitis mice. Delconte et al.[47] showed that fasting-induced NK cell redistribution could improve anti-tumor immunity.[47] Specifically, fasting-induced NK cell redistribution from the spleen into the bone marrow promoted NK cell priming and IFN-γ production by IL-12–expressing myeloid cells. Strikingly, NK cells that returned to the spleen after refeeding also secreted more IFN-γ than Ad-Lib controls, which aided in tumor control. IF also affected NK cell fatty acid oxidation to improve tumor control, independent of immune cell redistribution.

Finally, Janssen et al[45] speculated that a potential benefit of fasting-induced immune cell redistribution is protecting the pool of the current immune cells and reducing immune cell proliferation during nutrient deprivation. Accelerated immune cell production from distinct hematopoietic stem cell clones (i.e., clonal hematopoiesis) and clonal expansion of extramedullary and vascular-resident immune cells are associated with adverse cardiovascular health.[97–99] While the potential benefits of immune cell redistribution on cardiovascular health have been acknowledged, it remains necessary to determine whether immune cell redistribution has a direct impact on cardiovascular health.

LIMITATIONS AND FUTURE DIRECTIONS

The ability of fasting-induced immune cell redistribution to impact vascular function is intriguing, yet there are some translational limitations from the available data and potential concerns with the repeated movement of immune cells away from their prefasting location. First, most of the available data are from studies that observed immune cell redistribution in response to a single fasting-refeeding cycle, which may have different immunologic effects than long-term IF. It is imperative to explore whether long-term IF leads to adaptations in immune cells, reducing their tendency for movement with repeated exposure. Contrary to this notion, Janssen et al showed that when mice fasted 24 hours every other day for 2 weeks, fasting continued to reduce circulating Ly6C^{hi} monocyte levels during each fasting window, suggesting that immune cells continue to traverse to the bone marrow after each bout of fasting and do not adapt to the fasting response. These results further indicate that IF regimens with a greater fasting frequency (i.e., 5:2, ADF) might confer better vascular outcomes by more consistent inflammatory vascular-associated immune cell redistribution. Second, although data suggest that fasting-induced immune cell redistribution occurs in humans,[44] the relationships between fasting, immune cell redistribution, and vascular health must be more rigorously studied. The most logical next step would be to conduct an IF clinical trial in participants with vascular dysfunction while using advanced in vivo and ex vivo labeling techniques to evaluate the immune cell subsets that disappear from circulation during fasting and reappear during refeeding. This would enable researchers to clinically correlate the fasting-induced redistribution of immune cells with changes in vascular function.

Next, the potential benefits of vascular-associated immune cell redistribution on vascular function might be cell specific. For instance, Lim et al showed that functionally distinct LYVE-1 (lymphatic vessel endothelial hyaluronan receptor 1)–positive macrophages that presumably arise from bone marrow progenitors regulate arterial stiffness by engaging smooth muscle pericellular hyaluronic acid to reduce collagen production by MMP-9 (matrix metalloproteinase-9).[100] Furthermore, Delconte et al.[47] showed that NK cells that returned to the spleen after refeeding also secreted more IFN-γ than Ad-Lib controls. Because NK cell IFN-γ exacerbates endothelial dysfunction,[92] restoring vascular-associated NK cells

during refeeding could increase IFN-γ–mediated vascular dysfunction. Thus, research is needed to determine whether fasting-induced immune cell redistribution of several different immune cell subsets promotes a net benefit to vascular health, even if the redistribution of specific immune cells might not confer vascular benefits. Pharmaceuticals and other approaches could then be developed to leverage the redistribution of specific immune cells to maximize cardioprotective benefits.

CONCLUSIONS

Numerous studies have shown that IF markedly improves CVD risk factors such as obesity, hypertension, and type 2 diabetes. Arterial stiffness and endothelial dysfunction, 2 key aspects of vascular dysfunction, are strong risk factors for cardiovascular health and all-cause mortality. Studies investigating the effects of IF on vascular function are relatively scarce. Yet, the consensus from the available data is that fasting length and frequency are 2 critical determinants of IF's impact on vascular function. The mechanistic underpinnings of how specific IF modalities improve vascular function are poorly understood, but improved vascular function via IF generally coincides with robust changes to the immune system. With the recent identification of fasting-induced immune cell redistribution as a potential contributor to health, we propose that the relationship between fasting-induced immune cell redistribution and vascular health should be further explored. Future experiments should focus on validating the impact of vascular-associated immune cell redistribution on vascular function and whether redistribution is prevalent in humans. These experiments could have implications for human vascular health.

REFERENCES

1. Koppold DA, Breinlinger C, Hanslian E, et al. International consensus on fasting terminology. *Cell Metabolism*. Published online July 2024:S1550413124002699. doi:10.1016/j.cmet.2024.06.013

2. Persynaki A, Karras S, Pichard C. Unraveling the metabolic health benefits of fasting related to religious beliefs: A narrative review. *Nutrition*. 2017;35:14-20. doi:10.1016/j.nut.2016.10.005

3. Gonzalez JE, Cooke WH. Influence of an acute fast on ambulatory blood pressure and autonomic cardiovascular control. *American Journal of Physiology-Regulatory, Integrative and Comparative Physiology*. 2022;322:R542-R550. doi:10.1152/ajpregu.00283.2021

4. International Food Information Council. 2024 Health and Food Survey. June 20, 2024. https://foodinsight.org/2024-foodhealth-survey/

5. Catterson JH, Khericha M, Dyson MC, et al. Short-Term, Intermittent Fasting Induces Long-Lasting Gut Health and TOR-Independent Lifespan Extension. *Current Biology*. 2018;28:1714-1724.e4. doi:10.1016/j.cub.2018.04.015

6. de Cabo R, Mattson MP. Effects of Intermittent Fasting on Health, Aging, and Disease. Longo DL, ed. *N Engl J Med*. 2019;381:2541-2551. doi:10.1056/NEJMra1905136

7. Chen Y, Su J, Yan Y, et al. Intermittent Fasting Inhibits High-Fat Diet–Induced Atherosclerosis by Ameliorating Hypercholesterolemia and Reducing Monocyte Chemoattraction. *Front Pharmacol*. 2021;12:719750. doi:10.3389/fphar.2021.719750

8. Dorighello GG, Rovani JC, Luhman CJF, et al. Food restriction by intermittent fasting induces diabetes and obesity and aggravates spontaneous atherosclerosis development in hypercholesterolaemic mice. *Br J Nutr*. 2014;111:979-986. doi:10.1017/S0007114513003383

9. Mérian J, Ghezali L, Trenteseaux C, et al. Intermittent Fasting Resolves Dyslipidemia and Atherogenesis in Apolipoprotein E-Deficient Mice in a Diet-Dependent Manner, Irrespective of Sex. *Cells*. 2023;12:533. doi:10.3390/cells12040533

10. Togo J, Sung HK. Intermittent fasting—a double edged sword for atherosclerosis. *Life Metabolism*. 2024;3:loae015. doi:10.1093/lifemeta/loae015

11. Bartholomew CL, Muhlestein JB, May HT, et al. Randomized controlled trial of once-per-week intermittent fasting for health improvement: the WONDERFUL trial. Bäck M, ed. *European Heart Journal Open*. 2021;1:oeab026. doi:10.1093/ehjopen/oeab026

12. Wilkinson MJ, Manoogian ENC, Zadourian A, et al. Ten-Hour Time-Restricted Eating Reduces Weight, Blood Pressure, and Atherogenic Lipids in Patients with Metabolic Syndrome. *Cell Metabolism*. 2020;31:92-104.e5. doi:10.1016/j.cmet.2019.11.004

13. Al Zein M, Zein O, Diab R, et al. Intermittent fasting favorably modulates adipokines and potentially attenuates atherosclerosis. *Biochemical Pharmacology*. 2023;218:115876. doi:10.1016/j.bcp.2023.115876

14. Okoshi K, Cezar MDM, Polin MAM, et al. Influence of intermittent fasting on myocardial infarction-induced cardiac remodeling. *BMC Cardiovasc Disord*. 2019;19:126. doi:10.1186/s12872-019-1113-4

15. Ahmet I, Wan R, Mattson MP, Lakatta EG, Talan M. Cardioprotection by Intermittent Fasting in Rats. *Circulation*. 2005;112:3115-3121. doi:10.1161/CIRCULATIONAHA.105.563817

16.Dutzmann J, Kefalianakis Z, Kahles F, et al. Intermittent Fasting After ST-Segment–Elevation Myocardial Infarction Improves Left Ventricular Function: The Randomized Controlled INTERFAST-MI Trial. *Circ: Heart Failure*. Published online May 2, 2024:e010936. doi:10.1161/CIRCHEARTFAILURE.123.010936

17. Zheng H, Wu S, Liu X, et al. Association Between Arterial Stiffness and New-Onset Heart Failure: The Kailuan Study. *ATVB*. 2023;43. doi:10.1161/ATVBAHA.122.317715

18. Mattace-Raso FUS, van der Cammen TJM, Hofman A, et al. Arterial Stiffness and Risk of Coronary Heart Disease and Stroke: The Rotterdam Study. *Circulation*. 2006;113:657-663. doi:10.1161/CIRCULATIONAHA.105.555235

19. Davignon J, Ganz P. Role of Endothelial Dysfunction in Atherosclerosis. *Circulation*. 2004;109. III27-III32. doi:10.1161/01.CIR.0000131515.03336.f8

20. Tsao CW, Aday AW, Almarzooq ZI, et al. Heart Disease and Stroke Statistics—2023 Update: A Report From the American Heart Association. *Circulation*. 2023;147. doi:10.1161/CIR.0000000000001123

21. Alinezhad-Namaghi M, Eslami S, Nematy M, et al. Association of time-restricted feeding, arterial age, and arterial stiffness in adults with metabolic syndrome. *Health Science Reports*. 2023;6:e1385. doi:10.1002/hsr2.1385

22. Eldeeb A, Mahmoud M, Ibrahim A, Yousef E, Sabry A. Effect of Ramadan fasting on arterial stiffness parameters among Egyptian hypertensive patients with and without chronic kidney disease. *Saudi J Kidney Dis Transpl*. 2020;31:582. doi:10.4103/1319-2442.289444

23. Demirci E, Özkan E. Improvement in endothelial function in hypertensive patients after Ramadan fasting: effects of cortisol. *Turkish Journal of Medical Sciences*. 2023;53:439-445. doi:10.55730/1300-0144.5603

24. Azemi AK, Siti-Sarah AR, Mokhtar SS, Rasool AHG. Time-Restricted Feeding Improved Vascular Endothelial Function in a High-Fat Diet-Induced Obesity Rat Model. *Veterinary Sciences*. 2022;9:217. doi:10.3390/vetsci9050217

25. Stekovic S, Hofer SJ, Tripolt N, et al. Alternate Day Fasting Improves Physiological and Molecular Markers of Aging in Healthy, Non-obese Humans. *Cell Metabolism*. 2019;30:462-476.e6. doi:10.1016/j.cmet.2019.07.016

26. Razzak RLA, Abu-Hozaifa BM, Bamosa AO, Ali NM. Assessment of enhanced endothelium-dependent vasodilation by intermittent fasting in Wistar albino rats. *Indian J Physiol Pharmacol*. 2011;55:336-342.

27. Cui J, Lee S, Sun Y, et al. Alternate Day Fasting Improves Endothelial Function in Type 2 Diabetic Mice: Role of Adipose-Derived Hormones. *Front Cardiovasc Med*. 2022;9:925080. doi:10.3389/fcvm.2022.925080

28. Guo Y, Luo S, Ye Y, Yin S, Fan J, Xia M. Intermittent Fasting Improves Cardiometabolic Risk Factors and Alters Gut Microbiota in Metabolic Syndrome Patients. *The Journal of Clinical Endocrinology & Metabolism*. 2021;106:64-79. doi:10.1210/clinem/dgaa644

29. Hoddy KK, Bhutani S, Phillips SA, Varady KA. Effects of different degrees of insulin resistance on endothelial function in obese adults undergoing alternate day fasting. *NHA*. 2016;4:63-71. doi:10.3233/NHA-1611

30.Klempel MC, Kroeger CM, Norkeviciute E, Goslawski M, Phillips SA, Varady KA. Benefit of a low-fat over high-fat diet on vascular health during alternate day fasting. *Nutr & Diabetes*. 2013;3:e71-e71. doi:10.1038/nutd.2013.14

31. Bhutani S, Klempel MC, Kroeger CM, et al. Alternate day fasting with or without exercise: Effects on endothelial function and adipokines in obese humans. *e-SPEN Journal*. 2013;8:e205-e209. doi:10.1016/j.clnme.2013.07.005

32. Majeed BA, Eberson LS, Tawinwung S, Larmonier N, Secomb TW, Larson DF. Functional aortic stiffness: role of CD4+ T lymphocytes. *Front Physiol*. 2015;6. doi:10.3389/fphys.2015.00235

33. Lintermans LL, Stegeman CA, Heeringa P, Abdulahad WH. T Cells in Vascular Inflammatory Diseases. *Front Immunol*. 2014;5. doi:10.3389/fimmu.2014.00504

34. Silvestre-Roig C, Braster Q, Ortega-Gomez A, Soehnlein O. Neutrophils as regulators of cardiovascular inflammation. *Nat Rev Cardiol*. 2020;17:327-340. doi:10.1038/s41569-019-0326-7

35. Rahman K, Vengrenyuk Y, Ramsey SA, et al. Inflammatory Ly6Chi monocytes and their conversion to M2 macrophages drive atherosclerosis regression. *Journal of Clinical Investigation*. 2017;127:2904-2915. doi:10.1172/JCI75005

36. Fang P, Li X, Shan H, et al. Ly6C $^{+}$ Inflammatory Monocyte Differentiation Partially Mediates Hyperhomocysteinemia-Induced Vascular Dysfunction in Type 2 Diabetic db/db Mice. *ATVB*. 2019;39:2097-2119. doi:10.1161/ATVBAHA.119.313138

37. Williams JW, Zaitsev K, Kim KW, et al. Limited proliferation capacity of aortic intima resident macrophages requires monocyte recruitment for atherosclerotic plaque progression. *Nat Immunol*. 2020;21:1194-1204. doi:10.1038/s41590-020-0768-4

38. Guzik TJ, Hoch NE, Brown KA, et al. Role of the T cell in the genesis of angiotensin II–induced hypertension and vascular dysfunction. *The Journal of Experimental Medicine*. 2007;204:2449-2460. doi:10.1084/jem.20070657

39. Liu C, Yalavarthi S, Tambralli A, et al. Inhibition of neutrophil extracellular trap formation alleviates vascular dysfunction in type 1 diabetic mice. *Sci Adv*. 2023;9:eadj1019. doi:10.1126/sciadv.adj1019

40. Chan CT, Sobey CG, Lieu M, et al. Obligatory Role for B Cells in the Development of Angiotensin II–Dependent Hypertension. *Hypertension*. 2015;66:1023-1033. doi:10.1161/HYPERTENSIONAHA.115.05779

41. Dos Passos RR, Santos CV, Priviero F, et al. Immunomodulatory Activity of Cytokines in Hypertension: A Vascular Perspective. *Hypertension*. 2024;81:1411-1423. doi:10.1161/HYPERTENSIONAHA.124.21712

42. Sprague AH, Khalil RA. Inflammatory cytokines in vascular dysfunction and vascular disease. *Biochemical Pharmacology*. 2009;78:539-552. doi:10.1016/j.bcp.2009.04.029

43. Zhang C. The role of inflammatory cytokines in endothelial dysfunction. *Basic Res Cardiol*. 2008;103:398-406. doi:10.1007/s00395-008-0733-0

44. Jordan S, Tung N, Casanova-Acebes M, et al. Dietary Intake Regulates the Circulating Inflammatory Monocyte Pool. *Cell*. 2019;178:1102-1114.e17. doi:10.1016/j.cell.2019.07.050

45. Janssen H, Kahles F, Liu D, et al. Monocytes re-enter the bone marrow during fasting and alter the host response to infection. *Immunity*. 2023;56:783-796.e7. doi:10.1016/j.immuni.2023.01.024

46. Nagai M, Noguchi R, Takahashi D, et al. Fasting-Refeeding Impacts Immune Cell Dynamics and Mucosal Immune Responses. *Cell*. 2019;178:1072-1087.e14. doi:10.1016/j.cell.2019.07.047

47. Delconte RB, Owyong M, Santosa EK, et al. Fasting reshapes tissue-specific niches to improve NK cell-mediated anti-tumor immunity. *Immunity*. Published online June 2024:S1074761324002759. doi:10.1016/j.immuni.2024.05.021

48. Wang L, Cheng M, Wang Y, et al. Fasting-activated ventrolateral medulla neurons regulate T cell homing and suppress autoimmune disease in mice. *Nat Neurosci*. 2024;27:462-470. doi:10.1038/s41593-023-01543-w

49. Malinowski B, Zalewska K, Węsierska A, et al. Intermittent Fasting in Cardiovascular Disorders—An Overview. *Nutrients*. 2019;11:673. doi:10.3390/nu11030673

50. Torres-Peña JD, Arenas-de Larriva AP, Alcala-Diaz JF, Lopez-Miranda J, Delgado-Lista J. Different Dietary Approaches, Non-Alcoholic Fatty Liver Disease and Cardiovascular Disease: A Literature Review. *Nutrients*. 2023;15:1483. doi:10.3390/nu15061483

51. Mattson M, Wan R. Beneficial effects of intermittent fasting and caloric restriction on the cardiovascular and cerebrovascular systems. *The Journal of Nutritional Biochemistry*. 2005;16:129-137. doi:10.1016/j.jnutbio.2004.12.007

52. Mattson MP, Longo VD, Harvie M. Impact of intermittent fasting on health and disease processes. *Ageing Research Reviews*. 2017;39:46-58. doi:10.1016/j.arr.2016.10.005

53. Nicoll R, Henein M. Caloric Restriction and Its Effect on Blood Pressure, Heart Rate Variability and Arterial Stiffness and Dilatation: A Review of the Evidence. *IJMS*. 2018;19:751. doi:10.3390/ijms19030751

54. Sezen Y, Altiparmak IH, Erkus ME, et al. Effects of Ramadan fasting on body composition and arterial stiffness. *J Pak Med Assoc*. 2016;66:1522-1527.

55. Wilkinson IB, Mäki-Petäjä KM, Mitchell GF. Uses of Arterial Stiffness in Clinical Practice. *ATVB*. 2020;40:1063-1067. doi:10.1161/ATVBAHA.120.313130

56. Laurent S, Cockcroft J, Van Bortel L, et al. Expert consensus document on arterial stiffness: methodological issues and clinical applications. *European Heart Journal*. 2006;27:2588-2605. doi:10.1093/eurheartj/ehl254

57. Schwartz JE, Feig PU, Izzo JL. Pulse Wave Velocities Derived From Cuff Ambulatory Pulse Wave Analysis: Effects of Age and Systolic Blood Pressure. *Hypertension*. 2019;74:111-116. doi:10.1161/HYPERTENSIONAHA.119.12756

58. Del Giorno R, Troiani C, Gabutti S, Stefanelli K, Gabutti L. Comparing oscillometric and tonometric methods to assess pulse wave velocity: a population-based study. *Annals of Medicine*. 2021;53:1-16. doi:10.1080/07853890.2020.1794538

59. Tousoulis D, Kampoli AM, Tentolouris Nikolaos Papageorgiou C, Stefanadis C. The Role of Nitric Oxide on Endothelial Function. *CVP*. 2012;10:4-18. doi:10.2174/157016112798829760

60. Félétou M, Vanhoutte PM. Endothelium-Derived Hyperpolarizing Factor: Where Are We Now? *ATVB*. 2006;26:1215-1225. doi:10.1161/01.ATV.0000217611.81085.c5

61. Sobey CG. Potassium Channel Function in Vascular Disease. *ATVB*. 2001;21:28-38. doi:10.1161/01.ATV.21.1.28

62. Wilkinson IB, MacCallum H, Cockcroft JR, Webb DJ. Inhibition of basal nitric oxide synthesis increases aortic augmentation index and pulse wave velocity *in vivo*. *Brit J Clinical Pharma*. 2002;53:189-192. doi:10.1046/j.1365-2125.2002.1528adoc.x

63. Qiu H, Zhu Y, Sun Z, et al. Short Communication: Vascular Smooth Muscle Cell Stiffness As a Mechanism for Increased Aortic Stiffness With Aging. *Circulation Research*. 2010;107:615-619. doi:10.1161/CIRCRESAHA.110.221846

64. Lacolley P, Regnault V, Laurent S. Mechanisms of Arterial Stiffening: From Mechanotransduction to Epigenetics. *ATVB*. 2020;40:1055-1062. doi:10.1161/ATVBAHA.119.313129

65. Safar ME, Asmar R, Benetos A, et al. Interaction Between Hypertension and Arterial Stiffness: An Expert Reappraisal. *Hypertension*. 2018;72:796-805. doi:10.1161/HYPERTENSIONAHA.118.11212

66. Kim HL. Arterial stiffness and hypertension. *Clin Hypertens*. 2023;29:31. doi:10.1186/s40885-023-00258-1

67. Boutouyrie P, Chowienczyk P, Humphrey JD, Mitchell GF. Arterial Stiffness and Cardiovascular Risk in Hypertension. *Circ Res*. 2021;128:864-886. doi:10.1161/CIRCRESAHA.121.318061

68. Ait-Oufella H, Collin C, Bozec E, et al. Long-term reduction in aortic stiffness: a 5.3-year follow-up in routine clinical practice. *Journal of Hypertension*. 2010;28:2336-2341. doi:10.1097/HJH.0b013e32833da2b2

69. Butlin M, Tan I, Spronck B, Avolio AP. Measuring Arterial Stiffness in Animal Experimental Studies. *ATVB*. 2020;40:1068-1077. doi:10.1161/ATVBAHA.119.313861

70. Jaminon A, Reesink K, Kroon A, Schurgers L. The Role of Vascular Smooth Muscle Cells in Arterial Remodeling: Focus on Calcification-Related Processes. *IJMS*. 2019;20:5694. doi:10.3390/ijms20225694

71. Sutton EF, Beyl R, Early KS, Cefalu WT, Ravussin E, Peterson CM. Early Time-Restricted Feeding Improves Insulin Sensitivity, Blood Pressure, and Oxidative Stress Even without Weight Loss in Men with Prediabetes. *Cell Metabolism*. 2018;27:1212-1221.e3. doi:10.1016/j.cmet.2018.04.010

72. Martens CR, Rossman MJ, Mazzo MR, et al. Short-term time-restricted feeding is safe and feasible in non-obese healthy midlife and older adults. *GeroScience*. 2020;42:667-686. doi:10.1007/s11357-020-00156-6

73. Schafer MJ, Mazula DL, Brown AK, et al. Late-life time-restricted feeding and exercise differentially alter healthspan in obesity. *Aging Cell*. 2019;18:e12966. doi:10.1111/acel.12966

74. Deng G, Long Y, Yu YR, Li MR. Adiponectin directly improves endothelial dysfunction in obese rats through the AMPK–eNOS Pathway. *Int J Obes*. 2010;34:165-171. doi:10.1038/ijo.2009.205

75. Chen H, Montagnani M, Funahashi T, Shimomura I, Quon MJ. Adiponectin Stimulates Production of Nitric Oxide in Vascular Endothelial Cells. *Journal of Biological Chemistry*. 2003;278:45021-45026. doi:10.1074/jbc.M307878200

76. Ouchi N, Walsh K. Adiponectin as an anti-inflammatory factor. *Clinica Chimica Acta*. 2007;380:24-30. doi:10.1016/j.cca.2007.01.026

77. Gentile CL, Weir TL. The gut microbiota at the intersection of diet and human health. *Science*. 2018;362:776-780. doi:10.1126/science.aau5812

78. Battson ML, Lee DM, Jarrell DK, et al. Suppression of gut dysbiosis reverses Western diet-induced vascular dysfunction. *American Journal of Physiology-Endocrinology and Metabolism*. 2018;314:E468-E477. doi:10.1152/ajpendo.00187.2017

79. Trikha SRJ, Lee DM, Ecton KE, et al. Transplantation of an obesity-associated human gut microbiota to mice induces vascular dysfunction and glucose intolerance. *Gut Microbes*. 2021;13:1940791. doi:10.1080/19490976.2021.1940791

80. Ecton KE, Graham EL, Risk BD, et al. Toll-like receptor 4 deletion partially protects mice from high fat diet-induced arterial stiffness despite perturbation to the gut microbiota. *Front Microbiomes*. 2023;2:1095997. doi:10.3389/frmbi.2023.1095997

81. Shi H, Zhang B, Abo-Hamzy T, et al. Restructuring the Gut Microbiota by Intermittent Fasting Lowers Blood Pressure. *Circ Res*. 2021;128:1240-1254. doi:10.1161/CIRCRESAHA.120.318155

82. Theofilis P, Sagris M, Oikonomou E, et al. Inflammatory Mechanisms Contributing to Endothelial Dysfunction. *Biomedicines*. 2021;9:781. doi:10.3390/biomedicines9070781

83. Sproston NR, Ashworth JJ. Role of C-Reactive Protein at Sites of Inflammation and Infection. *Front Immunol*. 2018;9:754. doi:10.3389/fimmu.2018.00754

84. Zhang Z, Na H, Gan Q, et al. Monomeric C-reactive protein via endothelial CD31 for neurovascular inflammation in an ApoE genotype-dependent pattern: A risk factor for Alzheimer's disease? *Aging Cell*. 2021;20:e13501. doi:10.1111/acel.13501

85. Antoniades C, Bakogiannis C, Tousoulis D, Antonopoulos AS, Stefanadis C. The CD40/CD40 Ligand System. *Journal of the American College of Cardiology*. 2009;54:669-677. doi:10.1016/j.jacc.2009.03.076

86. Kida T, Tsubosaka Y, Hori M, Ozaki H, Murata T. Bile Acid Receptor TGR5 Agonism Induces NO Production and Reduces Monocyte Adhesion in Vascular Endothelial Cells. *ATVB*. 2013;33:1663-1669. doi:10.1161/ATVBAHA.113.301565

87. Forbes JD, Van Domselaar G, Bernstein CN. The Gut Microbiota in Immune-Mediated Inflammatory Diseases. *Front Microbiol*. 2016;7. doi:10.3389/fmicb.2016.01081

88. Moore JP, Vinh A, Tuck KL, et al. M2 macrophage accumulation in the aortic wall during angiotensin II infusion in mice is associated with fibrosis, elastin loss, and elevated blood pressure. *American Journal of Physiology-Heart and Circulatory Physiology*. 2015;309:H906-H917. doi:10.1152/ajpheart.00821.2014

89. Williams H, Mack CD, Li SCH, Fletcher JP, Medbury HJ. Nature versus Number: Monocytes in Cardiovascular Disease. *IJMS*. 2021;22:9119. doi:10.3390/ijms22179119

90. Trott DW, Machin DR, Phuong TTT, et al. T cells mediate cell non-autonomous arterial ageing in mice. *The Journal of Physiology*. 2021;599:3973-3991. doi:10.1113/JP281698

91. Lesniewski LA, Durrant JR, Connell ML, et al. Aerobic exercise reverses arterial inflammation with aging in mice. *American Journal of Physiology-Heart and Circulatory Physiology*. 2011;301:H1025-H1032. doi:10.1152/ajpheart.01276.2010

92. Kossmann S, Schwenk M, Hausding M, et al. Angiotensin II–Induced Vascular Dysfunction Depends on Interferon-γ–Driven Immune Cell Recruitment and Mutual Activation of Monocytes and NK-Cells. *ATVB*. 2013;33:1313-1319. doi:10.1161/ATVBAHA.113.301437

93. Frank JA, Kumagai LF, Dougherty TF. STUDIES ON THE RATES OF INVOLUTION AND RECONSTITUTION OF LYMPHATIC TISSUE [1]. *Endocrinology*. 1953;52:656-668. doi:10.1210/endo-52-6-656

94. Wing EJ, Magee DM, Barczynski LK. Acute starvation in mice reduces the number of T cells and suppresses the development of T-cell-mediated immunity. *Immunology*. 1988;63:677-682.

95. Yang J, Zhang L, Yu C, Yang XF, Wang H. Monocyte and macrophage differentiation: circulation inflammatory monocyte as biomarker for inflammatory diseases. *Biomark Res*. 2014;2:1. doi:10.1186/2050-7771-2-1

96. Ella K, Sűdy ÁR, Búr Z, et al. Time restricted feeding modifies leukocyte responsiveness and improves inflammation outcome. *Front Immunol*. 2022;13:924541. doi:10.3389/fimmu.2022.924541

97. Heyde A, Rohde D, McAlpine CS, et al. Increased stem cell proliferation in atherosclerosis accelerates clonal hematopoiesis. *Cell*. 2021;184:1348-1361.e22. doi:10.1016/j.cell.2021.01.049

98. Robbins CS, Chudnovskiy A, Rauch PJ, et al. Extramedullary Hematopoiesis Generates Ly-6C(high) Monocytes That Infiltrate Atherosclerotic Lesions. *Circulation*. 2012;125:364-374. doi:10.1161/CIRCULATIONAHA.111.061986

99. Tyrrell DJ, Wragg KM, Chen J, et al. Clonally expanded memory CD8+ T cells accumulate in atherosclerotic plaques and are pro-atherogenic in aged mice. *Nat Aging*. 2023;3:1576-1590. doi:10.1038/s43587-023-00515-w

100. Lim HY, Lim SY, Tan CK, et al. Hyaluronan Receptor LYVE-1-Expressing Macrophages Maintain Arterial Tone through Hyaluronan-Mediated Regulation of Smooth Muscle Cell Collagen. *Immunity*. 2018;49:326-341.e7. doi:10.1016/j.immuni.2018.06.008

CHAPTER 3: DIFFERENTIAL EFFECTS OF ACUTE VERSUS CHRONIC INTERMITTENT FASTING ON ARTERIAL STIFFNESS: THE POTENTIAL ROLE OF A NOVEL GUT-IMMUNE AXIS [2]

SUMMARY

Intermittent fasting (IF) is a popular dietary strategy and has been shown to improve cardiovascular health and alter the gut microbiota and immune system. However, it is unclear whether intermittent fasting affects arterial stiffness, a potential risk factor for cardiovascular disease, by influencing the gut microbiota and immune function. Furthermore, the effects of acute intermittent fasting (a single fasting-refeeding cycle) versus chronic intermittent fasting (once-weekly 24-hour intermittent fasting) remain largely unknown. In this study, we show that a single 24-hour fast acutely increased arterial stiffness for one day in lean mice (C57BL/6J) (431.7 ± 11.9 cm/sec vs. 508.5 ± 17.0 cm/sec, p=0.02) without any substantial changes to the gut microbiota or circulating cytokines. Arterial stiffness was unaltered in obese mice (B6.Cg-*Lep*^{ob}/J) throughout the single fasting-refeeding cycle. In contrast, compared to obese *ad libitum* mice, once-weekly 24-hour IF attenuated obesity-related arterial stiffness (47.8 ± 23.4 cm/sec vs. -21.6 ± 15.9 cm/sec, p=0.04) independent of body weight changes. De-stiffening persisted for at least five days after the last 24-hour fast, demonstrating the potential long-term effectiveness of intermittent fasting in enhancing vascular health. Mechanistically, we identified two novel gut microbe-immune interactions linked to obesity-related arterial stiffness and both were altered by IF. First, chronic IF decreased *Clostridia*_186 relative abundance, which corresponded with reduced circulating CCL2 and CXCL1 and perivascular adipose tissue lymphocyte accumulation. Second, chronic

[2] This research has been submitted to the journal *Arteriosclerosis, Thrombosis, and Vascular Biology*. To adhere to CSU Graduate School dissertation formatting, the following changes were made: 1) keywords and journal ending statements (i.e., funding, acknowledgments, nonstandard abbreviations and acronyms) are not displayed; 2) spacing has been adjusted to match CSU formatting. Citation information: **Graham EL**, Wrigley SD, Risk BD, Wei Y, Siebert JC, Zhang M, Dutt T, Tjalkens R, Rocha SM, Harris M, Poehlein L, Espinoza P, Bayer R, Hart R, Hinkle K, Gentile CL, Weir TL. Differential Effects of Acute Versus Chronic Intermittent Fasting on Arterial Stiffness: The Potential Role of a Novel Gut-Immune Axis

IF did not alter *Lachnospiraceae*_436 relative abundance in obese mice but abolished its positive relationships with CCL2, CXCL1, and arterial stiffness, indicating potential alterations in *Lachnospiraceae*_436 metabolite production. Overall, our results suggest that once-weekly 24-hour intermittent fasting attenuates obesity-related arterial stiffness, potentially by reducing components of an aberrant gut-immune-vascular axis.

INTRODUCTION

Cardiovascular disease (CVD) is the leading cause of death globally and has remained the leading cause of death in the United States for over a century[1]. Although there are numerous determinants of CVD, diet is a crucial modifiable risk factor [2]. Thus, easy-to-follow, cost-accessible dietary strategies are crucial for preventing and treating CVD.

Intermittent fasting (IF), repetitive periods of little-to-no energy intake (≤ 48 hrs)[3] followed by *ad libitum* eating, is currently one of the most popular dietary strategies globally [4,5]. IF's recent surge in popularity is due, in part, to an emphasis on when to eat, rather than what to eat, which may increase dietary compliance compared to other popular nutritional strategies [6]. Recently, IF has gained attention for its improvement of cardiovascular risk factors, including hypertension, hypercholesterolemia, and insulin resistance [7].

Stiffening of the large arteries (arterial stiffness) precedes overt CVD and is a strong independent risk factor of CVD onset and mortality [8,9]. Although few studies have investigated the effects of IF on arterial stiffness, we previously reported that the development of obesity-related arterial stiffness is strongly related to alterations in the gut microbiome. For example, antibiotic treatment ameliorated arterial stiffness and inflammation in a diet-induced obese mouse model [10] while transplantation of fecal microbiota from obese humans with elevated stiffness recapitulated arterial stiffness in gnotobiotic mice fed a standard, low-fat diet [11]. We have also shown that TLR4-deficient, high-fat-fed mice are partially protected from elevated arterial stiffness despite deleterious alterations in gut microbial composition and intestinal permeability [12]. These results indicate that gut-immune signaling has an important role in

regulating arterial stiffness. Given that IF has been shown to improve cardiovascular health and alter the gut microbiota and immune function[13,14] it is plausible that IF could improve arterial stiffness through similar mechanisms.

Another important consideration is whether the number of fasting bouts determines arterial de-stiffening. This is highlighted by the fact that arterial stiffness is regulated by acute factors such as blood pressure[15], nitric oxide signaling[16], and mechanotransduction [17,18], as well as chronic factors such as vascular wall remodeling and calcification [15,19–22]. Although our previous work demonstrates that the gut microbiota and inflammation regulate arterial stiffness chronically [10,23], even a single bout of fasting can impact gut microbial composition and inflammatory responses [24–29]. Thus, whether acute IF (a single fasting-refeeding cycle) and chronic IF (multi-week IF regimen) differentially impact arterial stiffness through distinct changes to the gut microbiota and immune system warrants further investigation.

Lastly, another fundamental question pertains to the durability of fasting-induced improvements post-refeeding. For example, most studies examining the health effects of fasting measure outcomes within 24 hours following the fasting session and in most cases, it is unclear if observed improvements persist beyond this period. Furthermore, whether persistence differs between a single bout of fasting and repeated bouts has not been examined. It is possible that a "training effect" occurs with repeated fasting and results in more prolonged benefits beyond the immediate refeeding, although this possibility has not been directly examined. Overall, these uncertainties underscore the need for further research regarding the persistence of fasting-induced health benefits.

To help answer these fundamental questions, we investigated the differential effects of a single fasting-refeeding cycle versus an 11-week once-weekly 24-hour IF protocol in mice with (obese; Ob) and without (lean; WT) elevated arterial stiffness. Our results indicate that a 24-hour fast differentially impacted arterial stiffness in lean and obese mice, yet these effects were short-lived and largely reverted after refeeding. The single fasting-refeeding cycle did not differentially impact the gut microbiota or splenocyte populations in lean or obese mice but slightly altered circulating cytokines in obese mice. Conversely, repeated bouts of once-weekly 24-hour IF attenuated arterial stiffness in obese mice, and

these improvements were independent of changes in body weight or food intake. Profound and persistent changes to the gut microbiota accompanied the arterial de-stiffening. Mechanistically, we observed that chronic IF diminished interactions between distinct gut microbial taxa and chemokines in obese mice, leading to reduced perivascular adipose tissue lymphocyte accumulation and arterial de-stiffening. IF also increased microbial butyrate production, which can impact gut barrier function and reduce inflammation. Taken together, these findings reveal that gut-immune interactions can be altered via chronic IF to attenuate obesity-related arterial stiffness.

METHODS

Data Availability

The authors declare that all supporting data and study materials are available within the article, in the supplemental material, or from the corresponding author upon reasonable request. All 16s rRNA sequencing data and related metadata findings reported in this manuscript are deposited in the Qiita (qiita.ucsd.edu) public repository (Study ID: 15617).

Animals, Experimental Design, and Euthanasia Procedures

All animal procedures were reviewed and approved by the Colorado State University Institutional Animal Care and Use Committee (protocol 1369).

Single Fasting-Feeding Cycle

5-week old lean (C57BL/6J; WT; n=28) and genetically obese (B6.Cg-*Lep*^{ob}/J; Ob; n=28) mice were obtained from Jackson Laboratories (Bar Harbor, ME). Mice were co-housed in a conventional facility under a 12:12 hour light/dark photocycle with access to standard rodent chow (Envigo 2918; irradiated diet consisting of 44.2% carbohydrates, 6.2% fat, and 18.6% protein) and normal drinking water. Mice were acclimated for two weeks with *ad libitum* chow and water. To examine the durability of IF effects, 6-8 mice per genotype were randomized into one of four groups such that terminal data were collected during either *ad libitum* feeding (AL) immediately after a 24-hour fast (Fast), one day after refeeding (Refeed(Day)), or

one week after refeeding (Refeed(Week)). Thus, this experimental design yielded 8 distinct groups: WT+AL, WT+Fast, WT+Refeed(Day), WT+Refeed(Week), Ob+AL, Ob+Fast, Ob+Refeed(Day), and Ob+Refeed(Week). On the day of euthanasia, body weight and food intake were obtained, glucose and ketones were measured via tail vein blood, mice were subjected to Doppler ultrasound to measure pulse wave velocity, feces were collected, and mice were immediately anesthetized with isoflurane and euthanized by exsanguination via cardiac puncture. Blood was collected in a 1 mL syringe coated with 0.5 M EDTA (no. 15575020; Invitrogen) and then placed into BD Microtainer™ Capillary Blood Collectors (BD365974). Plasma was obtained by centrifugation at 2,000 g for 10 min at 4°C. The plasma was immediately flash-frozen in liquid nitrogen and stored at -80°C until downstream analyses. The spleen was excised, weighed, and placed into cold Corning™ RPMI 1640 Medium 1X without L-Glutamine (MT15040CV) and kept on ice until downstream processing. Any other collected tissues were weighed, immediately snap-frozen in liquid nitrogen, and stored at -80°C until downstream processing.

Long-Term Intermittent Fasting Protocol

Another cohort of 5-week-old lean (C57BL/6J; WT; n=24) and genetically obese (B6.Cg-*Lep*^{ob}/J; Ob; n=24) mice were obtained from Jackson Laboratories (Bar Harbor, ME) and subjected to an identical acclimation protocol as described above. After acclimation, 12 mice per genotype were randomized into two groups to follow an *ad libitum* (AL) diet or a once-weekly 24-hour intermittent fast (IF). Thus, this experimental design yielded four distinct groups: WT+AL, WT+IF, Ob+AL, and Ob+IF. Body weight and food intake were measured weekly during cage and water changes. Pulse wave velocity was measured at weeks 1, 5-6, and 9 of the dietary protocol, and glucose homeostasis via an intraperitoneal glucose tolerance test (ipGTT; GTT) was conducted at week 10 of the protocol. Feces were collected at week eight and at termination (week 11). On the day of euthanasia, body weight, food intake, and feces were collected, and mice were anesthetized with isoflurane and euthanized by exsanguination via cardiac puncture. Blood, spleen, and other tissues were collected and processed identically to the acute fasting-refeeding cycle protocol. A small portion of the thoracic aorta and the small intestine was placed into cassettes and fixed

with 10% neutral buffered formalin until downstream histological analyses. To address the durability of IF effects, all *in vivo* and euthanasia measurements were taken at least 24 hours (1-4 days) after the refeeding period.

To enhance rigor, an additional validation cohort of 5-week-old lean (C57BL/6J; WT; n=9) and genetically obese (B6.Cg-Lepob/J; Ob; n=18) mice were obtained from Jackson Laboratories (Bar Harbor, ME) and subjected to an identical acclimation period as reported above. After acclimation, all WT mice were placed on an *ad libitum* (AL) diet. Ob mice were randomized to either an *ad libitum* (AL) diet or once-weekly 24-hour intermittent fasting (IF). Thus, this experimental design yielded three distinct groups: WT+AL, Ob+AL, and Ob+IF. Body weight and food intake were measured weekly during cage and water changes. Pulse wave velocity was measured at week 10, 4-5 days following the last 24-hour fasting bout.

Measurement of Arterial Stiffness

Aortic pulse wave velocity (PWV) was used to determine in vivo arterial stiffness using a Doppler Flow Velocity System (Indus Instruments, Webster, TX) via methods described previously by our laboratory[10,11,30]. PWV (in cm/s) was calculated as PWV = (distance between the two probes)/($\Delta time_{abdominal\ aortal} - \Delta time_{carotid\ artery}$).

Glucose, Ketones, Glucose Tolerance Test, and Insulin ELISA

For mice subjected to the acute fasting-refeeding protocol, glucose and ketones (beta-hydroxybutyrate; BHB) were measured using tail vein blood, an AlphaTRAK 2 glucometer (Abbott Laboratories, Chicago, IL), and Nova Max Plus Glucose and Ketone Meter (ADW Diabetes, Pompano Beach, FL), respectively. For mice subjected to the 11-week intermittent fasting protocol, glucose homeostasis was determined at week ten via an intraperitoneal glucose tolerance test and insulin ELISA, as previously described[12]. Briefly, following a six-hour fast, mice received an intraperitoneal injection of 2g/kg dextrose, and blood glucose was assessed at 0-, 15-, 30-, 45-, 60-, 90-, and 120-minutes post-injection using tail-vein blood and an AlphaTRAK 2 glucometer. Fasting blood was spun at 2,000 g for 10 min at

4°C, and the resultant serum was used to measure insulin levels via ELISA (Ultra-Sensitive Mouse Insulin ELISA Kit, 90080).

Stool Sample Collection, Processing, and Analyses of 16s rRNA Amplicon Sequencing Data

Stool samples from all mice were collected fresh, immediately placed on ice, and then stored at -80°C until DNA extraction. Fecal DNA extraction was completed using the FastDNA® Kit (MP Biomedicals, 116540400) per manufacturer protocol. Quantitative PCR was used to quantify total fecal 16srRNA DNA. Reactions were optimized for the 16s rRNA gene using universal bacterial primers (forward 5′-AAACTCAAAKGAATTGACGG-3′, reverse 5′-CTCACRRCACGAGCTGAC-3′). Cycling conditions using the Bio-Rad C1000 Touch thermal cycler were as follows: 95°C for 3 min and then 40 cycles of 95°C 15 s, 61°C 15 s, 72°C 10 s, 85°C 5 s followed by fluorescence detection. To calculate total fecal 16srRNA DNA, quantified amounts (ng) of 16s rRNA amplicons generated from DNA obtained from pooled fecal samples from experimental mice were serially diluted to create standard curves.

Amplification of the V4 region of the 16S rRNA gene was carried out following the Earth Microbiome Project protocol using the 515F-806R primer set [31] containing a unique 12bp error-correcting barcode included on the forward primer. Cycling and sequencing conditions were carried out as previously described[30]. DNA extraction controls, no template PCR controls, and the Zymo mock community (Zymo Research, D6305) were included on each sequencing plate. Sequence reads were imported into QIIME2 (version 2023.5) for quality filtering[32]. Briefly, sequence reads were demultiplexed and examined for quality filtering utilizing a Phred score cutoff of 30. Upon examination of the demultiplexed data, the reverse reads did not meet the quality filtering parameter, and analyses proceeded with single-end forward read sequences. In both studies, 12 base pairs were trimmed off the 5' end. Sequences from the acute fasting-refeeding cycle were truncated to 250 base pairs, while sequences from the 11-week IF study were truncated to 234 base pairs. All reads were binned into sub-OTUs (sOTUs) using the Deblur pipeline implementation in QIIME2[33]. Taxonomic assignments were made using Silva (version 13.8) [34]. Samples with low reads or

suspected contamination were removed, and mitochondrial and chloroplast sequences were filtered from the remaining samples.

The resulting feature tables and taxonomy files were combined and imported with corresponding metadata into MicrobiomeAnalyst for secondary workflow [35]. Based on sample prevalence, the minimum count filter was set at 4, and the low count filter was set at 10%. Data normalization was performed based on total sum scaling. Alpha diversity was examined utilizing the Shannon diversity index at the genus taxonomic level, and beta diversity was calculated using Bray-Curtis distances at the genus taxonomic level.

Gut microbial relative abundance data from Ob+AL and Ob+IF mice (11-week IF protocol) were used in a subsequent mediation analysis. This determined whether plasma chemokines (see methods below) mediate the relationship between microbial relative abundances and arterial stiffness in obese mice. Our mediation analysis steps are adapted from Tingley et al.[36] and utilize the "mediation" package available in Rstudio. Coefficient estimates, 95% confidence intervals, and p-values of the total, direct, and indirect effects were calculated by nonparametric bootstrapping (1,000 simulations) using the percentile method. P-values of the indirect effects (mediator) are reported in the supplementary.

Plasma Cytokine and Chemokine Immunoassays

Multiplex immunoassay panels were used to detect plasma cytokine/chemokine levels. The ProcartaPlex Mouse Cytokine & Chemokine Panel 1 26plex (EPX260-26088-901) and the ProcartaPlex Mouse Chemokine Panel 1 9plex (EPX090-20821-901) were used on the acute fasting-refeeding cycle and 11-week intermittent fasting plasma samples, respectively, as per the manufacturer's instructions. Only analytes with a signal over the detection limit were included in the analyses. To quantify CXCL1 and CCL2 levels in the colon and liver, we used the Mouse CXCL1 (KC) ELISA Kit (EMCXCL1) and the Mouse CCL2/MCP1 ELISA Kit (NBP1-92659), respectively, as per the manufacturer's instructions. Colon and liver samples were homogenized 1:10 (weight (mg): volume (uL)) using the NAVY bead lysis kit (NC0520622), a bullet blender (Next Advance, Averill Park, NY), and ice-cold Cell Extraction Buffer (FNN0011) supplemented with 1mM PMSF and 50 uL of Halt Protease Inhibitor Cocktail per 5

mL of Cell Extraction Buffer. In the ELISA wells, liver homogenates were further diluted to a final dilution of 1:20.

Adipose Tissue *Ccl2* Gene Expression

Total RNA was isolated from epididymal, mesenteric, and subcutaneous adipose tissue using the RNeasy® Mini Kit as per the manufacturer's instructions. For real-time PCR, reverse transcription was performed using iScript™ Reverse Transcription Supermix. PCR reactions were performed in 96-well plates using transcribed cDNA and SsoAdvanced Universal SYBR Green Supermix**.** Primers utilized were *Ccl2* (forward 5′-CTCACCTGCTGCTACTCATTC -3′, reverse 5′ TGGATCCACACCTTGCATTTA-3′), *Gapdh* (forward 5′-GTGAAGGTCGGTGTGAACGGATTT-3′, reverse 5′-TGGCAACAATCTCCACTTTGCCAC-3′), and *β_2-microglobulin* (B2M) (forward 5′-CGGTCGCTTCAGTCGTCAG-3′, reverse 5′-ATGTTCGGCTTCCCATTCTCC 3′). Cycling conditions using the Bio-Rad C1000 touch thermal cycler were as follows: 95°C for 3 min and then 40 cycles of 95°C 15 s, 58°C 30 s, 72°C 60 s followed by fluorescence detection. Fold changes were calculated as $2^{-\Delta\Delta Ct}$ compared to a normalization factor including both GAPDH and B2M[37] as reference genes. Ob+AL was used as the reference group.

Splenocyte Isolation and Flow Cytometry on Single Cell Suspensions

Spleens were homogenized using a syringe plunger and passed through a 70 μm filter to prepare a single-cell suspension. Erythrocytes were lysed using ACK Lysis Buffer (Fisher Scientific, A1049201). Cells were seeded into 96-well V-bottom plates, washed, and stained with Zombie NIR live/dead stain (BioLegend, 423105) for 15 minutes at room temperature in the dark. Cells were washed and incubated with Fc block solution (BioLegend, 101319) at 4°C for 20 min, protected from light, and then further stained with optimal titrations of specific surface antibodies at 4°C for 30 min, protected from light. The antibodies (catalog number regarding antibody clone, titration) used were as follows **(Table 3.S6)**: Brilliant Violet 570™ anti-mouse CD45 (103136, 1:200); PE anti-mouse CD335 (NKp46), (137604, 1:400); Alexa Fluor®

532 Anti-Mouse CD3 (58-0032-82, 1:100); Brilliant Violet 605™ anti-mouse CD19 (115539, 1:200); Pacific Blue™ anti-mouse/human CD11b (101224, 1:200); BD Horizon™ BV480 Rat Anti-Mouse I-A/I-E (566088, 1:600); Brilliant Violet 785™ anti-mouse CD11c (117335, 1:400); PerCP anti-mouse Ly-6G (127653, 1:100). All antibodies were ordered from BioLegend except I-A/I-E, which was ordered through BD Biosciences. After staining, cells were fixed with 4% paraformaldehyde (Fisher Scientific, J61899.AP) at room temperature for 20 min, protected from light. Cells were washed and left at 4°C overnight in FACS buffer (Fisher Scientific, 00-4222-26). Cell counts were acquired the following day using a Cytek® Aurora 4L flow cytometer, where 150,000-250,000 events were recorded. To calculate absolute cell counts, 25 uL of the single-cell suspensions were mixed with 25 uL CountBright™ Absolute Counting Beads (Fisher Scientific, C36950) and 200 uL of a live/dead solution (1:200 7AAD to FACS buffer), and 30,000-50,000 events were recorded on the cytometer. Splenocyte subpopulations were identified by a pre-determined gating strategy **(Figure 3.S8)** on Flowjo (version 10.9), and total cell counts per population were enumerated.

Aorta and Small Intestine Histology Processing and Analyses

Brightfield imaging was performed on hematoxylin and eosin (H&E) stained thoracic aorta sections with surrounding perivascular adipose tissue (previously fixed and paraffin-embedded). Cover slipped and mounted slides were loaded into a fully automated Olympus VS200 (Evident, Waltham, MA, USA) scanning microscope equipped with a Hamamatsu ORCA-Fusion camera (Hamamatsu Photonics, Shizuoka, Japan). For intima-media and total wall thickness, mounted slides were imaged at 200× resolution using an extended apochromat X-line 20× air (0.8 N.A.) objective at the Colorado State University Biological Imaging and Neuroanalysis (BIN) Core. For basophilic granulocytes and lymphocytes, mounted slides were imaged at 400× resolution using an extended apochromat X-line 40× air (0.95 N.A.) Scanning parameters (including binning, lamp intensity, and exposure time) were curated and validated per stain type by a single-trained microscopist and held constant for all sample imaging. All images were collected with Olympus ASW software (V3.4.1). Quantification of intima-media and total wall thickness were determined through algorithmic neural network curation, optimization, and validation at the Colorado State University

BIN Core utilizing VisioPharm artificial intelligence modules (2023.09.3.15043). Lymphocytes (predominantly T and B cells) training labels were based off standard lymphocyte identification parameters including small size, round to slightly oval nucleus with dense chromatin, and small cytoplasmic area. Basophilic granulocytes training labels were based on round to oval shaped nuclei with cytoplasm containing abundant hematoxylin rich granules. As with thickness measurements, quantification of lymphocytes and basophilic granulocytes were identified via algorithmic neural network curation, optimization, and validation at the Colorado State University BIN Core utilizing VisioPharm artificial intelligence modules (2023.09.3.15043). A single non-biased trained analyst generated all neural network training labels spanning H&E. Specific anatomical demarcations were subsequently validated by a board-certified veterinary pathologist.

Spiraled, fixed, and paraffin-embedded small intestine sections were stained with hematoxylin and eosin (H&E) following deparaffinization and rehydration with xylene and graded ethanol (xylene, 100% EtOH, 95% EtOH, 80% EtOH, 50% EtOH, 1X PBS). Slides were scanned at 20X on a Vectra Polaris scanning microscope. The images were imported into VisioPharm (version 2023.09.3.15043 x64) and processed through an artificial intelligence (AI) workflow to isolate intestinal mucosa and quantitative assessment of villous height, crypt depth, and villous-to-crypt ratio. AI quantification was performed on intestinal regions with representative villi in the longitudinal section and not regions with villi in the cross-section. Output measurements were a micrometer average of villous and crypt lengths (i.e., villous height and crypt depth) based on the long axis of each structure.

Visualization Of LineAr Regression Elements (VOLARE) Pipeline

Single Fasting-Refeeding Cycle

To uncover relationships between mouse physiological parameters, gut microbial composition, and the immune system during a single fasting-refeeding cycle in lean and obese mice, we leveraged the Visualization Of LineAr Regression Elements (VOLARE) pipeline[38]. Briefly, metadata files were created from collected data, and the metadata were then separated into three categories/bins. The first bin was

defined as “Clinical Data” corresponding to physiological parameters (plasma glucose, plasma ketone, cecum weight, cecum length, spleen weight, and pulse wave velocity measurements). The second bin was defined as “Microbes” and corresponded to feature relative abundance data derived from 16s rRNA sequencing. The third bin was defined as “Splenocyte and Plasma Cytokines” which included the splenocyte flow cytometry and the plasma cytokine/chemokines multiplex data. Individual outcome measures within these bins are referred to as analytes. Pairwise linear regressions (comparing any two analytes within or between bins) were fit within each genotype (WT, Ob) and intervention (AL, Fast, Refeed(Day), Refeed(Week)). The results were visualized and summarized in a top table. The top tables for lean and obese mice only reported pairwise linear regression models that passed the following thresholds: an adjusted r-squared (adjRsq) > 0.35, at least one slope p-value (Pslope) < 0.05, a maximum influential observation (maxInfluence) < 2, and a maximum absolute skew < 3. Slope semantics were defined using default regression coefficients semantics. Results from the VOLARE pipeline were analyzed in Rstudio.

11-Week Intermittent Fasting Protocol

Metadata files were created from data collected from Ob+AL and Ob+IF mice, and the metadata were then separated into three categories/bins. The first bin was defined as “PWV Data” corresponding to a week 1-9 change in pulse wave velocity or week 9 PWV values. The second analyte bin was described as “Microbes” and corresponded to feature relative abundance data derived from 16s rRNA sequencing. The third analyte bin was defined as “Plasma Chemokines,” which included the plasma chemokine multiplex data derived from multiplex immunoassays. Pairwise linear regressions (comparing any two analytes within or between analyte bins) were fit. The results were visualized and summarized in a top table. The top table only reported pairwise linear regression models that passed the following thresholds: an adjusted r-squared (adjRsq) > 0.20, F-statistic p-value (pF) < 0.05, a maximum influential observation (maxInfluence) < 2, and a maximum absolute skew < 3. Slope semantics were defined using default regression coefficients semantics. Results from the VOLARE pipeline were analyzed in Rstudio.

Cecal Content Short Chain Fatty Acid Processing, Acquisition, and Analysis

Short chain fatty acid (SCFA) analyses were carried out as previously described [39]. In brief, 0.34 mL of cold 3 M HCl and 0.06 mL of internal standard solution containing 1 mg/mL of 13C2-sodium acetate and 0.1 mg/mL of 13C4-sodium butyrate in water were added to ~20 mg of frozen cecal samples. Samples were vigorously shaken for 15 min at 4°C, followed by sonication for 10 min in a cold water bath, and then shaken for another 15 min at 4°C and centrifuged at 15,000 g for 15 min at 4°C. Supernatants (200 µL) were recovered, and added to 350 µL cold methyl tert-butyl ether (MTBE), followed by vortexing for 3 s x 10 times. About 80 µL of the top MTBE layer were recovered after centrifugation at 3,000 g for 5 min at 4°C, and stored at -20°C until analysis.

The MTBE extract (1 µL) of SCFAs were injected into a Trace 1310 GC coupled to a Thermo ISQ-LT MS, at a 5:1 split ratio. The inlet was held at 240°C. SCFA separation was achieved on a 30m DB-WAXUI column (J&W, 0.25 mm ID, 0.25 µm film thickness). Oven temperature was held at 100°C for 0.5 min, ramped at 10°C/min to 175°C, then ramped to 240°C at 40°C/min, and held at 240°C for 3 min. Helium carrier gas flow was held at 1.2 mL/min. Temperatures of transfer line and ion source were both held at 250°C. SIM mode was used to scan ions 45, 60, 62, 73, 74, 88 at a rate of 10 scans/sec under electron impact mode. The injection order of samples was again randomized. QC samples were analyzed after every 6 samples. The calibration curve was acquired at the end of the sequence. GC-MS data was processed using Chromeleon 7.2.10 software (Thermo Scientific). Peak areas were extracted for target compounds detected in biological samples and normalized to the peak area of the appropriate internal standard or surrogate in each sample. To calculate SCFA concentrations from peak area, known concentrations of acetic acid, propionic acid, and butyric acid were serially diluted to create standard curves.

Statistical Analyses

Data are presented as either mean ± standard error of the mean (SEM), mean with individual values (scatterpoints), or the log2 fold change between groups. Data analyses and visualizations were conducted in GraphPad Prism (version 9) or Rstudio (2024.04.1+748) using the ggplot2 package. Student's unpaired

t-tests were used to analyze differences between two groups. If applicable, one-way ANOVAs followed by Tukey's multiple comparisons test were used to examine differences between more than two groups. If the data violated the assumption of homoscedasticity, a Welch ANOVA followed by Dunnett's T3 multiple comparisons test was used instead of the one-way ANOVA. Two-way ANOVAs (Type II SS's) followed by Tukey's multiple comparisons test were used to analyze interactions between genotype and intervention. Mixed effect linear regression models with a Kenward-Roger's degrees of freedom approximation and Type II analyses of variance table output were used for repeated measures data. In these models, group and time points were fixed effects, and individual mouse ID was the random effect. If data were heteroscedastic, robust standard errors were used for the two-way ANOVAs or mixed effect models. For gut microbiota data, alpha diversity was analyzed using the nonparametric Kruskal-Wallis test or mixed effect models. Beta diversity was analyzed using permutational multivariate analysis of variance (PERMANOVA). Differences in microbial features between Ob+AL and Ob+IF mice were examined via a consensus analysis, which included Mann-Whitney (FDR adjusted p-value=0.05), negative binomial (EdgeR, FDR adjusted p-value=0.05), and linear discriminant analysis effect size (LEfSe, FDR adjusted p-value=0.1, fold change cutoff=2.0) tests. A p-value ≤ 0.05 was considered statistically significant unless otherwise indicated.

RESULTS

A Single 24-Hour Fast Acutely Increased Arterial Stiffness in Lean Mice

We first investigated the impact of a single fasting-refeeding cycle on body weight, food intake, glucose and ketone homeostasis, and arterial stiffness in lean and obese mice. The experimental design for the single fasting-refeeding cycle is presented in **Figure 3.1A**. Changes in body weight over the acute fasting-refeeding cycle did not differ between WT and Ob mice ($p_{interaction}=0.54$) **(Figure 3.1B)**. However, further analyses stratified by genotype revealed that WT mice lost weight during the 24-hour fast (22.8 ±0.3 g vs. 20.2 ± 0.9, $p<0.01$) and rebounded after 24 hours of refeeding (22.8 ± 0.3 g vs. 23.8 ± 0.5 g, $p=0.34$). Obese mice lost ~3 grams during the 24-hour fast, (statistically insignificant) (37.1 ± 0.9 g vs. 34.0 ± 1.1, $p=0.17$) and rebounded after 24 hours of refeeding (37.1 ± 0.9 g vs. 36.4 ± 1.0, $p=0.96$)

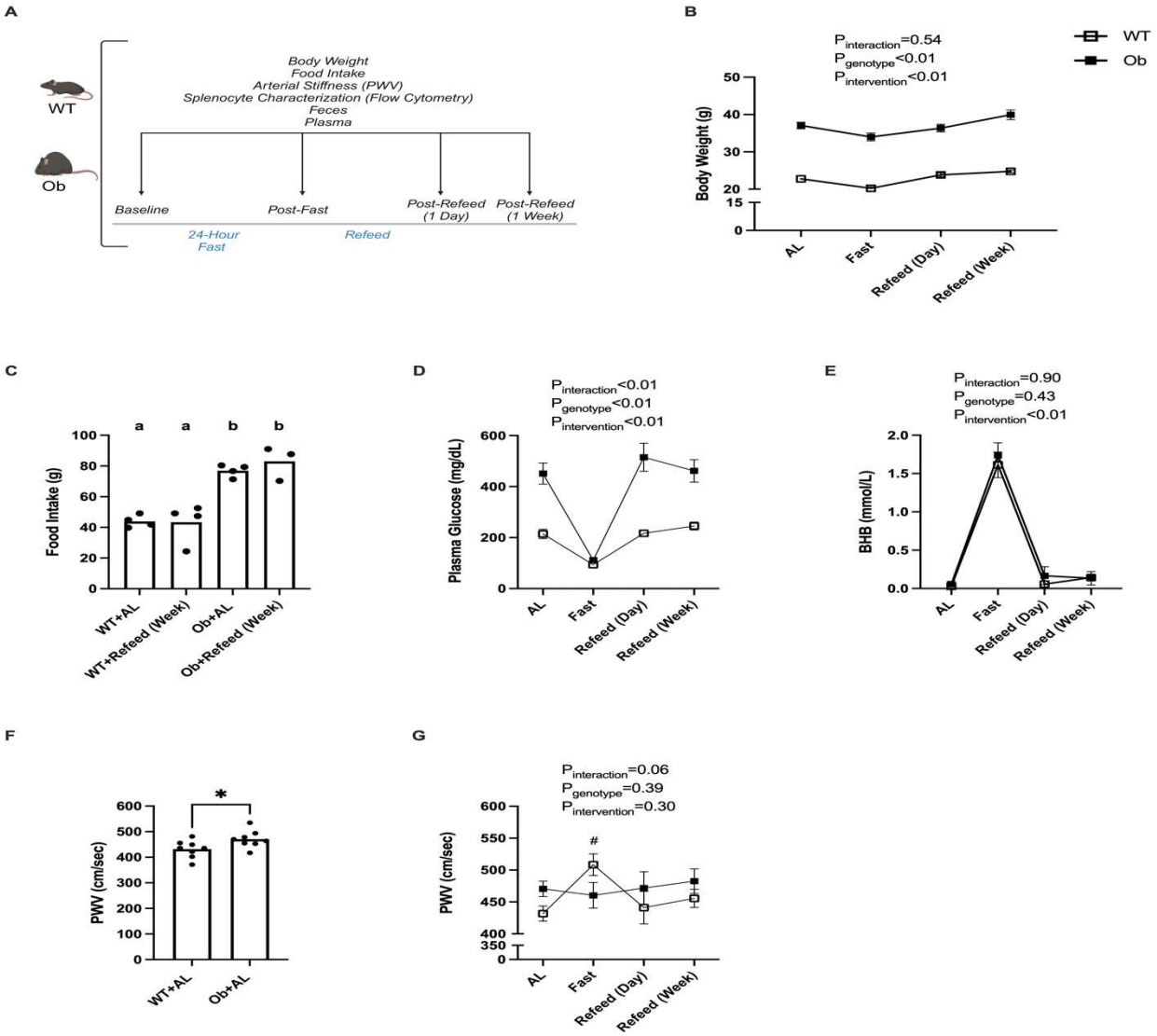

Figure 3.1. A single fasting-refeeding cycle transiently impacted physiological parameters in lean and obese mice. A) Schematic of experimental design. Created at Biorender.com. **B)** Changes in body weight in lean and obese mice. N=6-8 mice per group. **C)** Food intake between *ad libitum* and one-week post-refeed time points. N=3-4 cages per group. **D-E)** Changes in plasma glucose **D)** and plasma beta-hydroxybutyrate **E)** in lean and obese mice. N=6-8 mice per group. **F)** Pulse wave velocity in *ad libitum* lean and obese mice. N=8 mice per group. **G)** Changes in pulse wave velocity in lean and obese mice. N=6-8 mice per group. WT=lean; Ob=obese; AL=*ad libitum* fed; Fast=fasted for 24 hours; Refeed(Day)=mice that were fasted for 24 hours then refed for 24 hours; Refeed(Week)=mice that were fasted for 24 hours then refed for one week; PWV=pulse wave velocity; BHB= plasma beta-hydroxybutyrate. Different letters indicate significant differences between groups. *indicates a p-value less than 0.05. # indicates a p-value less than 0.05 between WT+AL vs WT+Fast.

(**Figure 3.1B**). The single fasting-refeeding cycle did not affect total weekly food intake **(Figure 3.1C)**, thus reducing the potential confound of altered caloric intake on other outcome variables. Plasma glucose was reduced in both WT (214.5 ± 17.9 mg/dL vs. 94.0 ± 3.5 mg/dL, $p<0.01$) and Ob mice (451.0 ± 41.7 mg/dL vs. 111.4 ± 8.8 mg/dL, $p<0.01$) **(Figure 3.1D)**. These reductions occurred in tandem with increases in plasma ketones (BHB) regardless of genotype ($p<0.01$) **(Figure 3.1E)**. As we've previously observed [23], Ob+AL mice displayed significantly higher PWV than WT+AL mice at baseline (470.7 ± 12 cm/sec vs. 431.7 ± 12.0 cm/sec, $p=0.04$) **(Figure 3.1F)**, which validated our use of a genetically obese mouse as a model of obesity-related arterial stiffness. Surprisingly, WT mice experienced a significant increase in PWV after the 24-hour fast (431.7 ± 11.9 cm/sec vs. 508.5 ± 17.0 cm/sec, $p=0.02$) but quickly reverted to baseline values just 24 hours after refeeding (431.7 ± 11.9 cm/sec vs 441.0 ± 25.6 cm/sec, $p=0.98$) and remained stable one week after the refeed (431.7 ± 11.9 cm/sec vs 455.6 ± 14.3 cm/sec, $p=0.77$). In contrast, acute IF did not affect PWV in Ob mice (**Figure 3.1G, Table 3.S1)**. Although interesting, this acute rise in PWV was only temporary and unlikely to impact long-term vascular health.

The Observed Effects of a Single Fasting-Refeeding Cycle Are Transient

Changes to gut microbial composition, the immune system (circulating cytokines levels and splenocyte counts), and VOLARE relationships during the acute fasting-refeeding cycle are detailed in the supplemental results as well as in **Figures 3.S1-3.S3**. Briefly, the fasting-refeeding cycle did not impact the gut microbiota in lean or obese mice **(Figure 3.S1)**. The fasting-refeeding cycle differentially impacted CCL4, IL-12, and CXCL1 in Ob mice compared to lean mice. Specifically, in obese mice, CCL4 and IL-12 remained elevated even after a week of refeeding, while CXCL1 was acutely increased after the 24-hour fast but rebounded to normal levels upon refeeding. Concentrations for all three of these cytokines remained stable throughout the fasting-refeeding cycle in WT mice **(Figure 3.S2)**.

After adjusting for genotype, spleen T cells, B cells, natural killer (NK) cells, neutrophils, and other innate immune populations with varying expression of CD11b/CD11c/MHCII were significantly reduced following the 24-hour refeed. These reductions were mostly temporary, as most splenocyte

populations (except for neutrophils and $CD11b^+$ $MHCII^+$ $CD11c^+$ cells) reverted to values not significantly different from AL controls after a week of refeeding **(Figure 3.S3)**. A similar phenomenon in spleen T cells was shown by Wing et al. [40].

Finally, we leveraged the VOLARE pipeline to observe whether the acute fasting-refeeding cycle differentially impacted linear relationships between any two analytes within the "Clinical Data", "Microbes", and/or "Splenocyte and Plasma Cytokines" bins (VOLARE section in Methods section for further clarification on bins and analytes). This analysis revealed that 24-hour fasting altered several analyte relationships in both WT and Ob mice, yet most of these relationships (83% in WT mice and 63% in Ob mice) reverted to baseline after 24 hours of *ad libitum* feeding. Overall, these data suggest that most physiological alterations from a single fasting-refeeding cycle are likely short-lived.

11 Weeks of Once-Weekly 24-hour Intermittent Fasting Reduced Arterial Stiffness in Obese Mice

Long-term IF protocols improve cardiometabolic health; therefore, we postulated that although a single bout of 24-hour fasting had little sustained effect on arterial stiffness, repeated 24-hour fasting **(Figure 3.2A)** might elicit more meaningful changes. Throughout the 11-week protocol, no changes in body weight were observed in WT mice. Although body weight was reduced in Ob+IF mice compared to Ob+AL at weeks 5, 6,10, and 11 (at the beginning of the week and at termination) **(Figure 3.2B, Table 3.S2)**, AUC analyses revealed that weight gain was relatively stable in Ob mice throughout the 11 weeks (739.4 ± 9.9 vs. 708.4 ± 10.6 g, p=0.17). **(Figure 3.2B)**. 10-week food intake was not significantly different between AL and IF groups, regardless of genotype **(Figure 3.2C)**.

At week 10, baseline fasting glucose levels were significantly lower in Ob+IF mice than Ob+AL mice (193.2 ± 6.6 mg/dL vs. 154.7 ± 16.2 mg/dL, p=0.03). IF enhanced glucose tolerance in WT mice (GTT AUC: (3166.0 ± 154.7 vs. 2299.0 ± 101.4, p<0.01) and in Ob mice so that GTT AUC was not significantly different from WT+AL mice (3166.0 ± 154.7 vs. 3943.0 ± 232.4, p=0.07) or Ob+AL mice (4390.0 ± 128.7 vs. vs. 3943.0 ± 232.4, p=0.47) **(Figure 3.2D)**. Plasma insulin levels were unchanged

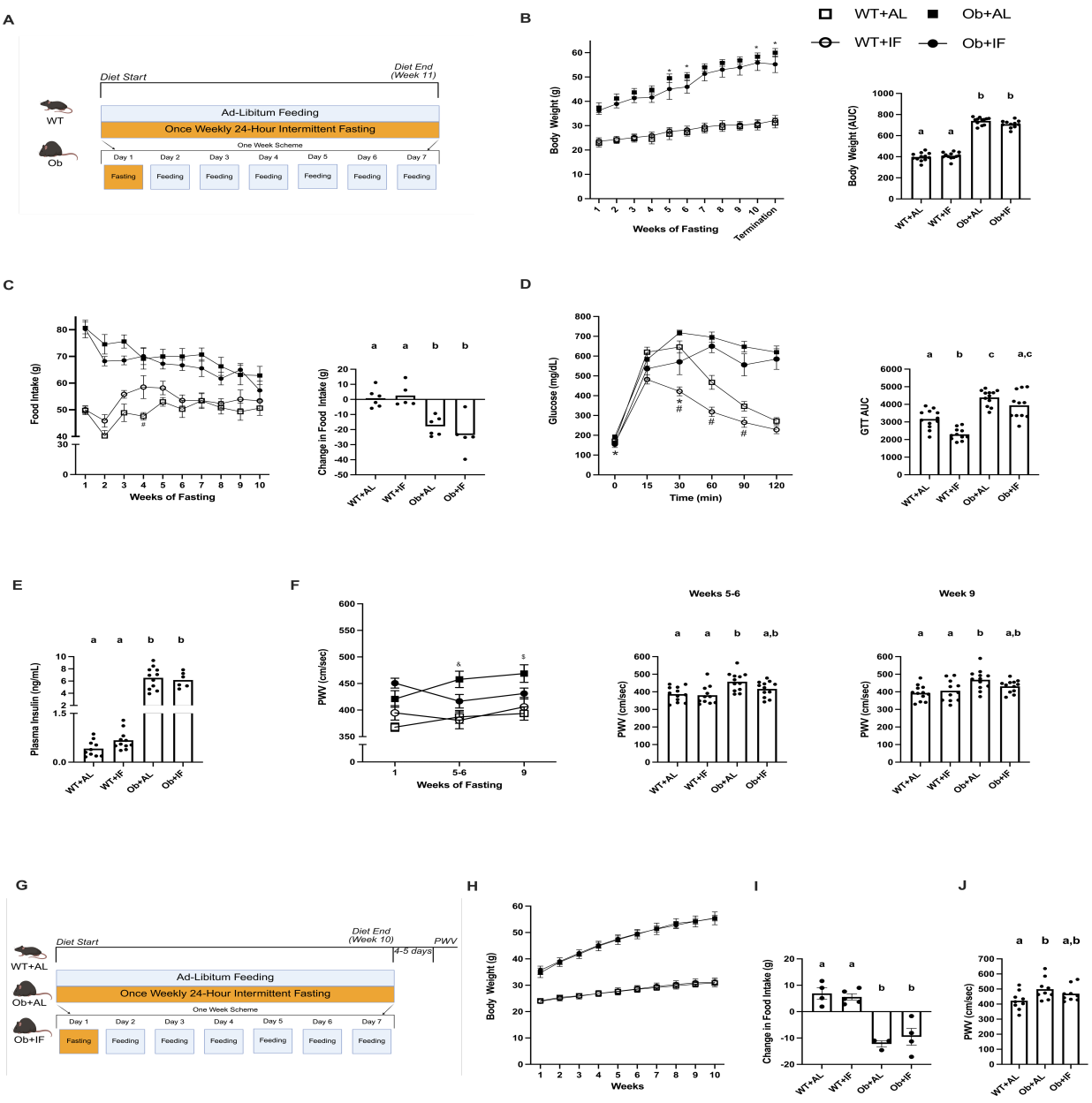

Figure 3.2. Once-weekly 24-hour intermittent fasting attenuated arterial stiffness in obese mice. A) Schematic of experimental design for cohort 1. Created at Biorender.com. **B)** Changes in body weight. N=11-12 mice per group per week. **C)** Changes in food intake. N=4-6 cages per group per week. **D)** Changes in plasma glucose during intraperitoneal glucose tolerance test at week 10. N=11-12 mice per group per time point. **E)** Differences in plasma insulin levels between groups. Blood for plasma insulin was taken immediately before glucose tolerance test. N=6-11 mice per group. **F)** Changes in pulse wave velocity. N=11-12 mice per group per week. **G)** Schematic of experimental design for cohort 2. Created at Biorender.com. **H)** Changes in body weight. N=9-10 mice per group per week. **I)** Changes in food intake. N=3-5 cages per group. **J)** Changes in pulse wave velocity at week 10. N=9 mice per group. WT=lean; Ob=obese; AL=*ad libitum* feeding; IF=once-weekly 24-hour intermittent fasting; PWV=pulse wave velocity; AUC=area under the curve. Different letters indicate significant differences between groups.* indicates a p-value less than 0.05 between Ob+AL vs Ob+IF. $^{\#}$ indicates a p-value less than 0.05 between WT+AL vs WT+IF. $^{\&}$ indicates a p-value of 0.08 in Ob+AL mice between week 1 and week 5-6. $^{\$}$ indicates a p-value less than 0.05 in Ob+AL mice between week 1 and week 9.

between IF and AL groups within each genotype, suggesting that IF improved insulin sensitivity in WT and Ob mice **(Figure 3.2E)**.

Throughout IF, PWV measures were stable in WT+AL and WT+IF mice. In contrast, PWV continued to rise in Ob+AL mice throughout the experiment (week 1 vs weeks 5-6: 420.9 ± 15.6 cm/sec vs. 457.8 ± 15.4 cm/sec, p=0.08) (week 1 vs. week 9: 420.9 ± 15.6 cm/sec vs. 468.7 ± 16.6 cm/sec, p=0.02) and was consistently higher than WT+AL mice (week 1 p-value=0.04; weeks 5-6 p-value<0.01; week 9 p-value<0.01) **(Figure 3.2F).** However, this gradual elevation was not apparent in Ob+IF mice **(Figure 3.2F)**. Furthermore, compared to Ob+AL mice, change in PWV was significantly reduced in Ob+IF mice at weeks 5-6 (37.0 ± 15.7 cm/sec vs. -36.5 ± 20.0 cm/sec, p=0.02) and week 9 (47.8 ± 23.4 cm/sec vs. -21.6 ± 15.9 cm/sec, p=0.04). No differences in PWV changes were found between WT+AL and WT+IF mice throughout the protocol **(Figure 3.2F)**. Furthermore, the reductions in PWV occurred independent of any structural changes to the aorta, as no differences in wall thickness and intima-media thickness were seen between the groups **(Figure 3.S4E)**. Since pulse wave velocity was always measured at least 24 hours (1-4 days) after *ad libitum* refeeding, these results highlight the potential durability of IF to reduce arterial stiffness.

Since we observed week-dependent changes in body weight in Ob+IF mice, we next investigated whether reductions in body weight influenced arterial stiffness. PWV was not associated with changes in body weight at either weeks 5-6 or week 9 in Ob+AL and Ob+IF mice **(Figure 3.S4A-3.S4D)**. These results suggest that body weight did not drive PWV in either group. To determine whether we could recapitulate persistent arterial de-stiffening and to be certain of body weight-independent effects, we subjected an additional cohort of WT+AL, Ob+AL, and Ob+IF mice to a 10-week once-weekly 24-hour IF protocol **(Figure 3.2G)** and obtained PWV measures 4-5 days following the 24-hour fast at week 10. Regardless of genotype, no differences in body weight or food intake between AL and IF groups were observed **(Figure 3.2H-3.2I)**. Again, PWV was significantly different between WT+AL and Ob+AL (422.6 ± 20.6 cm/sec vs. 499.3 ± 23.8 cm/sec, p=0.04) while Ob+AL mice displayed an intermediate

phenotype (WT+AL vs. Ob+IF: 422.6 ± 20.6 cm/sec vs 469.2 ± 17.5 cm/sec, p=0.27) (Ob+IF vs. Ob+AL: 469.2 ± 17.5 cm/sec vs 499.3 ± 23.8 cm/sec, p=0.57) **(Figure 3.2J)**. Overall, these results strongly indicate that repeated bout of once-weekly 24-hour fasting led to persistent PWV reductions in Ob+IF mice independent of changes in body weight and vascular wall thickening (aortic remodeling).

11 Weeks of Intermittent Fasting Altered Gut Microbial Composition and Butyrate Production in Obese Mice

IF has previously been shown to modify the composition of the gut microbiota [41,42] and we and others have reported that alterations in the gut microbiome can drive vascular phenotypes[10,13,14,23]. Therefore, we hypothesized that recurrent IF may reduce arterial stiffness via sustained adaptations to the gut microbiota. Within each group, Shannon's diversity index (alpha diversity) did not change during the last month of the IF protocol. However, after accounting for time (week), fasting significantly increased alpha diversity in WT mice and slightly increased alpha diversity in Ob mice so Ob+IF mice were not significantly different from WT+IF or Ob+AL groups **(Figure 3.3A)**. IF did not impact total fecal 16s rRNA DNA in either WT or Ob mice at termination, suggesting no impact of chronic IF on total gut microbial load **(Figure 3.3B)**. Principal Coordinates Analysis of Bray-Curtis distances revealed significant clustering between Ob+AL and Ob+IF mice, particularly along axis 2, yet no clustering between WT groups **(Figure 3.3C-3.3D).** No community dispersion was seen between Ob groups (PERMDISP p-value=0.40). Differential relative abundance of feature-level sOTUs between Ob+IF and Ob+AL mice were determined by identifying consensus sOTUs across different algorithms (Mann-Whitney, negative binomial (EdgeR), and linear discriminant analysis effect size (LEfSe) tests). All three tests revealed that IF increased the relative abundance of the feature *Bacteroides*_304 (Mann-Whitney FDR-adjusted p-value <0.001; EdgeR FDR-adjusted p-value =0.02; LEfSE FDR-adjusted p-value=0.04) **(Table 3.S3)**. In contrast, IF decreased the relative abundance of *Clostridia_UCG_014*_186 (*Clostridia*_186) (Mann-Whitney FDR-adjusted p-value <0.01; EdgeR FDR-adjusted p-value <0.01; LEfSE FDR-adjusted p-value=0.04) **(Table 3.S3)**, which was inversely associated with *Bacteroides*_304 (r= -0.43,

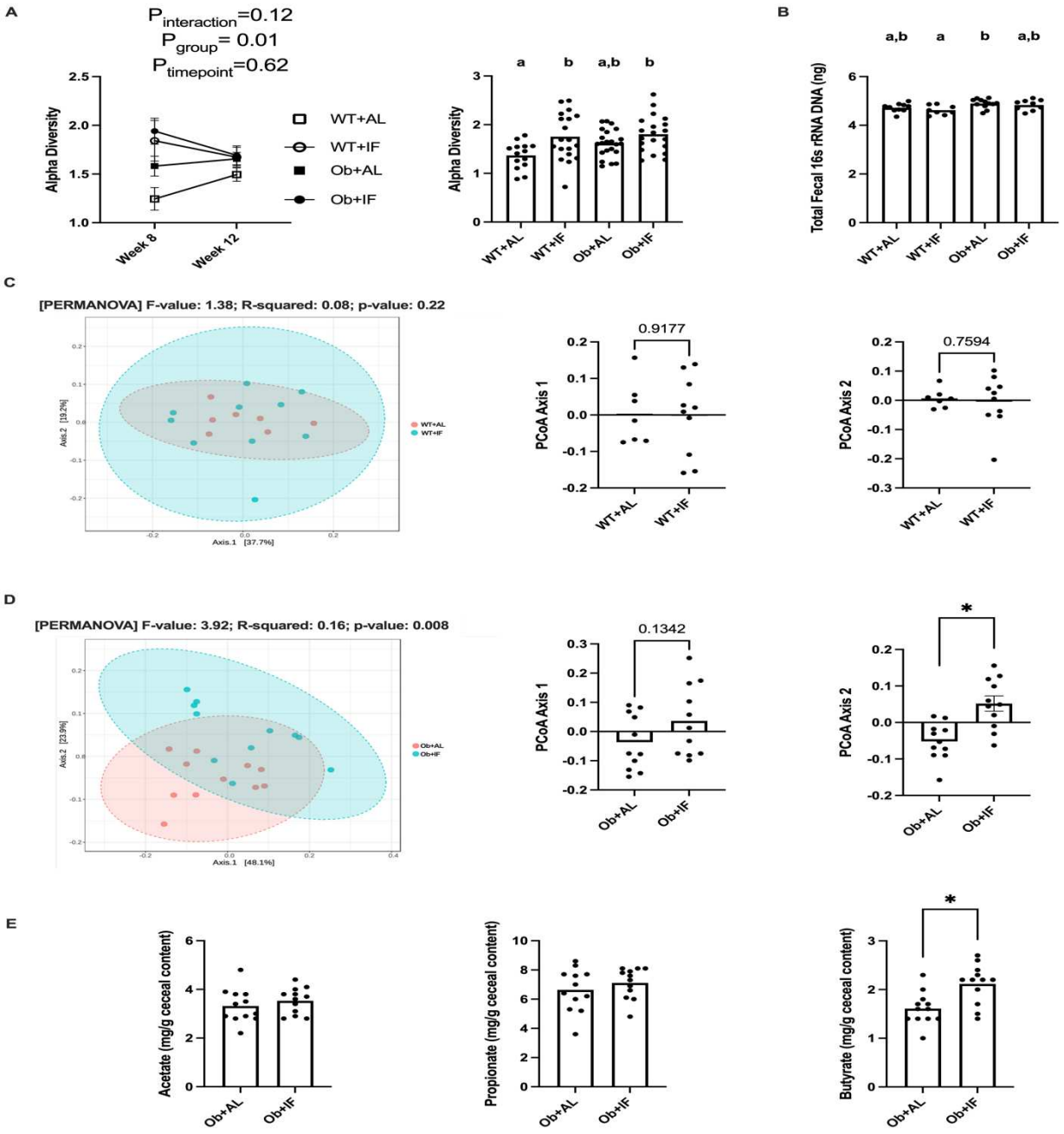

Figure 3.3. Once-weekly 24-hour intermittent fasting altered the gut microbiota in obese mice. A) Changes in the gut microbiota Shannon's alpha diversity metric at the genus level during the last month of the dietary protocol **(left)**. Barplot **(right)** visualizes differences in alpha diversity between groups irrespective of time point. N=7-11 mice per group per week. **B)** Differences in total fecal 16s rRNA DNA at termination. N=8-12 mice per group. **C-D)** Principal Coordinates Analysis of Bray-Curtis distances at the genus level between WT+AL versus WT+IF mice **C)** and Ob+AL versus Ob+IF mice **D)**. N=7-11 mice per group. Principal Coordinates Analysis axes 1 and 2 represent the principal coordinates (new uncorrelated variables that are constructed as linear combinations or mixtures of the initial variables) that explain the largest and second largest variability, respectively, in gut microbial composition. **E)** Differences in cecal short-chain fatty acid concentrations in obese mice. N=12 mice per group. WT=lean; Ob=obese; AL=*ad libitum* feeding; IF=once-weekly 24-hour intermittent fasting. Different letters indicate significant differences between groups. *indicates a p-value of less than 0.05.

p=0.045) **(Figure 3.S5A)**, suggesting that the two might be competing with each other for substrates during IF. We tried to identify *Bacteroides*_304 and *Clostridia*_186 further using the Basic Local Alignment Search Tool (BLAST, https://blast.ncbi.nlm.nih.gov/Blast.cgi). The BLAST output identified that *Bacteroides*_304 is likely a *Bacteroides thetaiotaomicron (B.thetaiotaomicron;* E value=2e-10^{7}, 100% homology) species member, while BLAST could not improve the granularity of the *Clostridia*_186 feature. Relative reductions in *Muribaculaceae*_200 (Mann-Whitney FDR-adjusted p-value <0.01; LEfSE FDR-adjusted p-value =0.04), *Muribaculaceae*_619 (EdgeR FDR-adjusted p-value <0.01; LEfSE FDR-adjusted p-value =0.07), *Muribaculaceae*_375 (EdgeR FDR-adjusted p-value <0.01; LEfSE FDR-adjusted p-value =0.09), *Monoglobus*_149 (EdgeR FDR-adjusted p-value <0.01; LEfSE FDR-adjusted p-value =0.09), *Akkermansia*_690 (EdgeR FDR-adjusted p-value =0.02; LEfSE FDR-adjusted p-value =0.07), and *Lachnospiraceae_612* (EdgeR FDR-adjusted p-value =0.03; LEfSE FDR-adjusted p-value =0.07), were observed in two out of the three analyses **(Table 3.S3)**. Ob+IF mice also displayed altered gut morphology, as highlighted by a reduced villous height:crypt depth ratio compared to Ob+AL **(Figure 3.S4F)**. Although reduced villous height:crypt ratio is typically associated with inflammation, Ob mice have elongated villi compared to WT mice[43]. Thus, the reduced villous height:crypt depth could indicate reduced nutrient absorption in the small intestine, which in turn could impact substrates available for assimilation by the gut microbiota in the colon.

Eleven weeks of once-weekly 24-hour fasting altered gut microbial metabolism, as highlighted by increased cecal butyrate levels in Ob+IF mice compared to Ob+AL mice (1.6 ± 0.1 mg/g vs 2.1 ± 0.1 mg/g, p<0.01). Other short-chain fatty acids, including acetate (3.3 ± 0.2 mg/g vs 3.5 ± 0.2 mg/g, p=0.40) and propionate (6.6 ± 0.4 mg/g vs 7.1 ± 0.3 mg/g, p=0.37), were not affected by IF **(Figure 3.3E)**.

Next, we associated changes in *Bacteroides*_304 and *Clostridia*_186, the two microbes whose relative abundance was most noticeably impacted by IF, with butyrate production. We observed a significant inverse association between *Clostridia*_186 relative abundance and cecal butyrate concentration (R=-0.51, p=0.02) and a weak albeit trending association between *Bacteroides*_304 relative

abundance and cecal butyrate concentration (R=0.36, p=0.1) **(Figure 3.S5B)**. These results were surprising, as *B. thetaiotaomicron* can metabolize host mucin glycans to produce acetate during low nutrient availability, while members of the *Clostridia* genera can make butyrate from host glycans. Interestingly, data report that *B. thetaiotaomicron*-derived acetate can be used as a substrate for butyrate production by other gut microbes, a process known as cross-feeding [44]. Indeed, further correlation analyses indicated a significant positive relationship between cecal acetate and butyrate concentrations, which was mainly driven by relatively high concentrations of acetate and butyrate in Ob+IF mice (r=0.52, p<0.01) (**Figure 3.S5C)**. In contrast, we did not observe a significant correlation between cecal propionate and butyrate concentrations (**Figure 3.S5C)**. Additionally, there was no correlation between *Bacteroides*_304 and cecal acetate (Figure S5D), implying that the relative increase in *Bacteroides*_304 was not increasing cecal acetate levels. These results propose that the "fasting gut microbiota" could have an improved capacity to convert acetate (possibly *Bacteroides*_304-derived) to butyrate. Thus, we used the pattern search function (SparCC) [45] in MicrobiomeAnalyst and identified the most positively and negatively associated taxa with *Bacteroides*_304 in obese mice **(Figure 3.S5E)**. Interestingly, all the top 10 most positively associated microbes were elevated in Ob+IF compared to Ob+AL mice (FDR-adjusted p-value=0.16). Furthermore, many of these taxa have the capacity to produce butyrate from acetate [46,47]. Overall, these results suggest that *Bacteroides*_304 may be a unique microbe better suited to survive during IF compared to other microbes with similar glycan degradation capabilities (e.g., Clostridia_186). Furthermore, our results support the possibility that IF could be enhancing gut butyrate production by microbial cross-feeding.

11 Weeks of Intermittent Fasting Altered Relationships Between Gut Microbes and Arterial Stiffness Without Impacting Relative Abundance

We leveraged the VOLARE pipeline to correlate gut microbe relative abundance to arterial stiffness measurements (either change in PWV from weeks 1-9 or week 9 PWV values) in obese mice. The VOLARE network revealed 6 microbes whose relationships with arterial stiffness were different

between Ob+AL and Ob+IF mice **(Table 3.S4)**. For example, *Lachnospiraceae*_436 relative abundance was positively associated with a change in PWV in Ob+AL mice (p=0.04) but not Ob+IF mice (p=0.52). Other examples include *Lachnospiraceae*_414 and *Lactobacillus*_209, which were inversely associated with changes in PWV in the Ob+AL group (p<0.01, p=0.04, respectively) yet not in Ob+IF mice (p=0.52, p=0.51, respectively). Strikingly, all the identified microbes (except Monoglobus_149) were not identified by the consensus analysis, indicating that the relative abundance of these microbes was not determining their relationship with arterial stiffness in either Ob+AL or Ob+IF mice. These results indicate two critical findings and avenues of further exploration: 1) IF can influence relationships between gut microbial features and changes in arterial stiffness without impacting relative abundance, potentially indicating functional changes in gut microbial metabolism; 2) Distinct gut microbes harbored within the Ob+AL gut might help to counteract the largely detrimental effects of an obesity-related microbiota on arterial stiffness.

11 Weeks of Intermittent Fasting Reduced Circulating Cytokine Concentrations

Next, since changes to the gut microbiota can impact inflammation, we investigated whether once-weekly 24-hour IF impacted the immune system. IF did not strongly affect splenocyte counts **(Figure 3.S6A-3.S6J)**. Since terminal measures were taken at least 24 hours after the last fast, this finding contradicts what was observed in the acute fasting-refeeding cycle study (i.e., 24-hour refeeding depleted splenocytes). Thus, mice may adapt throughout a longitudinal IF protocol to stabilize splenocyte counts.

In contrast, long-term IF did impact circulating chemokine levels in WT and Ob mice. IF significantly reduced 2 cytokines (CCL5, CCL7) and modestly reduced 2 others (CCL3, CCL2) in WT mice. Even more striking was that IF significantly reduced 9 cytokines in Ob mice (CXCL10, CXCL1, CCL5, CCL3, CCL7, CCL2, CXCL2, CCL11, CCL4). These reductions were especially pronounced in Ob mice, as cytokine levels dropped by more than 50% compared to Ob+AL levels **(Figure 3.S7)**. Furthermore, all circulating cytokines were strongly associated with each other in Ob mice, suggesting profound inflammation and immunosuppression in Ob+AL and Ob+IF mice, respectively. Thus, 11 weeks

of once-weekly 24-hour IF appears to impact circulating cytokine levels in Ob mice more profoundly than WT mice.

Intermittent Fasting Impedes Obesity-Related Arterial Stiffness by Altering Gut-Immune Interactions

IF significantly impacted the gut microbiota, immune system, and arterial stiffness in obese mice. To examine associations among these changes, we first correlated microbial features significantly altered by IF (identified as significant in 2/3 of the differential abundance analyses) with plasma chemokine levels in obese mice. Indeed, *Clostridia*_186 relative abundance was significantly and positively associated with most plasma cytokines (CXCL1, CCL5, CCL3, CCL2, CXCL2, CCL11, CCL4), followed by *Muribaculaceae*_375 (CXCL1, CCL5, CCL2, CXCL2, CCL11, CCL4), and *Muribaculaceae*_200 (CXCL1, CCL2, CXCL2). *Muribaculaceae*_619 relative abundance was inversely associated with all cytokines (**Figure 3.4A)**. Interestingly, although *Bacteroides*_304 was significantly increased in Ob+IF mice in 3/3 consensus analysis tests, it only had a significant inverse association with CXCL10 (**Figure 3.4A)**.

Next, we conducted a mediation analysis to identify whether IF reduces arterial stiffness by impacting gut-immune interactions in obese mice. The mediation analysis determined that plasma CXCL1 and CCL2 levels at least partially mediated the relationship between *Clostridia*_186 relative abundance and PWV measures in obese mice. Plasma CCL7 levels were also identified to mediate the relationship between *Muribaculaceae*_200 and PWV **(Table 3.S5)**. *Bacteroides*_304 was not identified in the mediation analysis. These findings indicate that IF-mediated reductions in distinct gut microbial features, particularly *Clostridia*_186, are linked to decreases in specific plasma cytokines (CCL2 and CXCL1) and arterial stiffness in obese mice. Furthermore, the absence of *Bacteroides*_304 from the correlation plot and mediation analysis, along with its positive relationship with butyrate producers in Ob+IF mice **(Figure 3.S5E)**, support that this microbe could be indirectly reducing cytokines (CCL2 and CXCL1, yet not CCL7) through increases in butyrate via potential cross-feeding (**Figure 3.4B)**.

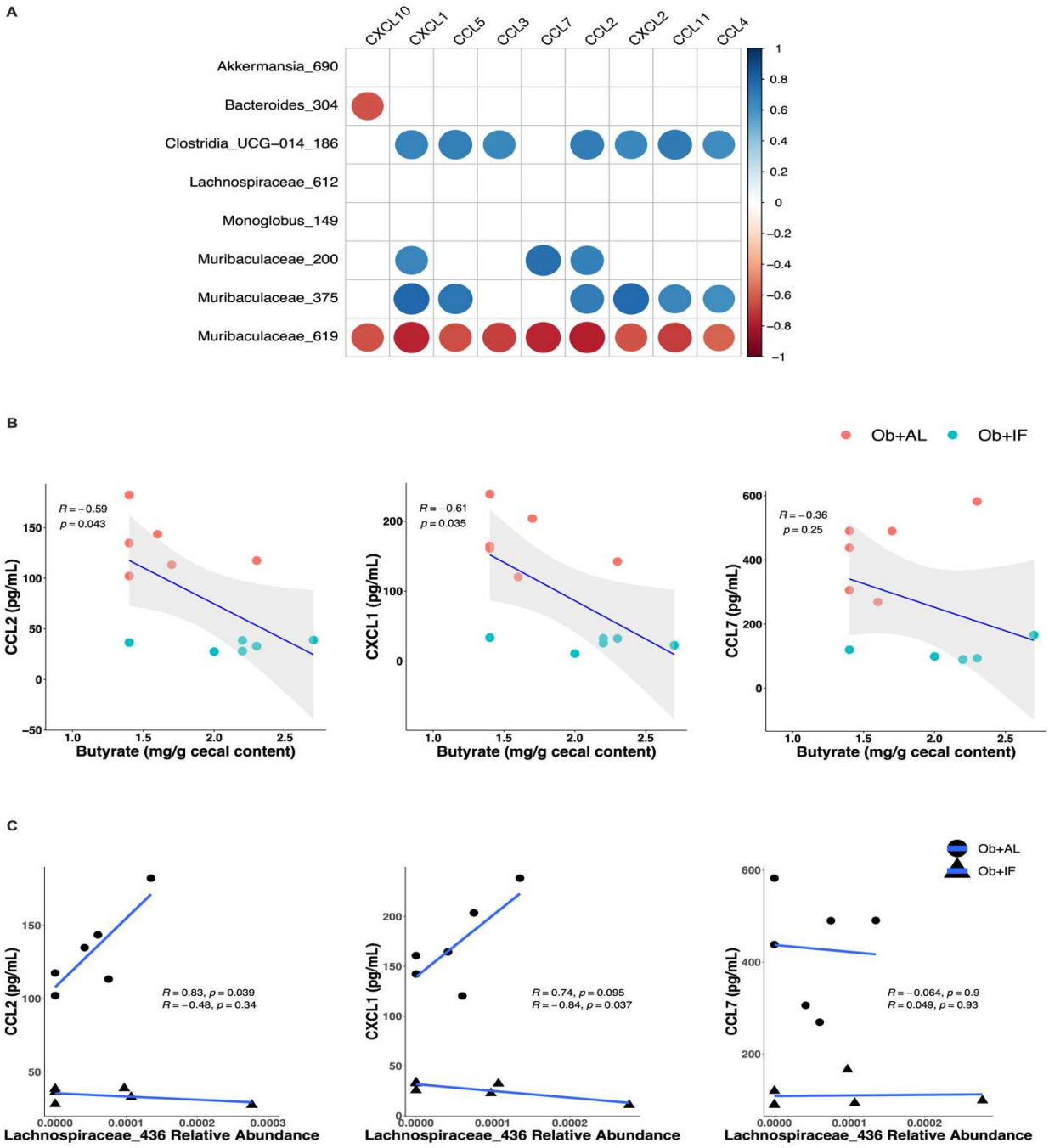

Figure 3.4. Once-weekly 24-hour intermittent fasting altered gut microbe-immune interactions. A) Pearson correlation plot visualizing associations between relative abundances of gut microbial features significantly altered by intermittent fasting (identified via consensus analysis) and plasma chemokines in obese mice. N=6 mice per group. Colored circles indicate $p<0.05$. **B)** Scatterplot and Pearson correlations between cecal butyrate concentrations and plasma CCL2 **(left)**, CXCL1 **(middle)**, and CCL7 **(right)** concentrations in obese mice. N=6 mice per group. **C)** Scatterplot and Pearson correlations between *Lachnospiraceae*_436, whose relative abundance was not altered via IF fasting (identified via VOLARE analysis) and plasma CCL2 **(left)**, CXCL1 **(middle)**, and CCL7 **(right)** concentrations in obese mice. N=6 mice per group. Ob=obese; AL=*ad libitum* feeding; IF=once-weekly 24-hour intermittent fasting.

Finally, since the VOLARE analysis revealed that certain microbial features had differing relationships with arterial stiffness without changes in their relative abundance, we pondered whether this would also be true with circulating cytokine levels. We only included *Lachnospiraceae*_436 in this correlation analysis, as this microbial feature was the only one identified to have a significant positive relationship with arterial stiffness in Ob+AL mice and no ties with stiffness in Ob+IF mice. We also only correlated *Lachnospiraceae*_436 to CCL2, CXCL1, and CCL7 as they were the only cytokines identified in the mediation analysis. We observed positive relationships between *Lachnospiraceae*_436 relative abundance and CCL2 and CXCL1 levels in Ob+AL mice, yet no (CCL2) or an inverse (CXCL1) relationship in Ob+IF mice **(Figure 3.4C)**. Interestingly, *Lachnospiraceae*_436 was not associated with plasma CCL7 levels in either Ob group **(Figure 3.4C)**. Together, these results suggest that CCL2 and CXCL1 are distinct cytokines that regulate the gut microbiota's impacts on arterial stiffness. We also found that *Lachnospiraceae*_436 was associated with reduced acetate and butyrate in Ob+AL mice but not Ob+IF mice **(Figure 3.S5F)**, again indicating metabolic adaptations in this microbe during IF.

Intermittent Fasting Reduces Perivascular Adipose Tissue Lymphocytes

CCL2 and CXCL1 are two pro-inflammatory chemokines that govern the recruitment of inflammatory immune cells to the vasculature, which can subsequently drive development of arterial stiffness. Thus, we investigated whether IF reduced the number of immune cells within the vascular wall (thoracic aorta) and perivascular adipose tissue. IF did not reduce the number of basophilic granulocytes or lymphocytes in the vascular wall **(Figure 3.5A)**. However, IF reduced the number of perivascular adipose tissue (PVAT) lymphocytes closely surrounding the vascular wall by 50% (18.9 ± 5.3 vs. 9.3 ± 1.7, $p=0.12$) **(Figure 3.5B)**. Moreover, reduced PVAT lymphocytes were associated with attenuated arterial stiffness in obese mice **(Figure 3.5C)**. Thus, IF-mediated reductions in CCL2 and CXCL1 might attenuate obesity-related arterial stiffness by altering lymphocyte recruitment to the inflamed PVAT.

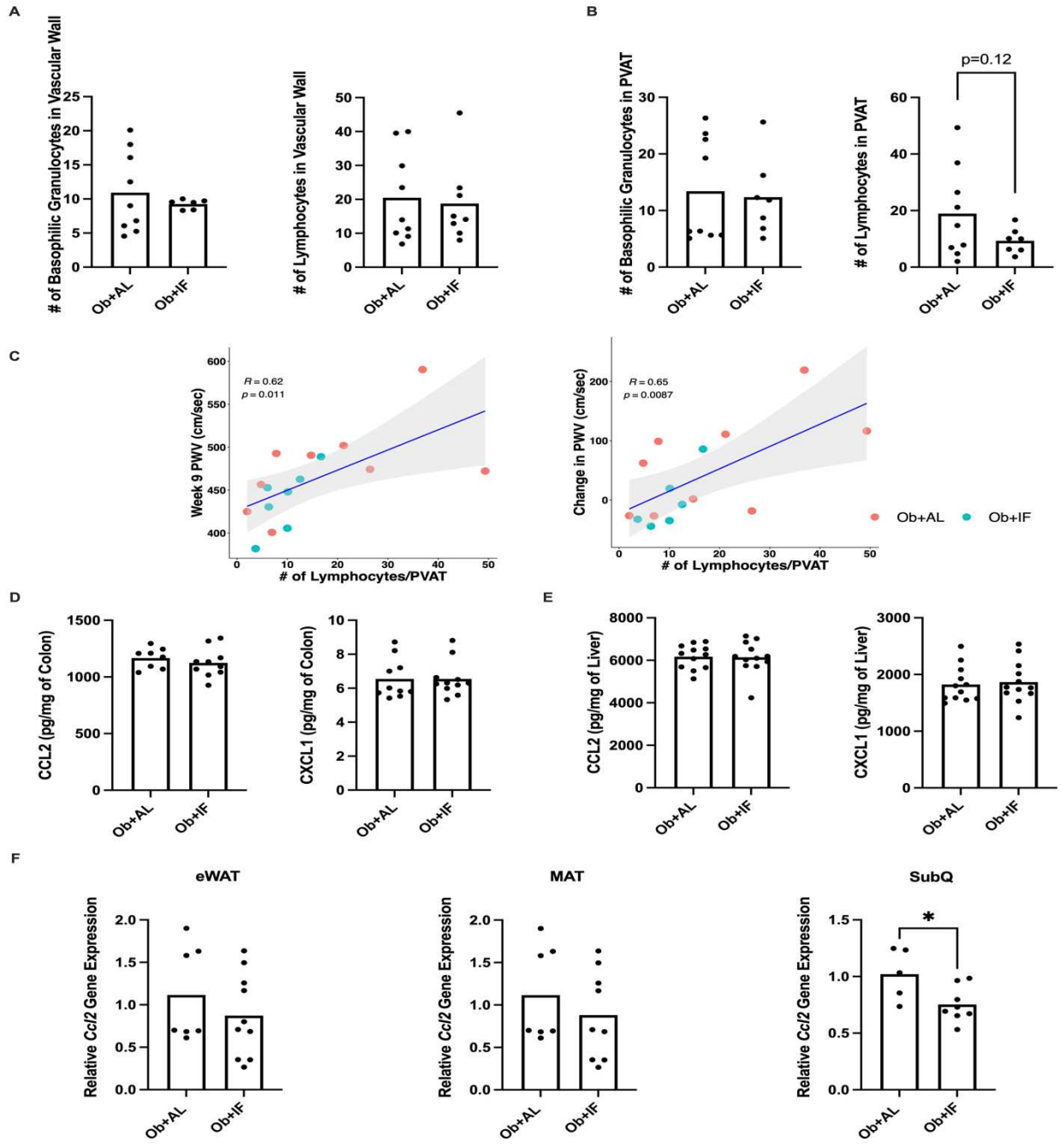

Figure 3.5. Once-weekly 24-hour intermittent fasting reduced perivascular adipose tissue lymphocyte accumulation. A-B) Normalized number of basophilic granulocytes and lymphocytes in thoracic aorta wall **(left)** and perivascular adipose tissue **(right)** in obese mice. N=6-9 mice per group per anatomical region (wall or perivascular adipose tissue). **C)** Scatterplot and Pearson correlations between the normalized number of lymphocytes in perivascular adipose tissue and week 9 pulse wave velocity **(left)** and change in pulse wave velocity **(right)** in obese mice. N=6-9 mice per group. **D-E)** Differences in colon **D)** and liver **E)** CCL2 and CXCL1 concentrations. N=8-12 mice per group per tissue. **F)** Relative *Ccl2* gene expression in epididymal **(left),** mesenteric **(middle),** and subcutaneous adipose tissue **(right)** in obese mice. N=5-10 mice per group per tissue. Ob=obese; AL=*ad libitum* feeding; IF=once-weekly 24-hour intermittent fasting; PWV=pulse wave velocity; Subq= subcutaneous adipose tissue, eWAT= epididymal white adipose tissue; MAT= mesenteric adipose tissue.

We also explored whether specific tissue(s) reduced CCL2 and CXCL1 production during IF. We first assessed the colon given our data linking the gut microbiota to plasma CCL2 and CXCL1 levels but found no impact of IF on colon CCL2 or CXCL1 levels **(Figure 3.5D)**. Next, we examined whether the gut microbiota could signal to the liver via the portal circulation. Again, we found no differences in liver CCL2 or CXCL1 levels **(Figure 53.E)**. Finally, we assessed whether IF influenced adipose tissue cytokine expression, as the gut microbiota can affect adipose tissue inflammation [48,49]. We found that IF only slightly reduced epididymal and mesenteric adipose tissue *Ccl2* gene expression, but significantly reduced expression in subcutaneous adipose tissue (1.0 ± 0.1 vs. 0.75 ± 0.1, $p=0.03$) **(Figure 3.5F)**. Although more analyses are warranted, this initial evidence suggests that the fasting gut microbiota could limit aberrant immune-vascular signaling by reducing adipose tissue cytokine production.

DISCUSSION

Recent data have demonstrated that IF elicits cardioprotective effects. Yet, some fundamental questions remain unanswered, including: 1) the effects of IF on arterial stiffness, 2) the potential differential effects of a single fast versus repeated fasting bouts, 3) whether IF-induced changes persist beyond the refeeding period, and 4) whether gut microbial-immune interactions could mediate potential improvements in arterial stiffness. In this study, we show that acute IF transiently increased arterial stiffness without impacting the gut microbiota or systemic inflammation in lean mice while having no substantial impact in obese mice. In contrast, chronic IF attenuated arterial stiffness only in obese mice, which was independent of weight loss and coincided with the suppression of aberrant gut microbe-immune interactions **(Figure 3.6)**. These results coincide with the emerging hypothesis that many of the cardiovascular benefits of chronic IF are independent of weight loss [7]. Furthermore, reduced arterial stiffness and gut-immune signaling persisted even after *ad libitum* feeding, indicating that persistent adaptations to the gut microbiota and immune system drive vascular health.

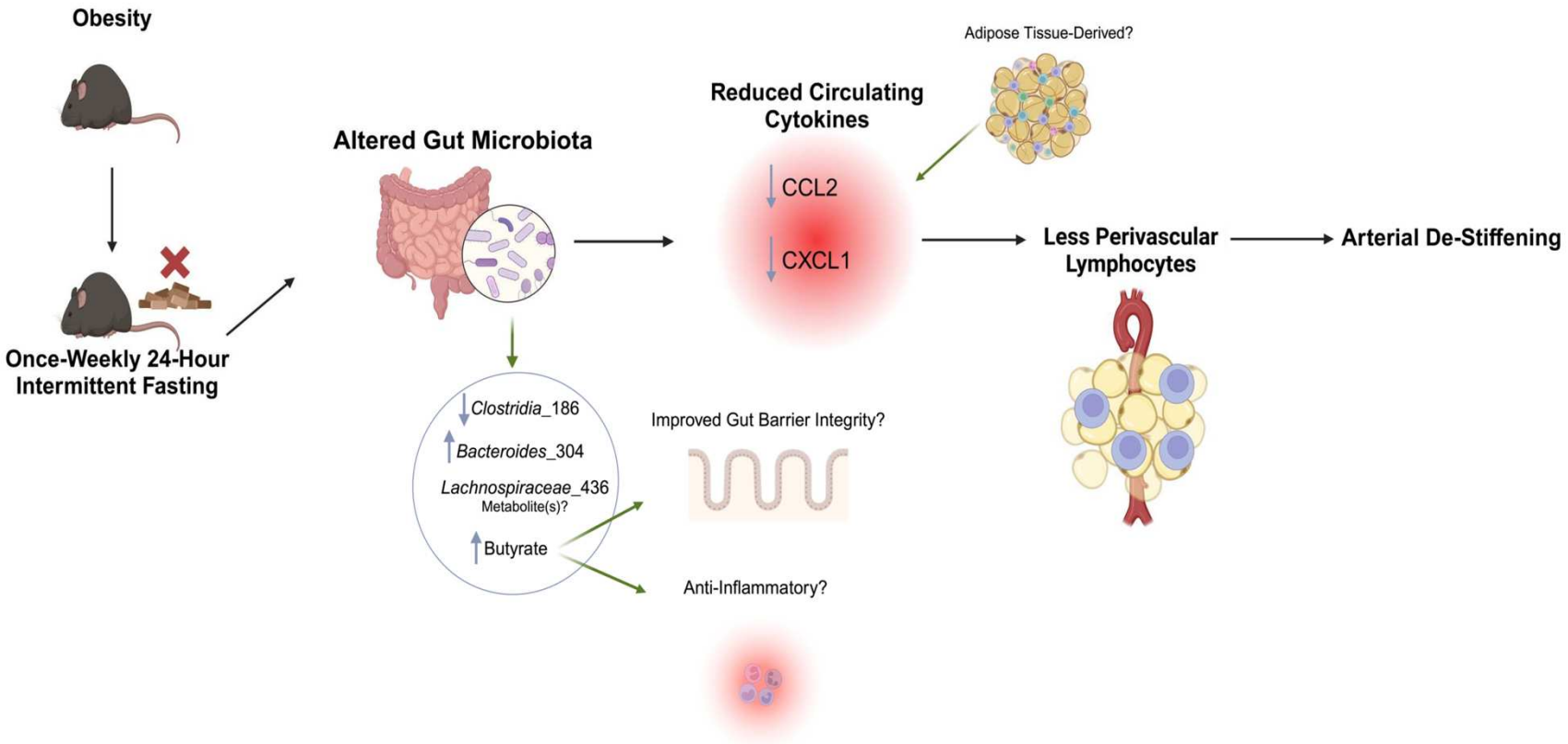

Figure 3.6. Once-weekly 24-hour intermittent fasting attenuated obesity-related arterial stiffness via potential gut-immune signaling. Once-weekly 24-hour intermittent fasting (IF) altered the gut microbiota in obese mice. In particular, IF reduced the relative abundance of *Clostridia*_186 and increased the relative abundance of *Bacteroides*_304 in conjunction with increased butyrate. Why the "fasted gut microbiota" confered a particular advtanage to *Bacteroides*_304, and whether *Bacteroides*_304 facilitated butyrate production due to cross-feeding warrents further investigation. Gut-derived butyrate could have reduced arterial stiffness through increased gut barrier integrity, limiting "harmful" microbial metabolites from reaching circulation, or by having direct anti-inflammatory activities as small amounts diffuse into the circulation. Whether butyrate acted by itself or in concert with other fasting-related microbial metabolites to reduce inflammation is another potential area of future research. Although IF did not impact *Lachnospiraceae*_436 relative abundance, it suppressed its positive relationship with arterial stiffness, possible indicating changes in its production of metabolites. IF-related alterations to the gut microbiota corresponded with reduced circulating cytokines, particularly CCL2 and CXCL1 (which could be adipose-tissue derived), reduced perivascular lymphocyte accumulation, and arterial de-stiffening. Created at Biorender.com.

Our first novel finding regarding arterial stiffness is that lean and obese mice respond differently to a single fasting-refeeding cycle, as we found that a 24-hour fast acutely increased arterial stiffness in lean mice yet did not impact arterial stiffness in genetically obese mice. To our knowledge, only one other study has assessed the impact of a single fast on obesity-related arterial stiffness. Fry and colleagues. [50] showed that an overnight fast reduced PWV in diet-induced obese mice by activating VSMC Sirtuin-1 (SIRT1) signaling and decreasing vascular inflammation and oxidative stress. However, since leptin at least partially regulates SIRT1 expression in mice [51], this might explain why we did not observe acute changes in our leptin-deficient obese mouse model. Furthermore, we found no striking differences in how the single fasting-refeeding cycle impacted metabolic parameters (i.e., glucose, ketones, body weight, etc.), gut microbial composition, or splenocyte populations between lean versus obese mice. We also did not observe large impacts of acute IF on circulating chemokines in lean mice, thus transient changes in systemic inflammation are presumably not contributing to the acute arterial stiffening.

Overall, these results were somewhat surprising since acute fasting-refeeding can drastically change gut microbial composition and the immune system in both mice and humans [52,53]. Specifically, Okada et al.[52] found that small intestinal *Lactobacillus murinus* was reduced in 36-hour fasted, 24-hour refed mice, which through its production of lactate greatly impacted colon epithelial cell turnover and risk of tumorigenesis. Maifeld et al. [53] showed that five days of modified fasting in humans increased *Clostridium sp.* and *Roseburia hominis* while reducing Eubacterium *rectale* and *Dorea longicatena*, and increased plasmacytoid dendritic cells, CD14+ monocytes and gamma delta T cells and reduced B cells and pro-inflammatory T cells. However, since the fasting durations of these two studies were different than the present study, it could be that fasting for more than 24 hours is needed to observe acute changes to the gut microbiota and immune system. Nevertheless, our results indicate that the metabolic, gut microbe, and immune parameters we analyzed during this single cycle do not predict acute arterial stiffening in lean mice. Thus, a single 24-hour fast might increase arterial stiffness in lean mice through other acute factors (i.e., stress [54–58], blood pressure[15], endothelial cell nitric oxide signaling [16]). However,

the increase in arterial stiffness returned to normal within 24 hours after refeeding, suggesting limited impact on chronic cardiovascular health.

In contrast to the single fasting-refeeding cycle, repeated bouts of once-weekly 24-hour IF attenuated arterial stiffness in obese mice, with these effects evident in as little as five weeks. We also show that arterial de-stiffening persists for at least 5 days following *ad libitum* refeeding, indicating that sustained arterial de-stiffening might be achievable through recurrent fasting. Indeed, a distinguishing feature of this study was the measurement of arterial stiffness several days after fasting, allowing us to differentiate between stable versus transient changes in arterial stiffness. This contrasts with previous studies which have either measured the impacts of IF on cardiovascular health within one day after fasting [13,59,60] or do not explicitly state how long after the fasting period parameters were measured [61,62].

Furthermore, our results suggest that arterial de-stiffening was not due to changes in body weight but was a result of long-term adaptations in gut microbe-immune interactions. Although previous work has linked IF with changes to the gut microbiota and immune system, our study offers novel insights into how IF impacts gut microbe-immune interactions to improve vascular health. For example, Shi et al.[13] determined that ten weeks of alternate day fasting (ADF) reduced blood pressure in spontaneous hypertensive stroke-prone (SHSP) rats. These reductions in blood pressure occurred with relative increases in *Bacteroides uniformis* and *Lactobacillus johnsonii* as well as reductions in *Muribaculum intestinale* and *Parasutterella excrementihominis*. Further microbiota transplantation studies revealed that reductions in blood pressure were dependent upon the IF-gut microbiota. However, changes in systemic or vascular-resident inflammation were not studied. In humans, Guo et al. [14] showed that eight weeks of modified IF altered the gut microbiota, improved markers of vascular health (i.e., increased total nitrate and reduced asymmetric dimethylarginine) and reduced inflammation (CD40L and malondialdehyde) in metabolic syndrome patients. Although this study established correlations between gut taxa relative abundances and these four markers, it failed to demonstrate the interconnectedness between the three biological systems. In contrast, our work highlights that gut-immune signaling was altered by IF to reduce

arterial stiffness. We identify *Clostridia* _186 as a distinct gut microbial feature reduced in Ob+IF mice, which was associated with reduced circulating CCL2 and CXCL1 levels, less lymphocyte PVAT accumulation, and arterial de-stiffening. Furthermore, despite no changes in its relative abundance, we found that IF suppressed *Lachnospiraceae*_436's positive relationships with CCL2, CXCL1, and arterial stiffness.

Although high CCL2 and CXCL1 levels are typically associated with poor cardiovascular health, their relationship with arterial stiffness has not been extensively studied. Wang et al. reported that inhibition of the CXCL1-CXCR2 axis reduced aortic thickness and collagen deposition but did not measure arterial stiffness[63]. Our results add to the existing data by demonstrating that CCL2 and CXCL1 are important regulators of obesity-related arterial stiffness and their reduction following IF may be subsequent to alterations in the gut microbiota, which may mediate arterial de-stiffening. These data align with previous results from our group indicating that alterations in the gut microbiota are a putative determinant of inflammation and vascular health [10,12].

These novel findings are hypothesis-generating and establish a foundation for more translational and mechanistic work on how IF alters aberrant gut-immune-vascular signaling during obesity. Translationally, to determine their abundance in the human gut during obesity and whether this abundance is altered by IF, metagenomic sequencing to more precisely identify *Clostridia* _186 and *Lachnospiraceae*_436 and capture their putative functional roles in fed and fasted states is necessary. This need is further emphasized by the fact that different species or strains within the same taxonomic group can have varying effects on the physiology of their hosts. A prime example is *Lachnospiraceae*, which on one hand has been shown to lower systemic inflammation and ameliorate atherosclerosis [64]; but is also associated with metabolic diseases such as type 2 diabetes, chronic kidney disease and ulcerative colitis [65].

Mechanistically, identifying how IF-induced alterations to the gut microbiota impacted circulating chemokines (CCL2 and CXCL1) during obesity will also be important. One hypothesis is that

IF reduces the systemic circulation of inflammatory microbial components and metabolites. Our data provide initial evidence for this hypothesis, as IF did not reduce colon or liver CCL2 and CXCL1, but did reduce their levels within the plasma, in obese mice. The suppressed positive relationships between *Lachnospiraceae*_436 and CCL2 and CXCL1 during IF, without changes in *Lachnospiraceae*_436 relative abundance, further supports this hypothesis. Thus, comparing gut and plasma metabolites during obesity and IF is a promising next step. This work could also determine which organs sense gut-derived metabolites during obesity and subsequently produce inflammatory chemokines. Our initial evidence suggests that the subcutaneous adipose tissue could be a particular target of the obese gut microbiota and its metabolites. Our finding of decreased PVAT lymphocytes could also indicate reduced microbial metabolite-inflammatory signaling within other adipose tissue depots. IF can also reduce bone marrow [26] and aortic [66] CCL2, suggesting these tissues as viable candidates as well.

Lastly, the relationship between increased *Bacteroides*_304 (*B.thetaiotaomicron*) and cecal butyrate should be further investigated. As discussed in the results section, these findings offer preliminary evidence suggesting that *Bacteroides*_304 could be a primary source of acetate for the "fasting gut microbiota" to synthesize butyrate. However, validation of elevated cross-feeding during IF is necessary. Furthermore, high levels of butyrate could contributing to the immunosuppression observed during IF. For instance, butyrate can increase gut barrier integrity [67], potentially reducing the impact of the obese gut microbiota on the vasculature. Butyrate can also directly reduce pro-inflammatory signaling in the gut and peripheral organs, such as the aorta [68–70]. Thus, whether butyrate is impacting arterial stiffness through its actions in the gut or periphery warrants further investigation.

Some limitations should be acknowledged. First, we used a genetic model of obesity (ob/ob), which might be less translatable to human health than diet-induced obese (DIO) mouse models. However, ob/ob and DIO mice present with similar metabolic abnormalities, including hyperphagic-like tendencies, hyperglycemia/glucose intolerance, arterial stiffness, immune dysfunction, and altered gut microbial composition [12,71,72]. Thus, the benefits of IF on the gut-immune-vascular axis mice that apply to

genetically obese mice likely apply to DIO mice. Second, we only used male mice in our experiments. Since IF might affect males and females differently, particularly regarding hormonal responses [73], our results should only be extrapolated to male mice. Third, although our initial mediation analysis found that CCL2 and CXCL1 were at least partially mediating the effects of the obese gut microbiota on arterial stiffness, further research is needed to observe a causal relationship between these chemokines and arterial stiffness. Additionally, although CCL2 is chemotactic towards CCR2-expressing lymphocytes, CXCL1 is typically involved in neutrophil and monocyte, not lymphocyte, recruitment. Furthermore, upon preliminary observation of H&E-stained thoracic aorta slides, we observed very little neutrophils within the vascular wall or PVAT. Therefore, the direct link between reduced CXCL1 and arterial de-stiffening during IF is still not clear. However, we do report that all circulating cytokine/chemokine concentrations correlated with each other, suggesting large-scale immunosuppression with IF. Therefore, reductions in CXCL1 due to IF may have decreased lymphocyte accumulation by affecting the production of other chemokines involved in T cell and B lymphocyte recruitment. Lastly, future studies should utilize metabolomics and meta-transcriptomics to uncover metabolites driving these interactions.

In conclusion, a single acute bout of IF was insufficient to reduce arterial stiffness in obese mice. However, chronic IF over a 10-week period attenuated arterial stiffness in obese mice and these effects persisted for at least 5 days beyond the refeeding period. This finding highlights the potential durability of chronic IF regimens to improve vascular health. Reduced arterial stiffness in obese mice was accompanied by profound changes to the gut microbiota, reduced systemic inflammation, and fewer perivascular-resident lymphocytes, suggesting that IF can improve vascular health by chronically altering interactions between the gut microbiota and immune system. Additionally, we identified distinct gut microbe-chemokine interactions implicated in obesity-related arterial stiffness that should be examined for their clinical relevance.

REFERENCES

1. Martin SS, Aday AW, Almarzooq ZI, et al. 2024 Heart Disease and Stroke Statistics: A Report of US and Global Data From the American Heart Association. *Circulation*. 2024;149(8). doi:10.1161/CIR.0000000000001209

2. Lichtenstein AH, Appel LJ, Vadiveloo M, et al. 2021 Dietary Guidance to Improve Cardiovascular Health: A Scientific Statement From the American Heart Association. *Circulation*. 2021;144(23). doi:10.1161/CIR.0000000000001031

3. Koppold DA, Breinlinger C, Hanslian E, et al. International consensus on fasting terminology. *Cell Metab*. 2024;36(8):1779-1794.e4. doi:10.1016/j.cmet.2024.06.013

4. Persynaki A, Karras S, Pichard C. Unraveling the metabolic health benefits of fasting related to religious beliefs: A narrative review. *Nutrition*. 2017;35:14-20. doi:10.1016/j.nut.2016.10.005

5. Gonzalez JE, Cooke WH. Influence of an acute fast on ambulatory blood pressure and autonomic cardiovascular control. *Am J Physiol-Regul Integr Comp Physiol*. 2022;322(6):R542-R550. doi:10.1152/ajpregu.00283.2021

6. Catterson JH, Khericha M, Dyson MC, et al. Short-Term, Intermittent Fasting Induces Long-Lasting Gut Health and TOR-Independent Lifespan Extension. *Curr Biol*. 2018;28(11):1714-1724.e4. doi:10.1016/j.cub.2018.04.015

7. de Cabo R, Mattson MP. Effects of Intermittent Fasting on Health, Aging, and Disease. Longo DL, ed. *N Engl J Med*. 2019;381(26):2541-2551. doi:10.1056/NEJMra1905136

8. Mitchell GF, Hwang SJ, Vasan RS, et al. Arterial Stiffness and Cardiovascular Events: The Framingham Heart Study. *Circulation*. 2010;121(4):505-511. doi:10.1161/CIRCULATIONAHA.109.886655

9. Vasan RS, Pan S, Xanthakis V, et al. Arterial Stiffness and Long-Term Risk of Health Outcomes: The Framingham Heart Study. *Hypertension*. 2022;79(5):1045-1056. doi:10.1161/HYPERTENSIONAHA.121.18776

10. Battson ML, Lee DM, Jarrell DK, et al. Suppression of gut dysbiosis reverses Western diet-induced vascular dysfunction. *Am J Physiol-Endocrinol Metab*. 2018;314(5):E468-E477. doi:10.1152/ajpendo.00187.2017

11. Trikha SRJ, Lee DM, Ecton KE, et al. Transplantation of an obesity-associated human gut microbiota to mice induces vascular dysfunction and glucose intolerance. *Gut Microbes*. 2021;13(1):1940791. doi:10.1080/19490976.2021.1940791

12. Ecton KE, Graham EL, Risk BD, et al. Toll-like receptor 4 deletion partially protects mice from high fat diet-induced arterial stiffness despite perturbation to the gut microbiota. *Front Microbiomes*. 2023;2:1095997. doi:10.3389/frmbi.2023.1095997

13. Shi H, Zhang B, Abo-Hamzy T, et al. Restructuring the Gut Microbiota by Intermittent Fasting Lowers Blood Pressure. *Circ Res*. 2021;128(9):1240-1254. doi:10.1161/CIRCRESAHA.120.318155

14. Guo Y, Luo S, Ye Y, Yin S, Fan J, Xia M. Intermittent Fasting Improves Cardiometabolic Risk Factors and Alters Gut Microbiota in Metabolic Syndrome Patients. *J Clin Endocrinol Metab*. 2021;106(1):64-79. doi:10.1210/clinem/dgaa644

15. Pierce GL, Coutinho TA, DuBose LE, Donato AJ. Is It Good to Have a Stiff Aorta with Aging? Causes and Consequences. *Physiology*. 2022;37(3):154-173. doi:10.1152/physiol.00035.2021

16. Wilkinson IB, MacCallum H, Cockcroft JR, Webb DJ. Inhibition of basal nitric oxide synthesis increases aortic augmentation index and pulse wave velocity *in vivo*. *Br J Clin Pharmacol*. 2002;53(2):189-192. doi:10.1046/j.1365-2125.2002.1528adoc.x

17. Qiu H, Zhu Y, Sun Z, et al. Short Communication: Vascular Smooth Muscle Cell Stiffness As a Mechanism for Increased Aortic Stiffness With Aging. *Circ Res*. 2010;107(5):615-619. doi:10.1161/CIRCRESAHA.110.221846

18. Lacolley P, Regnault V, Laurent S. Mechanisms of Arterial Stiffening: From Mechanotransduction to Epigenetics. *Arterioscler Thromb Vasc Biol*. 2020;40(5):1055-1062. doi:10.1161/ATVBAHA.119.313129

19. Boutouyrie P, Chowienczyk P, Humphrey JD, Mitchell GF. Arterial Stiffness and Cardiovascular Risk in Hypertension. *Circ Res*. 2021;128(7):864-886. doi:10.1161/CIRCRESAHA.121.318061

20. Ait-Oufella H, Collin C, Bozec E, et al. Long-term reduction in aortic stiffness: a 5.3-year follow-up in routine clinical practice. *J Hypertens*. 2010;28(11):2336-2341. doi:10.1097/HJH.0b013e32833da2b2

21. Butlin M, Tan I, Spronck B, Avolio AP. Measuring Arterial Stiffness in Animal Experimental Studies. *Arterioscler Thromb Vasc Biol*. 2020;40(5):1068-1077. doi:10.1161/ATVBAHA.119.313861

22. Jaminon A, Reesink K, Kroon A, Schurgers L. The Role of Vascular Smooth Muscle Cells in Arterial Remodeling: Focus on Calcification-Related Processes. *Int J Mol Sci*. 2019;20(22):5694. doi:10.3390/ijms20225694

23. Battson ML, Lee DM, Li Puma LC, et al. Gut microbiota regulates cardiac ischemic tolerance and aortic stiffness in obesity. *Am J Physiol-Heart Circ Physiol*. 2019;317(6):H1210-H1220. doi:10.1152/ajpheart.00346.2019

24. Graef FA, Celiberto LS, Allaire JM, et al. Fasting increases microbiome-based colonization resistance and reduces host inflammatory responses during an enteric bacterial infection. Baumler AJ, ed. *PLOS Pathog*. 2021;17(8):e1009719. doi:10.1371/journal.ppat.1009719

25. Janssen H, Kahles F, Liu D, et al. Monocytes re-enter the bone marrow during fasting and alter the host response to infection. *Immunity*. 2023;56(4):783-796.e7. doi:10.1016/j.immuni.2023.01.024

26. Jordan S, Tung N, Casanova-Acebes M, et al. Dietary Intake Regulates the Circulating Inflammatory Monocyte Pool. *Cell*. 2019;178(5):1102-1114.e17. doi:10.1016/j.cell.2019.07.050

27. Nagai M, Noguchi R, Takahashi D, et al. Fasting-Refeeding Impacts Immune Cell Dynamics and Mucosal Immune Responses. *Cell*. 2019;178(5):1072-1087.e14. doi:10.1016/j.cell.2019.07.047

28. Wang L, Cheng M, Wang Y, et al. Fasting-activated ventrolateral medulla neurons regulate T cell homing and suppress autoimmune disease in mice. *Nat Neurosci*. 2024;27(3):462-470. doi:10.1038/s41593-023-01543-w

29. Delconte RB, Owyong M, Santosa EK, et al. Fasting reshapes tissue-specific niches to improve NK cell-mediated anti-tumor immunity. *Immunity*. Published online June 2024:S1074761324002759. doi:10.1016/j.immuni.2024.05.021

30. Lee DM, Ecton KE, Trikha SRJ, et al. Microbial metabolite indole-3-propionic acid supplementation does not protect mice from the cardiometabolic consequences of a Western diet. *Am J Physiol-Gastrointest Liver Physiol*. 2020;319(1):G51-G62. doi:10.1152/ajpgi.00375.2019

31. Caporaso JG, Lauber CL, Walters WA, et al. Ultra-high-throughput microbial community analysis on the Illumina HiSeq and MiSeq platforms. *ISME J*. 2012;6(8):1621-1624. doi:10.1038/ismej.2012.8

32. Bolyen E, Rideout JR, Dillon MR, et al. Reproducible, interactive, scalable and extensible microbiome data science using QIIME 2. *Nat Biotechnol*. 2019;37(8):852-857. doi:10.1038/s41587-019-0209-9

33. Amir A, McDonald D, Navas-Molina JA, et al. Deblur Rapidly Resolves Single-Nucleotide Community Sequence Patterns. Gilbert JA, ed. *mSystems*. 2017;2(2):e00191-16. doi:10.1128/mSystems.00191-16

34. Robeson MS, O'Rourke DR, Kaehler BD, et al. RESCRIPt: Reproducible sequence taxonomy reference database management. Pertea M, ed. *PLOS Comput Biol*. 2021;17(11):e1009581. doi:10.1371/journal.pcbi.1009581

35. Chong J, Liu P, Zhou G, Xia J. Using MicrobiomeAnalyst for comprehensive statistical, functional, and meta-analysis of microbiome data. *Nat Protoc*. 2020;15(3):799-821. doi:10.1038/s41596-019-0264-1

36. Tingley D, Yamamoto T, Hirose K, Keele L, Imai K. **mediation** : *R* Package for Causal Mediation Analysis. *J Stat Softw*. 2014;59(5). doi:10.18637/jss.v059.i05

37. Vandesompele J, De Preter K, Pattyn F, et al. Accurate normalization of real-time quantitative RT-PCR data by geometric averaging of multiple internal control genes. *Genome Biol*. 2002;3(7):RESEARCH0034. doi:10.1186/gb-2002-3-7-research0034

38. Siebert JC, Neff CP, Schneider JM, et al. VOLARE: visual analysis of disease-associated microbiome-immune system interplay. *BMC Bioinformatics*. 2019;20(1):432. doi:10.1186/s12859-019-3021-0

39. Yao L, Davidson EA, Shaikh MW, Forsyth CB, Prenni JE, Broeckling CD. Quantitative analysis of short-chain fatty acids in human plasma and serum by GC–MS. *Anal Bioanal Chem*. 2022;414(15):4391-4399. doi:10.1007/s00216-021-03785-8

40. Wing EJ, Magee DM, Barczynski LK. Acute starvation in mice reduces the number of T cells and suppresses the development of T-cell-mediated immunity. *Immunology*. 1988;63(4):677-682.

41. Paukkonen I, Törrönen EN, Lok J, Schwab U, El-Nezami H. The impact of intermittent fasting on gut microbiota: a systematic review of human studies. *Front Nutr*. 2024;11:1342787. doi:10.3389/fnut.2024.1342787

42. Li L, Su Y, Li F, et al. The effects of daily fasting hours on shaping gut microbiota in mice. *BMC Microbiol*. 2020;20(1):65. doi:10.1186/s12866-020-01754-2

43. Stojanović O, Altirriba J, Rigo D, et al. Dietary excess regulates absorption and surface of gut epithelium through intestinal PPARα. *Nat Commun*. 2021;12(1):7031. doi:10.1038/s41467-021-27133-7

44. Chia LW, Mank M, Blijenberg B, et al. Bacteroides thetaiotaomicron Fosters the Growth of Butyrate-Producing Anaerostipes caccae in the Presence of Lactose and Total Human Milk Carbohydrates. *Microorganisms*. 2020;8(10):1513. doi:10.3390/microorganisms8101513

45. Friedman J, Alm EJ. Inferring Correlation Networks from Genomic Survey Data. Von Mering C, ed. *PLoS Comput Biol*. 2012;8(9):e1002687. doi:10.1371/journal.pcbi.1002687

46. Duncan SH, Holtrop G, Lobley GE, Calder AG, Stewart CS, Flint HJ. Contribution of acetate to butyrate formation by human faecal bacteria. *Br J Nutr*. 2004;91(6):915-923. doi:10.1079/BJN20041150

47. Duncan SH, Barcenilla A, Stewart CS, Pryde SE, Flint HJ. Acetate Utilization and Butyryl Coenzyme A (CoA):Acetate-CoA Transferase in Butyrate-Producing Bacteria from the Human Large Intestine. *Appl Environ Microbiol*. 2002;68(10):5186-5190. doi:10.1128/AEM.68.10.5186-5190.2002

48. Hersoug L -G., Møller P, Loft S. Gut microbiota-derived lipopolysaccharide uptake and trafficking to adipose tissue: implications for inflammation and obesity. *Obes Rev*. 2016;17(4):297-312. doi:10.1111/obr.12370

49. Virtue AT, McCright SJ, Wright JM, et al. The gut microbiota regulates white adipose tissue inflammation and obesity via a family of microRNAs. *Sci Transl Med*. 2019;11(496):eaav1892. doi:10.1126/scitranslmed.aav1892

50. Fry JL, Al Sayah L, Weisbrod RM, et al. Vascular Smooth Muscle Sirtuin-1 Protects Against Diet-Induced Aortic Stiffness. *Hypertension*. 2016;68(3):775-784. doi:10.1161/HYPERTENSIONAHA.116.07622

51. Song NY, Lee YH, Na HK, Baek JH, Surh YJ. Leptin induces SIRT1 expression through activation of NF-E2-related factor 2: Implications for obesity-associated colon carcinogenesis. *Biochem Pharmacol*. 2018;153:282-291. doi:10.1016/j.bcp.2018.02.001

52. Okada T, Fukuda S, Hase K, et al. Microbiota-derived lactate accelerates colon epithelial cell turnover in starvation-refed mice. *Nat Commun*. 2013;4(1):1654. doi:10.1038/ncomms2668

53. Maifeld A, Bartolomaeus H, Löber U, et al. Fasting alters the gut microbiome reducing blood pressure and body weight in metabolic syndrome patients. *Nat Commun*. 2021;12(1):1970. doi:10.1038/s41467-021-22097-0

54. Ahima RS, Prabakaran D, Mantzoros C, et al. Role of leptin in the neuroendocrine response to fasting. *Nature*. 1996;382(6588):250-252. doi:10.1038/382250a0

55. Haynes WG, Morgan DA, Walsh SA, Mark AL, Sivitz WI. Receptor-mediated regional sympathetic nerve activation by leptin. *J Clin Invest*. 1997;100(2):270-278. doi:10.1172/JCI119532

56. Young JB, Landsberg L. Diminished sympathetic nervous system activity in genetically obese (ob/ob) mouse. *Am J Physiol-Endocrinol Metab*. 1983;245(2):E148-E154. doi:10.1152/ajpendo.1983.245.2.E148

57. Mark AL, Shaffer RA, Correia MLG, Morgan DA, Sigmund CD, Haynes WG. Contrasting blood pressure effects of obesity in leptin-deficient ob/ob mice and agouti yellow obese mice: *J Hypertens*. 1999;17(Supplement):1949-1953. doi:10.1097/00004872-199917121-00026

58. Simonds SE, Pryor JT, Ravussin E, et al. Leptin Mediates the Increase in Blood Pressure Associated with Obesity. *Cell*. 2014;159(6):1404-1416. doi:10.1016/j.cell.2014.10.058

59. Sutton EF, Beyl R, Early KS, Cefalu WT, Ravussin E, Peterson CM. Early Time-Restricted Feeding Improves Insulin Sensitivity, Blood Pressure, and Oxidative Stress Even without Weight Loss in Men with Prediabetes. *Cell Metab*. 2018;27(6):1212-1221.e3. doi:10.1016/j.cmet.2018.04.010

60. Azemi AK, Siti-Sarah AR, Mokhtar SS, Rasool AHG. Time-Restricted Feeding Improved Vascular Endothelial Function in a High-Fat Diet-Induced Obesity Rat Model. *Vet Sci*. 2022;9(5):217. doi:10.3390/vetsci9050217

61. Razzak RLA, Abu-Hozaifa BM, Bamosa AO, Ali NM. Assessment of enhanced endothelium-dependent vasodilation by intermittent fasting in Wistar albino rats. *Indian J Physiol Pharmacol*. 2011;55(4):336-342.

62. Cui J, Lee S, Sun Y, et al. Alternate Day Fasting Improves Endothelial Function in Type 2 Diabetic Mice: Role of Adipose-Derived Hormones. *Front Cardiovasc Med*. 2022;9:925080. doi:10.3389/fcvm.2022.925080

63. Wang L, Zhao XC, Cui W, et al. Genetic and Pharmacologic Inhibition of the Chemokine Receptor CXCR2 Prevents Experimental Hypertension and Vascular Dysfunction. *Circulation*. 2016;134(18):1353-1368. doi:10.1161/CIRCULATIONAHA.115.020754

64. Kasahara K, Krautkramer KA, Org E, et al. Interactions between Roseburia intestinalis and diet modulate atherogenesis in a murine model. *Nat Microbiol*. 2018;3(12):1461-1471. doi:10.1038/s41564-018-0272-x

65. Vacca M, Celano G, Calabrese FM, Portincasa P, Gobbetti M, De Angelis M. The Controversial Role of Human Gut Lachnospiraceae. *Microorganisms*. 2020;8(4):573. doi:10.3390/microorganisms8040573

66. Chen Y, Su J, Yan Y, et al. Intermittent Fasting Inhibits High-Fat Diet–Induced Atherosclerosis by Ameliorating Hypercholesterolemia and Reducing Monocyte Chemoattraction. *Front Pharmacol*. 2021;12:719750. doi:10.3389/fphar.2021.719750

67. Kelly CJ, Zheng L, Campbell EL, et al. Crosstalk between Microbiota-Derived Short-Chain Fatty Acids and Intestinal Epithelial HIF Augments Tissue Barrier Function. *Cell Host Microbe*. 2015;17(5):662-671. doi:10.1016/j.chom.2015.03.005

68. Furusawa Y, Obata Y, Fukuda S, et al. Commensal microbe-derived butyrate induces the differentiation of colonic regulatory T cells. *Nature*. 2013;504(7480):446-450. doi:10.1038/nature12721

69. Chen G, Ran X, Li B, et al. Sodium Butyrate Inhibits Inflammation and Maintains Epithelium Barrier Integrity in a TNBS-induced Inflammatory Bowel Disease Mice Model. *eBioMedicine*. 2018;30:317-325. doi:10.1016/j.ebiom.2018.03.030

70. Aguilar EC, Leonel AJ, Teixeira LG, et al. Butyrate impairs atherogenesis by reducing plaque inflammation and vulnerability and decreasing NFκB activation. *Nutr Metab Cardiovasc Dis*. 2014;24(6):606-613. doi:10.1016/j.numecd.2014.01.002

71. Thaler JP, Yi CX, Schur EA, et al. Obesity is associated with hypothalamic injury in rodents and humans. *J Clin Invest*. 2012;122(1):153-162. doi:10.1172/JCI59660

72. Jais A, Paeger L, Sotelo-Hitschfeld T, et al. PNOCARC Neurons Promote Hyperphagia and Obesity upon High-Fat-Diet Feeding. *Neuron*. 2020;106(6):1009-1025.e10. doi:10.1016/j.neuron.2020.03.022

73. Cienfuegos S, Corapi S, Gabel K, et al. Effect of Intermittent Fasting on Reproductive Hormone Levels in Females and Males: A Review of Human Trials. *Nutrients*. 2022;14(11):2343. doi:10.3390/nu14112343

74. Deshmane SL, Kremlev S, Amini S, Sawaya BE. Monocyte Chemoattractant Protein-1 (MCP-1): An Overview. *J Interferon Cytokine Res*. 2009;29(6):313-326. doi:10.1089/jir.2008.0027

75. Hamza T, Barnett JB, Li B. Interleukin 12 a Key Immunoregulatory Cytokine in Infection Applications. *Int J Mol Sci*. 2010;11(3):789-806. doi:10.3390/ijms11030789

76. Korbecki J, Maruszewska A, Bosiacki M, Chlubek D, Baranowska-Bosiacka I. The Potential Importance of CXCL1 in the Physiological State and in Noncancer Diseases of the Cardiovascular System, Respiratory System and Skin. *Int J Mol Sci*. 2022;24(1):205. doi:10.3390/ijms24010205

CHAPTER 4: ASSESSING THE POTENTIAL DISCORDANT EFFECTS OF INTERMITTENT FASTING ON CARDIOVASCULAR HEALTH AND ACUTE SARS-COV-2 INFECTION

SUMMARY

Intermittent fasting improves cardiovascular health through restructuring the gut microbiota and reducing chronic, low-grade systemic inflammation. Reducing incessant inflammation is paramount for cardiovascular health, yet an active immune response is needed to resolve acute infection. Although the peak of the COVID-19 pandemic is in the rearview, SARS-COV-2 is still a widespread pathogen that causes severe health complications in the short- and long-term. Therefore, in this study, we addressed the potential discordant effects of intermittent fasting on cardiovascular health (arterial stiffness) and SARS-CoV-2 infection. Lean and obese mice were randomized to either *ad libitum* feeding or once-weekly 24-hour intermittent fasting for 12 weeks. At week 10, arterial stiffness was measured via pulse wave velocity. After 12 weeks, mice were inoculated with SARS-CoV-2 and measurements were taken 3- and 7 days post inoculation. Once-weekly 24-hour intermittent fasting reduced arterial stiffness in obese mice. Compared to *ad libitum* infected controls, once-weekly 24-hour intermittent fasting did not substantially alter infection-associated weight loss, anorectic behavior, body surface temperature, lung viral burden, or plasma S1- and S2 IgG titers in either lean or obese mice. Obese intermittent fasting mice exhibited relatively higher lung CD11b+ CD11c- MHCII- cells ($p<0.01$) and lower CD62L/CD86-expressing B cells ($p\leq 0.01$) at 3 days post SARS-CoV-2 infection. However, these alterations were transient and not apparent 7 days post infection. Finally, intermittent fasting did not significantly impact gut microbial composition during SARS-COV-2 infection in either lean or obese mice. Taken together, this is the first study to directly investigate the impact of intermittent fasting on cardiovascular health and SARS-CoV-2 infection in lean and obese mice. Our results suggest that once-weekly 24-hour intermittent fasting is a safe and efficacious in reducing obesity-related arterial stiffness without substantially impacting acute SARS-CoV-2 infection severity.

INTRODUCTION

Intermittent fasting (IF), repetitive periods of little-to-no energy intake (≤ 48 hrs.)[1] followed by *ad libitum* eating, continues to emerge as one of the most popular dietary strategies globally [2,3]. The popularity of IF may be due to its focus on when to eat rather than what to eat, the variety of approaches available, and its purported health benefits. Recent studies have investigated the efficacy of IF in ameliorating cardiovascular disease (CVD), the leading cause of death in the United States for the past century [4]. We have determined that once-weekly 24-hour IF attenuates obesity-related arterial stiffness, an independent predictor of CVD onset and mortality [5,6]. Arterial de-stiffening in obese mice was associated with profound changes to the gut microbiota, a crucial immune primer [7], and large-scale immunosuppression as highlighted by reductions in pro-inflammatory chemokines. Although most of our results were pertinent to obese mice, we also found that IF reduced circulating pro-inflammatory chemokines (CCL5, CCL3, and CCL7, CCL2) in lean mice, suggesting that IF might also impact the inflammatory response in lean mice.

The immune system is paramount during infection, clearing and neutralizing the pathogens while inducing immune memory to reduce the impact of secondary exposure. However, fasting can also alter immune cell redistribution, which has been proposed to exacerbate infection responses. For instance, Janssen et al.[8] discovered that Ly6C^{hi} monocytes that migrate to the bone marrow during fasting exhibit a surge to the lung parenchyma in response to refeeding and an intranasal LPS challenge. Additionally, a 24-hour fast followed by a 12-hour refeed increased myeloid cell recruitment to the lung parenchyma, elevated circulating cytokines, and accelerated death after *Pseudomonas aeruginosa* (PAE) inoculation [8]. Other longer-term IF studies show similar results, as 10 days of ADF exacerbated sickness behavior and plasma cytokine levels in response to intraperitoneal Poly(I:C) (TLR3 agonist) injection [9]. However, mice within the ADF group were fasted during data collection, which could indicate that the exacerbated responses were due to the single fast rather than the cumulative effects of ADF. Thus, the impacts of recurrent fasting bouts (chronic IF) on infection remain unclear. Our previous results suggest that the immunosuppressive effects of once-weekly 24-hour IF fasting could worsen acute infections. Despite our

positive cardioprotective findings, this potential concern limits the widespread endorsement of chronic IF as an all-encompassing “healthy” diet.

Although the peak of the COVID-19 pandemic is behind us, SARS-CoV-2 is still a common respiratory pathogen that can lead to acute and long-term health complications due to its actions on the musculoskeletal, neurological, and cardiorespiratory systems [10,11]. The gut microbiota and immune system are critical determinants of SARS-COV-2 infection severity and symptom resolution [12–15], raising the question of whether chronic IF could predispose the host to more severe SARS-COV-2 infection. Furthermore, since we’ve observed that IF preferentially affects the gut microbiota and immune system in obese mice, and obesity is a significant risk factor for more severe SARS-COV-2 infection[16], it is plausible that IF results in exacerbated SARS-COV-2 infection. Lastly, there is almost no data investigating the effect of IF on SARS-COV-2 infection. Some of the only available data are from observational studies that determined periodic fasting was associated with lower SARS-CoV-2 severity and less heart failure-associated hospitalization in COVID-19-positive patients[17,18]. Yet, these results could be confounded by the fact that the non-fasting cohort included a significantly higher proportion of smokers (prior or current) and higher levels of diabetes, COPD and asthma [17,18].

Therefore, this study is the first to directly examine whether chronic IF has discordant effects on cardiovascular health and SARS-COV-2 infection. We show that multi-week, once-weekly 24-hour IF reduces arterial stiffness in obese mice without substantially impacting lung SARS-COV-2 titers in either lean or obese mice. Moreover, IF did not dramatically impact infection-associated weight loss, circulating SARS-COV-2-specific antibodies, gut microbial ecology, or lung and spleen immune cell populations in either lean or obese mice. These findings reveal that once-weekly 24-hour fasting could be a safe and feasible dietary strategy to improve cardiovascular health with minimal impacts on acute SARS-COV-2 infection.

METHODS

Animals, Experimental Design, and Euthanasia Procedures

Animals were maintained in a BSL-3 facility at Colorado State University and all animal procedures were reviewed and approved by the Colorado State University Institutional Animal Care and Use Committee (protocols 3324 and 1369).

Intermittent Fasting and SARS-CoV-2 Infection Protocol

Five-week old lean (C57BL/6J; WT; n=30) and genetically obese (B6.Cg-*Lep*^{ob}/J; Ob; n=30) mice were obtained from Jackson Laboratories (Bar Harbor, ME). Mice were co-housed in a conventional facility under a 12:12 hour light/dark photocycle with access to standard rodent chow (Envigo 2918; irradiated diet consisting of 44.2% carbohydrates, 6.2% fat, and 18.6% protein) and normal drinking water. Mice were acclimated for two weeks with *ad libitum* chow and water. After acclimation, mice were randomized into two groups to receive an *ad libitum* (AL) diet or a once-weekly 24-hour intermittent fasting (IF) for 12 weeks (WT+AL, WT+IF, Ob+AL, and Ob+IF). At week 10 of the 12-week protocol, WT+AL, Ob+AL, and Ob+IF were subjected to pulse wave velocity for 4-5 days during the 24-hour fast. We did not subject WT+IF mice to PWV, as our previous results show that IF does not reduce arterial stiffness in WT mice. We were also particularly interested in recapitulating our previous results of an ntermediate vascular phenotype observed in Ob+IF mice compared to WT+AL and Ob+AL mice. During week 11, all IF mice and half of the AL mice were transferred to a biosafety level 3 (BSL-3) laboratory for acclimation prior to viral inoculation. Thus, the last 24-hour fast was done in BSL3. Body weight and food intake were measured weekly during cage and water changes.

After 12 weeks, body surface temperature was recorded with a standard infrared thermometer and all mice in BSL3 were inoculated with SARS-CoV-2 (MA10 mouse-adapted strain; SC2) while mice held in the conventional facility were inoculated with sterile saline (1x PBS), yielding six distinct groups (10 mice per group): WT+AL, WT+AL+SC2, WT+IF+SC2, Ob+AL, Ob+AL+SC2, Ob+IF+SC2. Following inoculation, all mice were given food *ad libitum*. At 3- and 7 days post-inoculation (DPI), 5 mice per group

per time point were assessed for body temperature, body weight, food intake, and feces were collected. Mice were anesthetized with isoflurane and euthanized by exsanguination via cardiac puncture. Blood was collected via 1 mL syringe coated with 0.5 M EDTA (no. 15575020; Invitrogen) and then placed into EDTA coated BD Microtainer™ Capillary Blood Collectors (BD365974). Plasma was obtained by centrifugation at 2,000 g for 10 min at 4°C. The plasma was immediately flash-frozen in liquid nitrogen and stored at -80°C until downstream analyses. The spleen and left lobe of the lung were excised and placed into cold Corning™ RPMI 1640 Medium 1X without L-Glutamine (MT15040CV) and kept on ice until downstream processing. The right superior and middle lobe were excised and placed into 1.5mL luer locked tubes with three stainless steel homogenizer beads per tube pre-filled with viral transport media (VTM; sterile Hanks Balanced Salt Solution (HBSS), 2% FBS, 100 µg/mL Gentamicin, 0.5 µg /mL Amphotericin B), homogenized and transferred to the -80 freezer until downstream analyses.

Measurement of Arterial Stiffness

Aortic pulse wave velocity (PWV) was used to determine *in vivo* arterial stiffness using a Doppler Flow Velocity System (Indus Instruments, Webster, TX) via methods described previously by our laboratory[19–21]. PWV (in cm/s) was calculated as PWV = (distance between the two probes)/($\Delta time_{abdominal} - \Delta time_{carotid}$).

Experimental Infection

SARS-CoV-2 MA10 was provided by Dr. Richard Bowen (Colorado State University). Stocks were prepared by infection of Vero E6 cells for two days when the cytopathic effect (CPE) was starting to be visible. Media was collected and clarified by centrifugation before being aliquoted for storage at −80°C. The stock titer (3.1 x 10^5 PFU/mL) was determined by plaque assay using Vero E6 cells as described previously [22]. The stock titer was diluted to 5 x 10^3 PFU in 40 uL of sterile saline for intranasal inoculations. During infection, mice were anesthetized with isoflurane, and 40 uL of the 5 X 10^3 PFU inoculum (20 uL in each nostril) was inoculated intranasally. Control mice were intranasally injected with 40 uL of sterile saline.

Lung SARS-CoV-2 Titers

In MA10-infected mice, lung SARS-CoV-2 titers were quantified by a median tissue culture infectious dose ($TCID_{50}$) assay. Briefly, the middle and upper portions of the right lung lobe were homogenized, and Vero E6 cells (ATCC CRL-1568) were grown to 90-100% confluency on 24-well cell culture plates at 37°C with 5% CO_2. Plates were washed with Dulbecco's Phosphate-Buffered Saline (DPBS, without calcium and magnesium), and 8-point, 5-fold dilutions of lung homogenate were added to wells. At least 4 replicates for each dilution were used. Incomplete media and Wuhan strain (provided by Dr. Richard Bowen) were used as positive and negative controls, respectively. After 1 hour of incubation, lung homogenate was removed, cells were washed with DPBS, and 500 uL of an agarose-media mix (Dulbecco's Modified Eagle Medium (DMEM) with 0.6% agarose and 4% FBS) were added to each well. Cells were incubated for 3 days at 37°C, with 5% CO_2. After 3 days, 4% 500 uL of paraformaldehyde (PFA) was added on top of the agarose mix in each well, and plates were incubated for 1 hour. PFA and the agarose mix were gently discarded, and 0.5% crystal violet dye solution was added to each well. After 5 minutes of incubation, plates were washed with DPBS and allowed to air dry for at least one day. The number of wells with visible CPE for each dilution was determined, and $TCID_{50}$/mL was calculated using the Improved Kärber Method [23].

Circulating S1 and S2 Antibody ELISAs

High-binding 96-half-well microplates (Corning, 9018) were coated with 50 uL of 50 ng recombinant spike 1 (S1) (40591-V08H-100) or spike 2 (S2) (40590-V08B-100) subunits overnight at 4°C. The next day, plates were washed five times with 180 uL of wash buffer (1X PBS with 0.05% Tween 20, and 180 uL of blocking buffer (1X PBS with 0.05% Tween 20, 2% BSA, and 2% normal goat serum (Jackson immunoresearch, 005-000-121) was added to each well. After two hours of incubation, 100 uL of diluted plasma (4-point, 5-fold dilutions) were added to each well in duplicate. Blocking buffer was used as a negative control. Plates were incubated for 1 hour and then washed 5 times with wash buffer. Next, 100 uL of horseradish peroxidase (HRP)-conjugated goat-anti-mouse IgG (Jackson

Immunoresearch, 115-035-003) (1:5000 dilution in blocking buffer) was added to each well, and plates were incubated for one hour. After 5X washes, 100 uL of TMB substrate was added to each well, followed by 50 uL of stop solution (1M sulphuric acid). Absorbance at 450 nm was immediately measured using a BioTek Synergy 2 plate reader (BioTek Instruments Inc., Winooski, VT, USA). Endpoint titers were calculated using the ELISA-R pipeline [24].

Spleen and Lung Immune Cell Isolation and Flow Cytometry on Single Cell Suspensions

In SC2-infected mice, spleens were homogenized using a syringe plunger and passed through a 70 μm filter to prepare a single-cell suspension. The left lobe of the lung was isolated, lightly scored with a sterile razor, and treated with digestion solution (RPMI-1640 medium with DNase IV (500 units/mL, D5025) and Liberase (0.5 mg/mL, 5401127001)) for 30 min at 37°C to dissociate and digest pulmonary collagen. The tissue was then homogenized and passed through a 70 μm filter. Erythrocytes were lysed using ACK Lysis Buffer (A1049201). Spleen and lung single cell suspensions were seeded into 96-well V-bottom plates, washed, and stained with Zombie NIR live/dead stain (Biolegend, 423105) for 15 minutes at room temperature in the dark. Cells were washed and incubated with Fc block solution (Biolegend, 101319) at 4°C for 20 min, protected from light, and then further stained with optimal titrations of specific surface antibodies at 4°C for 30 min, protected from light. The antibodies (catalog number regarding antibody clone, titration) used to identify broad lung and spleen immune cells subset at 3- and 7 DPI were as follows **(Table 4.S4)**: Brilliant Violet 570™ anti-mouse CD45 (103136, 1:200); PE anti-mouse CD335 (NKp46), (137604, 1:400); Alexa Fluor® 532 Anti-Mouse CD3 (58-0032-82, 1:100); Brilliant Violet 605™ anti-mouse CD19 (115539, 1:200); PE/Dazzle™ 594 anti-mouse CD62L (104447, 1:400); PE/Cyanine7 anti-mouse CD86 (105013, 1:200); Pacific Blue™ anti-mouse/human CD11b (101224, 1:200); Brilliant Violet 785™ anti-mouse CD11c (117335, 1:400); PerCP anti-mouse Ly-6G (127653, 1:100); and BD Horizon™ BV480 Rat Anti-Mouse I-A/I-E (566088, 1:600). After staining, cells were fixed with 4% paraformaldehyde (J61899.AP) at room temperature for 20 min, protected from light. Cells were washed and left at 4°C overnight in FACS buffer (00-4222-26). Cell counts were acquired the following

day using a Cytek® Aurora 4L flow cytometer. Splenocyte and lung immune cell subpopulations were identified by a pre-determined gating strategy **(Figure 4.S1)** on Flowjo (version 10.9).

Sample Collection, Processing, and Analyses of 16s rRNA Amplicon Sequencing Data

Stool samples from all mice were collected fresh, immediately placed on ice, and then stored at -80°C until DNA extraction. Fecal DNA extraction was completed using the FastDNA® Kit (MP Biomedicals, 116540400) per the manufacturer's protocol. Quantitative PCR was used to quantify total fecal 16srRNA DNA. Reactions were optimized for the 16s rRNA gene using universal bacterial primers (forward 5′-AAACTCAAAKGAATTGACGG-3′, reverse 5′-CTCACRRCACGAGCTGAC-3′). Cycling conditions using the Bio-Rad C1000 Touch thermal cycler were as follows: 95°C for 3 min and then 40 cycles of 95°C 15 s, 61°C 15 s, 72°C 10 s, 85°C 5 s followed by fluorescence detection. To calculate total fecal 16srRNA DNA, quantified amounts (ng) of 16s rRNA amplicons generated from DNA obtained from pooled fecal samples from experimental mice were serially diluted to create standard curves.

Amplification of the V4 region of the 16S rRNA gene was carried out following the Earth Microbiome Project protocol using the 515F-806R primer set [25] containing a unique Golay 12bp error-correcting barcode included on the forward primer. Cycling and sequencing conditions were carried out as previously described[20]. DNA extraction controls, no template PCR controls, and the Zymo mock community (Zymo Research, D6305) were included on each sequencing plate. Sequence reads were imported into QIIME2 (version 2023.5) for quality filtering [26]. Briefly, sequence reads were demultiplexed and examined for quality filtering utilizing a Phred score cutoff of 30. All analyses proceeded with single-end forward read sequences. Fecal sequences from the SC2 study were truncated to 157 base pairs. All reads were binned into sub-OTUs (sOTUs) using the Deblur pipeline implementation in QIIME2[27]. Taxonomic assignments were made using Silva (version 13.8) [28]. Samples with low reads or suspected contamination were removed, and mitochondrial and chloroplast sequences were filtered from the remaining samples.

The resulting feature tables and taxonomy files were combined and imported with corresponding metadata into MicrobiomeAnalyst for secondary workflow [29]. Based on sample prevalence, the minimum

count filter was set at 4, and the low count filter was set at 10%. Data normalization was performed based on total sum scaling. Alpha diversity was examined utilizing the Shannon diversity index at the genus taxonomic level, and beta diversity was calculated using Bray-Curtis distances at the genus taxonomic level.

Statistical Analyses

Data are presented as either mean ± standard error of the mean (SEM), mean with individual values (scatterpoints), or the log2 fold change between groups. Data analyses and visualizations were conducted in GraphPad Prism (version 9) or Rstudio (2024.04.1+748) using the ggplot2 package. One-way ANOVAs followed by Tukey's multiple comparisons test examined differences between groups. If the data violated the assumption of homoscedasticity, a Welch ANOVA followed by Dunnett's T3 multiple comparisons test was used instead of the one-way ANOVA. Two-way ANOVAs (Type II SS's) followed by Tukey's multiple comparisons test were used to analyze interactions between group and time (DPI). Mixed effect linear regression models with a Kenward-Roger's degrees of freedom approximation and Type II analyses of variance table output were used for repeated measures data. In these models, group and time points were fixed effects, and individual mouse ID was the random effect. If data were heteroscedastic, robust standard errors were used for the two-way ANOVAs or mixed effect models. Beta diversity was analyzed using permutational multivariate analysis of variance (PERMANOVA) and community dispersion was assessed by permutational multivariate analysis of dispersion (PERMDISP). Differences in microbial features between groups were examined via a consensus analysis, which included Mann-Whitney (FDR adjusted p-value=0.05), negative binomial (EdgeR, FDR adjusted p-value=0.05), and linear discriminant analysis effect size (LEfSe, FDR adjusted p-value=0.1, fold change cutoff=2.0) tests. A p-value $\leq$ 0.05 was considered statistically significant unless otherwise indicated.

RESULTS

Repeated Bouts of Once-Weekly 24-Hour Intermittent Fasting Reduced Obesity-Related Arterial Stiffness Without Substantially Impacting Acute SARS-CoV-2 Infection

The experimental design is presented in **Figure 4.1A**. As previously reported, once-weekly 24-hour IF reduced obesity-related related arterial stiffness without impacting body weight or food intake (**Figure 4.1B**). As in our previous results, this indicates that the arterial de-stiffening effects of once-weekly 24-hour IF are not due to weight loss in obese mice.

During acute SC2 infection, no changes in body weight were observed between WT groups **(Figure 4.1C)**. Similarly, no differences in body weight were observed between Ob+AL+SC2 and Ob+IF+SC2 mice **(Figure 4.1C)**. However, at 3 DPI, body weight of the Ob+AL controls was significantly lower than the Ob+IF+SC2 mice (59.1 ± 1.3g vs. 55.3 ± 1.7g, p=0.03), likely due to an acute dip in Ob+AL body weight after mock infection (week 12 vs 3 DPI in Ob+AL mice: 59.1 ± 1.3g vs. 55.3 ± 1.7g, p=0.03). We found no significant differences in body weight between Ob+AL mice and the infected groups at 7 DPI **(Figure 4.1C)**, suggesting that this dip in Ob+AL body weight was transient. These unsubstantial changes in body weight during infection correspond to previous results, suggesting that at least 10^4 PFU of SC2 MA10 is needed to observe significant weight loss in mice[30,31]. Moreover, we observed reductions in food intake in all SC2 infected groups (**Figure 4.1C)**, which is common during infection[32].

Compared to AL controls, IF did not differentially impact surface body temperature during infection in either WT or Ob mice ($p_{interaction}$=0.12) **(Figure 4.1D)**. We did observe lower temperatures 3 DPI compared to 7 DPI (p_{time}=0.02); however, this was probably driven by Ob mice as their temperature changes between 3 and 7 DPI were more robust (Ob+AL+SC2 mice: 29.8 ± 0.2℃ vs. 32.0 ± 0.40 ℃; Ob+IF+SC2 mice 29.2 ± 0.1℃ vs. 31.5 ± 0.1℃) than WT mice (WT+AL+SC2 mice: 31.8 ± 0.6℃ vs. 31.7 ± 0.2 ℃; WT+IF+SC2 mice 31.0 ± 0.2℃ vs. 31.2 ± 0.2℃). There were no significant differences in temperature between 0 and 7 DPI in any of the groups.

There were no differences in lung SARS-CoV-2 titers at 3 DPI **(Figure 4.1E)**. Virus was not detected in the lungs in any infected group at 7 DPI (data not shown), suggesting SC2 clearance at 7 DPI,

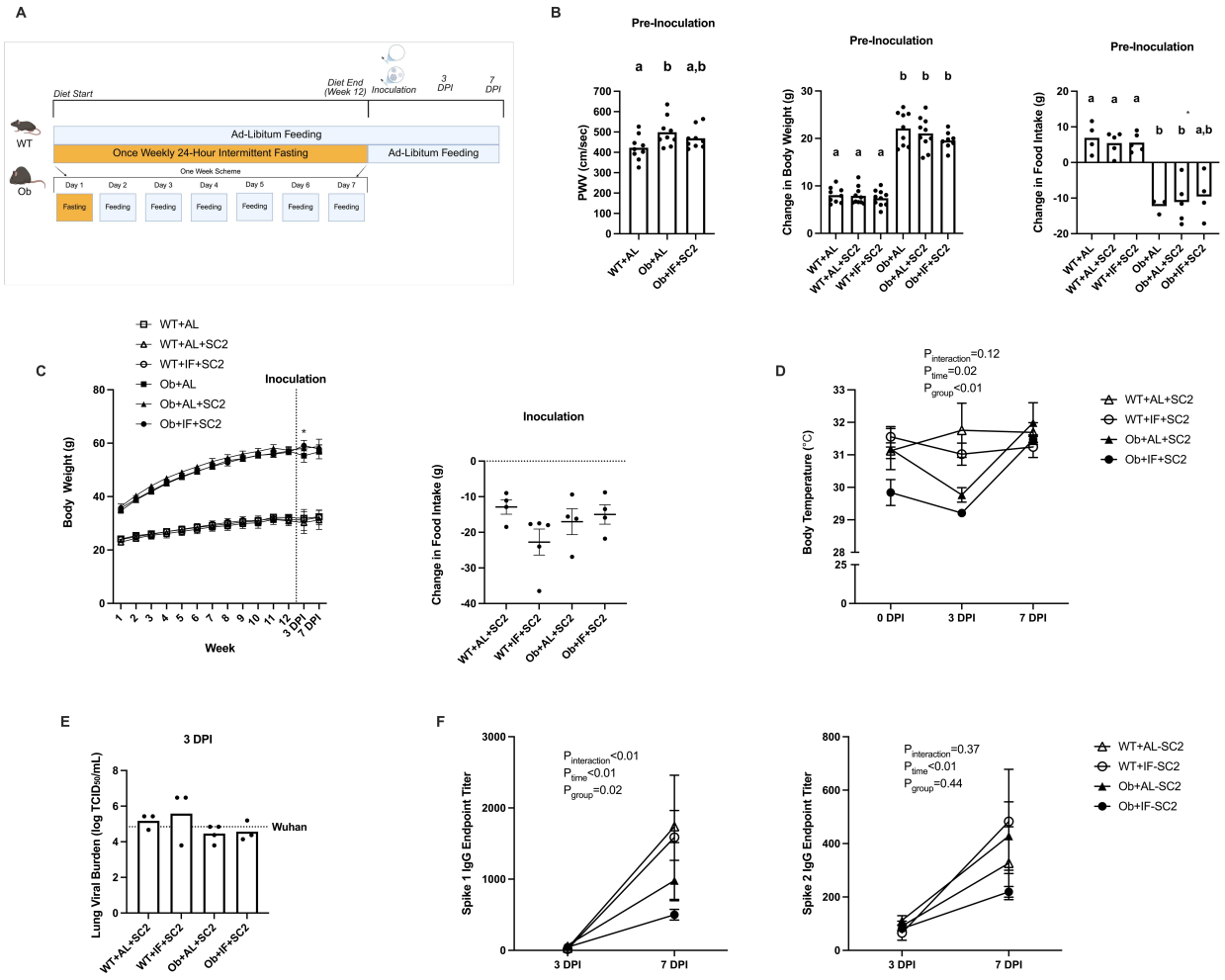

Figure 4.1. Once-weekly 24-hour intermittent fasting reduced obesity-related arterial stiffness without substantially impacting SARS-CoV-2 infection. A) Schematic of experimental design. Created at Biorender.com. **B)** Pre-inoculation pulse wave velocity (**left**), changes in body weight (**middle**), and changes in food intake (**left**). N=6-10 mice per group. **C)** Changes in body weight pre- and post-inoculation **(left)** and changes in food intake post-SARS-CoV-2 inoculation (**right**). N=9-10 mice per group per week (pre-infection), 4-5 mice per group per DPI, and N=4-5 cages per group, respectively. **D)** Changes in body surface temperature during SARS-CoV-2 infection. N=5-10 mice per group per DPI. **E)** Lung SARS-CoV-2 titers (burden) at 3 days post-inoculation. N=3-4 mice per group. Incomplete media and Wuhan strain (provided by Dr. Richard Bowen) were used as positive and negative controls, respectively. **F)** Changes in plasma S1- (**left**) and S2- (**right**) IgG endpoint titers during SARS-CoV-2 infection. N=3-5 mice per group per DPI. WT=lean; Ob=obese; AL=*ad libitum* feeding; IF=once-weekly 24-hour intermittent fasting; SC2=SARS-CoV-2 (MA10) infection; DPI= days post-inoculation. Different letters indicate significant differences between groups.* indicates a p-value less than 0.05 between Ob+AL vs Ob+IF+SC2.

as previously reported[30]. These results also indicate a similar time-course of acute SC2 infection between AL and IF mice, regardless of genotype. Spike 1 (S1) IgG endpoint titers were significantly elevated at 7 dpi compared to 3 DPI in all groups except for WT+IF+SC2 mice in which titers were still elevated but did not reach statistical significance (1587.0 ± 872.3 vs. 17.9 ± 10.3, p=0.12) **(Figure 4.1F)**. However, this result is likely due to the large variability in S1 IgG titers at 7 DPI, and on average, this group seemed to manifest an appropriate antibody response towards acute SC2 infection. Furthermore, pairwise comparisons revealed no significant differences in S1 IgG endpoint titers between WT+AL+SC2 and WT+IF+SC2 mice (3 DPI: 33.3 ± 19.3 vs. 17.9 ± 10.3, p=0.93) (7 DPI: 1738.7 ± 225.5 vs. 1587.0 ± 872.3, p=0.99) or Ob+AL+SC2 and Ob+IF+SC2 mice (3 DPI: 71.9 ± 9.9 vs. 46.1 ± 7.7, p=0.31) (7 DPI: 981.2 ± 283.4 vs. 501.05 ± 74.9, p=0.47) **(Figure 4.1F)**. Although Ob+IF+SC2 mice appeared to exhibit a diminished S1 IgG antibody response, this is likely not the case, as Ob+AL+SC2 mice had greater heterogeneity (range: 213.9-1954.8) compared to Ob+IF+SC2 mice (265.1-733.7). Similar overall results were found for Spike 2 (S2) IgG endpoint titers, as after adjusting for group, titers were significantly elevated at 7 DPI compared to 3 DPI (364.2 ± 66.4 vs. 89.3 ± 10.0, p<0.01). We found nonsignificant pairwise differences between WT+AL+SC2 and WT+IF+SC2 mice (3 DPI: 91.3 ± 18.5 vs. 65.8 ± 27.8, p=0.91; 7 DPI: 326.6 ± 136.5 vs. 482.7 ± 195.3, p=0.94) or Ob+AL+SC2 and Ob+IF+SC2 (3 DPI: 112.6 ± 17.6 vs. 81.6± 13.8, p=0.62; 7 DPI: 428.2 ± 128.0 vs. 219.3 ± 20.0, p=0.48) at either 3- or 7 DPI **(Figure 4.1F)**. Taken together, these data provide evidence that once-weekly 24-hour fasting reduces obesity-related arterial stiffness without substantially exacerbating acute SARS-CoV-2 infection severity or antibody responses in lean or obese mice.

Effect of Intermittent Fasting on Immune Cell Responses in the Lungs and Spleen During SARS-CoV-2 Infection

Next, we investigated whether IF mice had altered lung and spleen immune cell frequencies during SC2 infection **(Figure 4.S1A-4.S1B)**. Overall, these results were heterogeneous, making it challenging to decipher whether IF altered immune cell frequencies during SC2 infection. During flow

cytometry analysis, we noticed that several spleen samples, particularly within AL+SC2 groups at 7 DPI, had an overabundance of dead immune cells (≥50% of singlets in 3/5 mice in both genotypes). Because of this heterogeneity, there were no significant pairwise differences in dead splenocytes between any of the infected groups at 7 DPI. Additionally, within the same group, mice with a high proportion of dead splenocytes had noticeably different frequencies of live splenocyte subsets compared to those with a low proportion of dead splenocytes. Although including these samples would have increased our sample size, it would have confounded our results and likely limited our power to detect meaningful differences in live immune cell proportions. Thus, we proceeded with a sample size of 2-5 mice per group per DPI for spleen and 3-5 mice per group per DPI for lung.

In both WT and Ob mice, IF did not substantially alter the proportion of major lung and spleen immune cell populations during SC2 infection, including $CD3^+$ cells (T cells) and $NKp46^+$ cells (NK cells), $Ly6G^+$ cells (neutrophils), and $CD11b^-$ $CD11c^+$ cells **(Figure 4.2A-4.2D)**. IF did not impact lung or spleen $CD11b^+$ $CD11c^+$ or $CD11b^+$ $CD11c^-$ cell frequencies in WT mice (**Figure 4.2E-4.2F)**. However, lung $CD11b^+$ $CD11c^+$ and $CD11b^+$ $CD11c^-$ frequencies were significantly increased at 7 DPI compared to 3 DPI in Ob+AL+SC2 mice, whereas they were stable in Ob+IF+SC2 mice (**Figure 4.2E-4.2F)**. Furthermore, the $CD11b^+$ $CD11c^-$ subset was significantly higher in Ob+IF+SC2 mice compared to Ob+AL+SC2 mice at 3 DPI ($p<0.01$), but not 7 DPI ($p=0.97$) (**Figure 4.2F)**. Gating of lung $CD11b^+$ $CD11c^+$ and $CD11b^+$ $CD11c^-$ cells by MHCII identified these subsets as $CD11b^+$ $CD11c^+$ $MHCII^-$ and $CD11b^+$ $CD11c^-$ $MHCII^-$ cells, respectively (**Figure 4.S2A-4.S2D)**.

Finally, although the proportion of lung $CD19^+$ cells (B cells) did not change over the course of infection between groups ($p_{interaction}=0.74$), their frequency was suppressed in Ob+IF+SC2 mice compared to Ob+AL+SC2 mice throughout infection (0.42 ± 0.03 vs. 0.33 ± 0.04, $p=0.06$) **(Figure 4.2G)**. When gating on lung B cells by their expression of CD62L and CD86, we observed less lung $CD62L^+$ $CD86^+$ B cells ($p=0.01$) and $CD62L^-$ $CD86^+$ B cells ($p<0.01$) at 3 DPI in Ob+IF+SC2 mice compared to Ob+AL+SC2 mice (**Figure 4.S2E-4.S2F)**. No differences were found at 7 DPI. IF did not impact $CD62L^+$ $CD86^-$ or $CD62L^-$ $CD86^-$ B cell frequencies during infection **(Figure 4.2S2G-4.S2H)**.

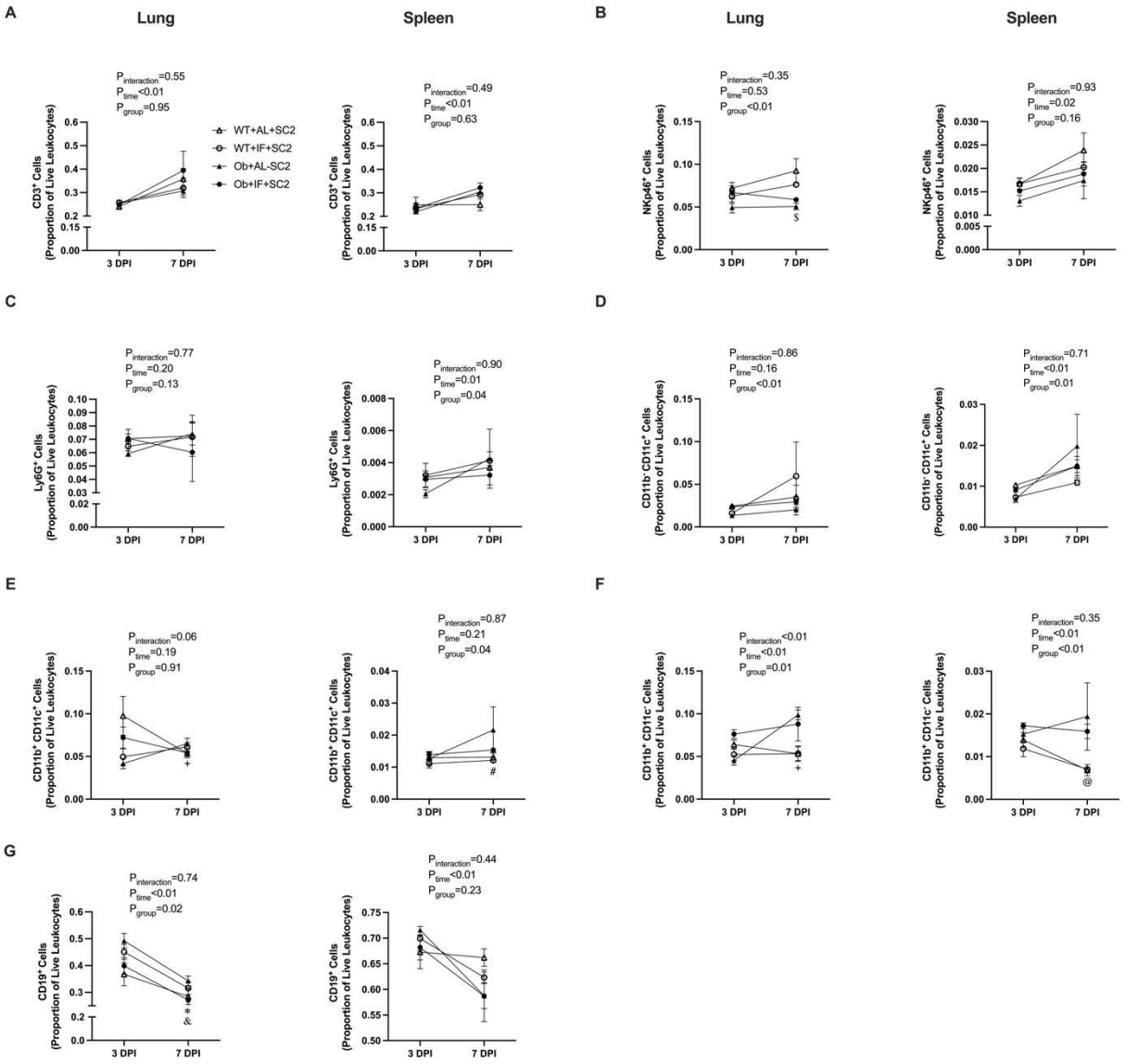

Figure 4.2. Effect of intermittent fasting on immune cell proportions during SARS-CoV-2 infection. Proportion of $CD3^+$**A)** $NKp46^+$ **B)** $Ly6G^+$ **C)** $CD11b^-$ $CD11c^+$ **D)** $CD11b^+$ $CD11c^+$ **E)** $CD11b^+$ $CD11c^-$ **F)** and $CD19^+$ **G)** cells in lung **(left)** and spleen **(right)** during SARS-CoV-2 infection. N=2-5 mice per group per DPI. WT=lean; Ob=obese; AL=*ad libitum* feeding; IF=once-weekly 24-hour intermittent fasting; SC2=SARS-CoV-2 (MA10) infection; DPI= days post-inoculation. $^{\$}$ indicates a p-value of less than 0.05 between Ob+AL+SC2 vs WT+AL+SC2 and WT+IF+SC2. $^{+}$ indicates a p-value of less than 0.05 between 3- and 7 DPI in Ob+AL+SC2 mice. $^{\#}$ indicates a p-value of less than 0.05 between Ob+IF+SC2 and WT+IF+SC2. $^{@}$ indicates a p-value of less than 0.05 between Ob+IF+SC2 vs WT+AL+SC2 and WT+IF+SC2.*indicates a p-value of 0.06 between Ob+AL+SC2 vs Ob+IF+SC2. $^{\&}$ indicates a p-value of less than 0.05 between Ob+AL+SC2 vs WT+AL+SC2.

Ad libitum and Intermittent Fasting Mice Have Similar Gut Microbial Profiles Following SARS-CoV-2 Infection

IF can impact the gut microbiota and changes to the gut microbiota during SARS-CoV-2 infection can influence infection severity [12–15]. Thus, we also assessed whether IF impacted gut microbial responses towards SC2 infection and whether responses differed between WT and Ob mice. Shannon's index (alpha diversity) was similar between AL and IF infected mice, regardless of genotype **(Figure 4.3A)**. However, after adjusting for time, alpha diversity was overall greater in Ob+IF+SC2 mice compared to Ob+AL controls ($p<0.01$) **(Figure 4.3A)**. Total fecal microbial load (16s rRNA DNA) was similar between AL and IF infected mice, regardless of genotype **(Figure 4.3B)**. Principal Coordinates Analyses of Bray-Curtis distances revealed substantial clustering of gut microbial composition between mice inoculated with PBS and SC2. Clustering was particularly evident along PCoA axis 1 in WT mice and PCoA axis 2 in Ob mice (after accounting for time) (**Figure 4.3C-4.3D)**.

When stratified by time (DPI), there were no differences in gut microbial beta diversity within WT mice. However, pairwise PERMANOVA analyses revealed differences in Ob+AL and Ob+AL+SC2 mice at 3 DPI (FDR-adjusted $p=0.04$) as well as Ob+AL and Ob+IF+SC2 mice at 7 DPI (FDR-adjusted $p=0.04$) **(Table 4.S1)**. To further characterize these differences, the differential relative abundance of feature-level sOTUs were determined by identifying consensus sOTUs across different algorithms. Compared to PBS-inoculated controls, the EdgeR algorithm identified relative increases in *Muribaculaceae*_159 and relative decreases in *Marvinbryantia*_34 in Ob+AL+SC2 mice at 3 DPI and Ob+IF+SC2 mice at 7 DPI **(Tables 4.S2-4.S3)**. However, EdgeR was the only algorithm out of three to identify any differential abundances. Thus, the consensus analysis failed to robustly identify microbes differentially abundant between Ob+AL and Ob+AL+SC2 mice at 3 DPI or Ob+AL and Ob+IF+SC2 mice at 7 DPI. As expected, the consensus analysis also failed to identify differentially abundant microbes between PBS- and SC2- inoculated WT mice at 3- and 7 DPI. Taken together, these results suggest that IF does not significantly impact gut microbial responses towards SC2 infection in either lean or obese mice.

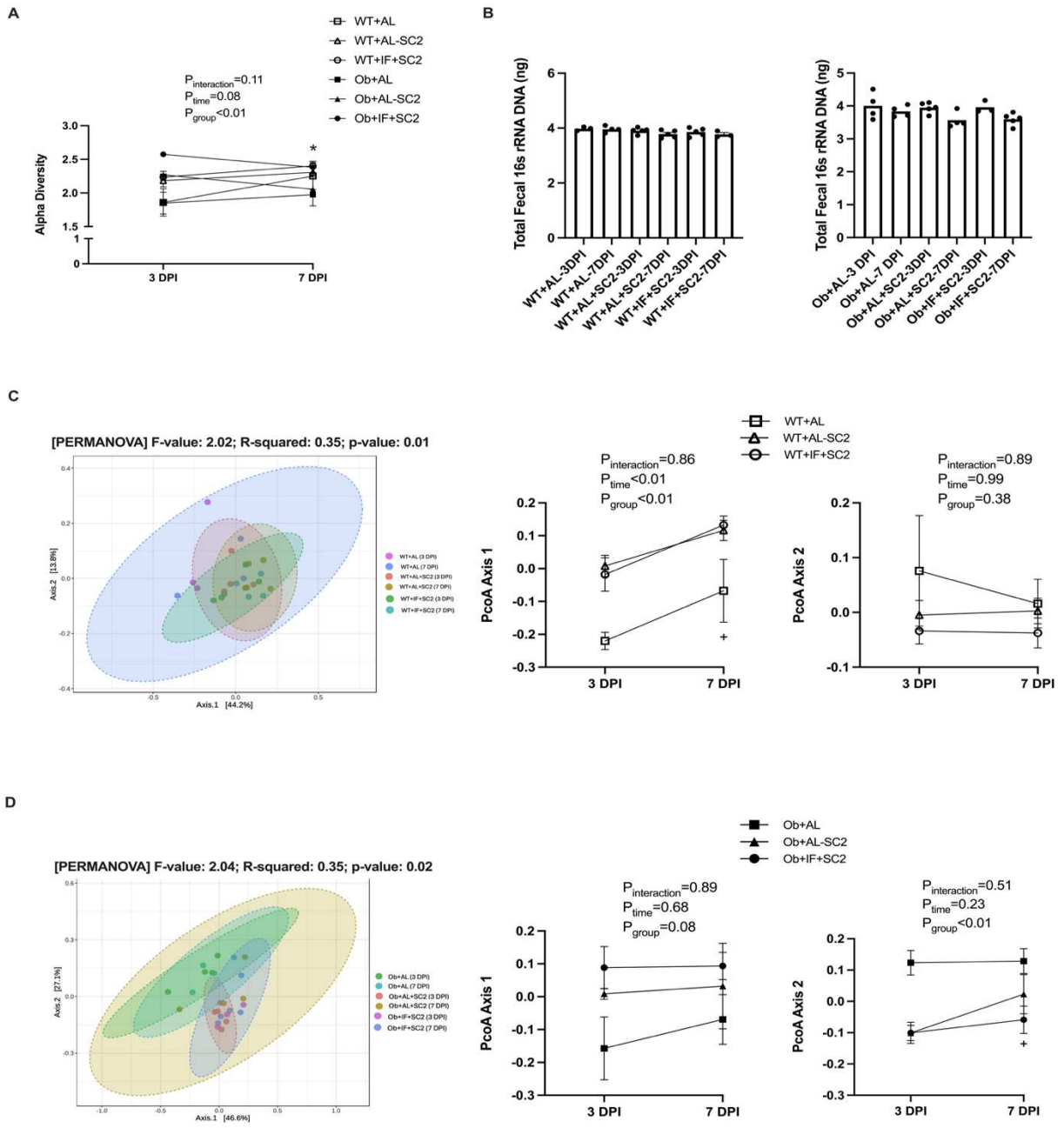

Figure 4.3. Effect of intermittent fasting on gut microbial composition during SARS-CoV-2 infection. A) Changes in gut microbiota alpha diversity (Shannon's index) at the genus level between mock (PBS)- and SARS-CoV-2-inoculated mice. N=3-5 mice per group per DPI. **B)** Differences in total fecal 16s rRNA DNA in WT **(left)** and Ob **(right)** mice at termination. N=3-5 mice per group per DPI. **C-D)** Principal Coordinates Analysis of Bray-Curtis distances at the genus level between WT **C)** and Ob **D)** mock- and SARS-CoV-2 inoculated mice. N=3-5 mice per group per DPI. Principal Coordinates Analysis axes 1 and 2 represent the principal coordinates (new uncorrelated variables that are constructed as linear combinations or mixtures of the initial variables) that explain the largest and second largest variability, respectively, in gut microbial composition. WT=lean; Ob=obese; AL=*ad libitum* feeding; IF=once-weekly 24-hour intermittent fasting; SC2=SARS-CoV-2 (MA10) infection; DPI= days post-inoculation. *indicates a p-value of less than 0.05 between Ob+AL vs. Ob+IF+SC2 mice. $^{+}$ indicates a p-value of less than 0.05 between PBS- and SC2 inoculated groups.

DISCUSSION

Our data suggest that IF improves cardiovascular health via reducing obesity-related arterial stiffness, at least partially through suppressing pro-inflammatory immune responses. However, as a dietary strategy that has sustained considerable popularity for its purported health benefits, it is necessary to identify whether IF possesses any adverse effects. Specifically, a robust and active immune response is critical to ward off invading pathogens, and our data, along with other work [8,33], suggests that IF may affect immune response. Thus, we hypothesized that IF exacerbates acute infection.

SARS-COV-2, the culprit of the COVID-19 pandemic, is still a prominent pathogen[34] that can cause acute and long-term health complications. To uncover whether IF improved cardiovascular health but exacerbated SARS-COV-2 infection severity, we confirmed that once-weekly 24-hour intermittent fasting attenuated obesity-related arterial stiffness. In the same cohort of mice, we then addressed whether IF worsens SARS-COV-2 infection severity as well as immune and gut microbial responses towards SARS-COV-2. Assessing the potential differences in how IF impacts infection in lean and obese mice is critical, since obesity is a risk factor for more severe SARS-COV-2 outcomes, including death, regardless of multiple COVID-19 vaccine doses [35]. In general, we show that IF does not substantially impact SARS-COV-2 infection responses in lean or obese mice, highlighted by no differences in infection-associated body weight, food intake, lung SARS-COV-2 burden, or circulating S1- and S2- antibodies.

To date, only a few studies have assessed links between IF and SARS-COV-2 severity in humans with obesity [17,18,36] and none have used well-controlled rodent experimental models. Observational data from Horne and colleagues [17] found that in the pre-vaccine era, periodic self-reported fasting increased hospitalization-free survival rates in COVID-19 patients (HR=0.61;CI 0.42 to 0.90; p=0.013). The positive effects of fasting remained significant in all multivariable analyses, with a HR range of 0.61-0.64 depending upon the fitted covariables (p=0.015-0.036). In a more recent study, Horne et al. included vaccination as a covariate and reported similar results[18], as periodic fasting was associated with reduced rates of heart failure hospitalization (HR=0.57;CI 0.37 to 0.90; p=0.015) and major adverse cardiovascular events (MACE) (HR=0.59;CI 0.40 to 0.87; p=0.008). These analyses included

cardiovascular events that occurred during acute COVID-19 (0-30 days after diagnosis) and post-acute phases (>30 days after diagnosis), suggesting that IF could impede both acute and post-COVID-19 cardiovascular sequelae. However, these were observational studies in free-living populations, and Horne and colleagues state that their statistical approaches do not completely control for all covariates/confounders [21]. This potential concern is highlighted by the fact that there was no standardized format for fasting, so their dataset likely included many different types of IF protocols which were not accounted for in their statistical analyses [38,39]. In addition, the non-fasting group included a significantly higher proportion of smokers (prior or current) and higher levels of diabetes, COPD and asthma[20,21], which are significant risk factors for severe SARS-COV-2 and long-term COVID-19 complications. Finally, a case report of a 36-year-old obese patient found that 9 months of 18:6 time-restricted eating (fasting for 18 hours a day and *ad libitum* eating for 6 hours a day) coupled with a 3-month refeeding phase improved cardiometabolic parameters (blood glucose, testosterone, LDL-C) and reduced systemic inflammation (C-reactive protein), but did not impact antibody responses towards SARS-COV-2 [36], which is in line with our results.

Along with the negligible effects of IF on SARS-COV-2 infection severity and antibody responses, we also show no significant changes most lung and spleen immune cell populations. However, we did observe increased $CD11b^+$ $CD11c^-$ MHCII- cells (innate immune cells, likely monocytes or eosinophils[37]) and reduced $CD62L^+$ $CD86^+$ and $CD62L^-$ $CD86^+$ B cells in the lungs of Ob+IF+SC2 mice at 3 DPI. Why we observed these alterations only at 3 DPI is unclear, although the proportional differences detected may not correspond to changes in absolute numbers of these cells within the lung. This is supported by the limited impact of IF on all other lung and spleen immune cell subsets, coupled with the lack of significant alterations in S1- and S2-antibody responses.

Lung B cells are an integral component of the immune response towards SARS-COV-2 infection, as mice deficient in B lymphocytes have substantially delayed SARS-COV-2 clearance[38]. Thus, although a heightened innate immune response during SARS-COV-2 might not always be advantageous [39,40], it is possible that the acute surge in $CD11b^+$ $CD11c^-$ MHCII- cells in Ob+IF+SC2 mice at 3 DPI may have

been essential to compensate for the absence of lung CD62L+ CD86+ and CD62L- CD86+ B cells. This hypothesis loosely aligns with data supporting the benefits of an active innate immune response during SARS-COV-2 infection. For example, Imbiakha et al.[31] showed that lung monocyte-derived macrophages accrued within the lung at 3 DPI (high viral load) followed by a decrease at 14 DPI (viral clearance). Nelson et al. [41] also showed that rhesus macaques infected with SARS-COV-2 exhibited decreased viral loads before the infiltration of T and B cells, further supporting the significant role of innate immunity in limiting SARS-COV-2 infection. In contrast, the lack of lung B cells at 3 DPI does not necessarily mean that Ob+IF+SC2 had a diminished adaptive immune response towards SARS-COV-2. CD86 and CD62L are markers of activation and migration, respectively [42–44]. Thus, the proportional loss of these B cell subsets within the lung at 3 DPI could also mean that IF enhanced their flux into the lung-draining lymph nodes early in infection, propagating the adaptive immune responses in obese mice. However, since we found no differences in these immune cell subsets at 7 DPI, these effects were likely transient and did not impact overall immune responses towards SARS-COV-2 infection in obese mice.

Alterations to the gut microbiota are a critical determinant of SARS-COV-2 infection severity in both humans and pre-clinical animal models. Yeoh et al.[14] found that *Faecalibacterium prausnitzii*, *Eubacterium rectale* and *Bifidobacteria* were reduced in COVID-19 patients, which corresponded with elevated inflammation including increased C-reactive protein (CRP) and inflammatory cytokines. In hamsters, SARS-COV-2 infection increased *Enterobacteriaceae* and *Desulfovibrionaceae* while reducing the short-chain fatty acid (SCFA) producers *Ruminococcaceae* and *Lachnospiraceae* [12]. Interestingly, SCFA supplementation did not impact infection outcomes[12]. Severe SARS-COV-2 infection reduced *Lachnospiraceae* and *Oscillospiraceae* and increased *Akkermansiaceae* in K18-hACE2 mice [45]. In this study, SARS-COV-2 infection altered the gut microbiota of both *ad libitum*- and IF-infected mice compared to mock-infected controls. However, we did not observe substantial differences in alpha or beta diversity between *ad libitum*- and IF-infected mice, suggesting that SARS-COV-2 may have a more pronounced impact on the gut microbiota compared to IF. To confirm this, a non-infected IF group would be necessary. Nevertheless, in contrast to other studies, we could not identify differentially abundant

microbes between mock- and SC2-inoculated groups, regardless of genotype. A potential reason for the differential effects on the gut microbiota could be that the impact of SARS-COV-2 MA10 on the gut microbiota differs from other SARS-COV-2 strains previously used, such as the hCoV-19_IPL_France strain[12] and USA-WA1/2020[45]. Specifically, SARS-COV-2 MA10 might slightly alter the relative abundance of many gut microbes rather than substantially affecting the relative abundance of a few keystone taxa. This provides valuable information, as changes to the gut microbiota following SARS-COV-2 MA10 infection does not seem to be well-characterized [46]. In general, future studies might want to refrain from using SARS-COV-2 MA10 when investigating links between SARS-COV-2 and the gut microbiota.

Importantly, our findings contribute to the growing body of literature investigating whether IF should be considered an overall healthy diet. Previous research has begun investigating these simultaneous effects due to IF's potential immunosuppressive effects with regard to cardiometabolic and autoimmune disorders but minimal impact on acute infections. Similar to our results, Jordan et al. [47] found that alternate-day fasting (ADF) reduced experimental autoimmune encephalomyelitis (EAE; model for multiple sclerosis) but did not affect immune responses towards *Listeria monocytogene*s (*L. monocytogenes)* infection. Data from Janssen et al.[8] indicated that a potential benefit of IF is immune cell redistribution, reducing clonal hematopoiesis and clonal expansion of extramedullary leukocytes which is associated with poor cardiovascular health [48–50]. In contrast, the same study reported that a single fasting-refeeding cycle increased myeloid cell recruitment to the lung parenchyma, elevated circulating cytokines, and accelerated death after *Pseudomonas aeruginosa* (PAE) inoculation [8]. Further analyses found that a single fasting-refeeding cycle -increased Ly6C^{hi} monocytes, TNF^{+} Ly6C^{hi} monocytes, and transcriptionally "old" monocyte recruitment to the lung parenchyma after LPS challenge[8]. The effects of IF on infection are only beginning to be understood; however, it seems as if infection responses might be largely dictated by the type of IF, with chronic IF (recurrent fasting-refeeding cycles) potentially being overall beneficial. Nevertheless, since this study solely focused on the effects of chronic IF on SARS-

CoV-2 infection, future research should explore the impact of chronic IF on other prevalent infectious diseases.

This study has some limitations. First, to infect mice from a C57 genetic background, we had to use the SARS-COV-2 MA10 strain as ancestral SARS-COV-2 strains are incapable of binding to the murine ACE2 ortholog [30]. Although SARS-COV-2 MA10 does stably infect C57BL/6J mice (the genetic background of our lean and obese mice), it induces a relatively mild infection [30]. The virulence of SARS-COV-2 MA10 compared to circulating SARS-COV-2 strains could be a major reason why our results differed from those of Horne et al. (especially their pre-vaccine era data) [17,18]. Therefore, other pre-clinical models, such as hamsters[51] and diet-induced obese transgenic hACE2 mouse lines[30], in combination with a more virulent strain of SARS-COV-2 could have yielded results more similar to the human observational studies. However, some studies caution against using hACE2 mice for obesity studies due to the hACE2 transgene being expressed at vastly different levels than in humans, obesity altering ACE2 expression, and adenovirus hACE2 inoculation promoting weight loss in obese mice independent of SARS-COV-2 infection[52,53]. Furthermore, we inoculated mice with 5 x 10^3 PFU of SARS-COV-2 MA10. Although higher PFUs of MA10 do not kill WT C57 mice[30], we settled on 5 x 10^3 PFU to ensure this dose would be tolerable in leptin-deficient obese mice. Moreover, we wanted to observe whether IF impacted host responses over the course of infection (7 days) and did not want mice to die early on during infection. Our results indicate that a more infectious dose of SARS-COV-2 MA10 (greater than or equal to 10^4 PFU) could be used when inoculating leptin-deficient obese mice. Similarly, leptin is a potent immunomodulator that increases activation and survival of many different immune cells [54,55]. Thus, using a leptin-deficient obese model could have altered the immune response towards SARS-COV-2, even further constraining the translational potential of this study. Finally, all animals were infected during *ad libitum* feeding and no IF was conducted during SARS-COV-2 infection. It would be intriguing to examine potential differences in SARS-COV-2 infection severity between mice who were subjected to IF before infection and those who were subjected to IF after infection.

In conclusion, once-weekly 24-hour IF attenuated arterial stiffness in obese mice while having minimal impact on SARS-COV-2 infection severity in lean or obese mice. This is the first study to directly investigate the simultaneous effects of this widely adopted dietary strategy on cardiovascular health and SARS-CoV-2 infection, offering preliminary evidence of its safety even with the ongoing prevalence of COVID-19. These findings further contribute to the accumulating body of literature indicating that chronic IF is a generally healthy diet that reduces chronic inflammation and without substantially impacting immune responses during acute infections.

REFERENCES

1. Koppold DA, Breinlinger C, Hanslian E, et al. International consensus on fasting terminology. *Cell Metabolism*. 2024;36(8):1779-1794.e4. doi:10.1016/j.cmet.2024.06.013

2. Persynaki A, Karras S, Pichard C. Unraveling the metabolic health benefits of fasting related to religious beliefs: A narrative review. *Nutrition*. 2017;35:14-20. doi:10.1016/j.nut.2016.10.005

3. Gonzalez JE, Cooke WH. Influence of an acute fast on ambulatory blood pressure and autonomic cardiovascular control. *American Journal of Physiology-Regulatory, Integrative and Comparative Physiology*. 2022;322(6):R542-R550. doi:10.1152/ajpregu.00283.2021

4. Martin SS, Aday AW, Almarzooq ZI, et al. 2024 Heart Disease and Stroke Statistics: A Report of US and Global Data From the American Heart Association. *Circulation*. 2024;149(8). doi:10.1161/CIR.0000000000001209

5. Mitchell GF, Hwang SJ, Vasan RS, et al. Arterial Stiffness and Cardiovascular Events: The Framingham Heart Study. *Circulation*. 2010;121(4):505-511. doi:10.1161/CIRCULATIONAHA.109.886655

6. Vasan RS, Pan S, Xanthakis V, et al. Arterial Stiffness and Long-Term Risk of Health Outcomes: The Framingham Heart Study. *Hypertension*. 2022;79(5):1045-1056. doi:10.1161/HYPERTENSIONAHA.121.18776

7. Belkaid Y, Hand TW. Role of the microbiota in immunity and inflammation. *Cell*. 2014;157(1):121-141. doi:10.1016/j.cell.2014.03.011

8. Janssen H, Kahles F, Liu D, et al. Monocytes re-enter the bone marrow during fasting and alter the host response to infection. *Immunity*. 2023;56(4):783-796.e7. doi:10.1016/j.immuni.2023.01.024

9. Zenz G, Jačan A, Reichmann F, Farzi A, Holzer P. Intermittent Fasting Exacerbates the Acute Immune and Behavioral Sickness Response to the Viral Mimic Poly(I:C) in Mice. *Front Neurosci*. 2019;13:359. doi:10.3389/fnins.2019.00359

10. Chen X, Laurent S, Onur OA, et al. A systematic review of neurological symptoms and complications of COVID-19. *J Neurol*. 2021;268(2):392-402. doi:10.1007/s00415-020-10067-3

11. Graham EL, D'Isabel S, Lofrano-Porto A, Smith DL. Musculoskeletal, Pulmonary, and Cardiovascular COVID-19 Sequelae in the Context of Firefighter Occupational Health: A Narrative Review. *IJERPH*. 2024;21(10):1383. doi:10.3390/ijerph21101383

12. Sencio V, Machelart A, Robil C, et al. Alteration of the gut microbiota following SARS-CoV-2 infection correlates with disease severity in hamsters. *Gut Microbes*. 2022;14(1):2018900. doi:10.1080/19490976.2021.2018900

13. Zuo T, Zhang F, Lui GCY, et al. Alterations in Gut Microbiota of Patients With COVID-19 During Time of Hospitalization. *Gastroenterology*. 2020;159(3):944-955.e8. doi:10.1053/j.gastro.2020.05.048

14. Yeoh YK, Zuo T, Lui GCY, et al. Gut microbiota composition reflects disease severity and dysfunctional immune responses in patients with COVID-19. *Gut*. 2021;70(4):698-706. doi:10.1136/gutjnl-2020-323020

15. Li Z, Chen J, Li Y, et al. Impact of SARS-CoV-2 infection on respiratory and gut microbiome stability: a metagenomic investigation in long-term-hospitalized COVID-19 patients. *npj Biofilms Microbiomes*. 2024;10(1):126. doi:10.1038/s41522-024-00596-4

16. Sattar N, McInnes IB, McMurray JJV. Obesity a Risk Factor for Severe COVID-19 Infection: Multiple Potential Mechanisms. *Circulation*. Published online April 22, 2020:CIRCULATIONAHA.120.047659. doi:10.1161/CIRCULATIONAHA.120.047659

17. Horne BD, May HT, Muhlestein JB, et al. Association of periodic fasting with lower severity of COVID-19 outcomes in the SARS-CoV-2 prevaccine era: an observational cohort from the INSPIRE registry. *BMJNPH*. Published online July 1, 2022:e000462. doi:10.1136/bmjnph-2022-000462

18. Horne BD, Anderson JL, Haddad F, et al. Periodic Fasting and Acute Cardiac Events in Patients Evaluated for COVID-19: An Observational Prospective Cohort Study. *Nutrients*. 2024;16(13):2075. doi:10.3390/nu16132075

19. Battson ML, Lee DM, Jarrell DK, et al. Suppression of gut dysbiosis reverses Western diet-induced vascular dysfunction. *American Journal of Physiology-Endocrinology and Metabolism*. 2018;314(5):E468-E477. doi:10.1152/ajpendo.00187.2017

20. Lee DM, Ecton KE, Trikha SRJ, et al. Microbial metabolite indole-3-propionic acid supplementation does not protect mice from the cardiometabolic consequences of a Western diet. *American Journal of Physiology-Gastrointestinal and Liver Physiology*. 2020;319(1):G51-G62. doi:10.1152/ajpgi.00375.2019

21. Trikha SRJ, Lee DM, Ecton KE, et al. Transplantation of an obesity-associated human gut microbiota to mice induces vascular dysfunction and glucose intolerance. *Gut Microbes*. 2021;13(1):1940791. doi:10.1080/19490976.2021.1940791

22. Bashor L, Gagne RB, Bosco-Lauth AM, Bowen RA, Stenglein M, VandeWoude S. SARS-CoV-2 evolution in animals suggests mechanisms for rapid variant selection. *Proc Natl Acad Sci U S A*. 2021;118(44):e2105253118. doi:10.1073/pnas.2105253118

23. Lei C, Yang J, Hu J, Sun X. On the Calculation of TCID50 for Quantitation of Virus Infectivity. *Virol Sin*. 2021;36(1):141-144. doi:10.1007/s12250-020-00230-5

24. Dutt TS, Spencer JS, Karger BR, et al. ELISA-R: an R-based method for robust ELISA data analysis. *Front Immunol*. 2024;15:1427526. doi:10.3389/fimmu.2024.1427526

25. Caporaso JG, Lauber CL, Walters WA, et al. Ultra-high-throughput microbial community analysis on the Illumina HiSeq and MiSeq platforms. *ISME J*. 2012;6(8):1621-1624. doi:10.1038/ismej.2012.8

26. Bolyen E, Rideout JR, Dillon MR, et al. Reproducible, interactive, scalable and extensible microbiome data science using QIIME 2. *Nat Biotechnol*. 2019;37(8):852-857. doi:10.1038/s41587-019-0209-9

27. Amir A, McDonald D, Navas-Molina JA, et al. Deblur Rapidly Resolves Single-Nucleotide Community Sequence Patterns. Gilbert JA, ed. *mSystems*. 2017;2(2):e00191-16. doi:10.1128/mSystems.00191-16

28. Robeson MS, O'Rourke DR, Kaehler BD, et al. RESCRIPt: Reproducible sequence taxonomy reference database management. Pertea M, ed. *PLoS Comput Biol*. 2021;17(11):e1009581. doi:10.1371/journal.pcbi.1009581

29. Chong J, Liu P, Zhou G, Xia J. Using MicrobiomeAnalyst for comprehensive statistical, functional, and meta-analysis of microbiome data. *Nat Protoc*. 2020;15(3):799-821. doi:10.1038/s41596-019-0264-1

30. Leist SR, Dinnon KH, Schäfer A, et al. A Mouse-Adapted SARS-CoV-2 Induces Acute Lung Injury and Mortality in Standard Laboratory Mice. *Cell*. 2020;183(4):1070-1085.e12. doi:10.1016/j.cell.2020.09.050

31. Imbiakha B, Sahler JM, Buchholz DW, et al. Adaptive immune cells are necessary for SARS-CoV-2–induced pathology. *Sci Adv*. 2024;10(1):eadg5461. doi:10.1126/sciadv.adg5461

32. Wang A, Huen SC, Luan HH, et al. Opposing Effects of Fasting Metabolism on Tissue Tolerance in Bacterial and Viral Inflammation. *Cell*. 2016;166(6):1512-1525.e12. doi:10.1016/j.cell.2016.07.026

33. Nagai M, Noguchi R, Takahashi D, et al. Fasting-Refeeding Impacts Immune Cell Dynamics and Mucosal Immune Responses. *Cell*. 2019;178(5):1072-1087.e14. doi:10.1016/j.cell.2019.07.047

34. Centers for Disease Control and Prevention. *COVID Data Tracker*. Department of Health and Human Services, CDC; 2025. https://covid.cdc.gov/covid-data-tracker

35. Piernas C, Patone M, Astbury NM, et al. Associations of BMI with COVID-19 vaccine uptake, vaccine effectiveness, and risk of severe COVID-19 outcomes after vaccination in England: a population-based cohort study. *The Lancet Diabetes & Endocrinology*. 2022;10(8):571-580. doi:10.1016/S2213-8587(22)00158-9

36. Tewani GR, Sharma H, M.K. Nair P. Prolonged Intermittent Fasting As a Preventive Strategy Against COVID-19: A Case Report. *Integrative Medicine Reports*. 2022;1(1):38-42. doi:10.1089/imr.2021.0027

37. Misharin AV, Morales-Nebreda L, Mutlu GM, Budinger GRS, Perlman H. Flow cytometric analysis of macrophages and dendritic cell subsets in the mouse lung. *Am J Respir Cell Mol Biol*. 2013;49(4):503-510. doi:10.1165/rcmb.2013-0086MA

38. Israelow B, Mao T, Klein J, et al. Adaptive immune determinants of viral clearance and protection in mouse models of SARS-CoV-2. *Sci Immunol*. 2021;6(64):eabl4509. doi:10.1126/sciimmunol.abl4509

39. Junqueira C, Crespo Â, Ranjbar S, et al. FcγR-mediated SARS-CoV-2 infection of monocytes activates inflammation. *Nature*. 2022;606(7914):576-584. doi:10.1038/s41586-022-04702-4

40. Ranjbar M, Cusack RP, Whetstone CE, et al. Immune Response Dynamics and Biomarkers in COVID-19 Patients. *IJMS*. 2024;25(12):6427. doi:10.3390/ijms25126427

41. Nelson CE, Namasivayam S, Foreman TW, et al. Mild SARS-CoV-2 infection in rhesus macaques is associated with viral control prior to antigen-specific T cell responses in tissues. *Sci Immunol*. 2022;7(70):eabo0535. doi:10.1126/sciimmunol.abo0535

42. Axelsson S, Magnuson A, Lange A, Alshamari A, Hörnquist EH, Hultgren O. A combination of the activation marker CD86 and the immune checkpoint marker B and T lymphocyte attenuator (BTLA) indicates a putative permissive activation state of B cell subtypes in healthy blood donors independent of age and sex. *BMC Immunol*. 2020;21(1):14. doi:10.1186/s12865-020-00343-2

43. Pape KA, Catron DM, Itano AA, Jenkins MK. The Humoral Immune Response Is Initiated in Lymph Nodes by B Cells that Acquire Soluble Antigen Directly in the Follicles. *Immunity*. 2007;26(4):491-502. doi:10.1016/j.immuni.2007.02.011

44. Morrison VL, Barr TA, Brown S, Gray D. TLR-Mediated Loss of CD62L Focuses B Cell Traffic to the Spleen during *Salmonella typhimurium* Infection. *The Journal of Immunology*. 2010;185(5):2737-2746. doi:10.4049/jimmunol.1000758

45. Seibert B, Cáceres CJ, Cardenas-Garcia S, et al. Mild and Severe SARS-CoV-2 Infection Induces Respiratory and Intestinal Microbiome Changes in the K18-hACE2 Transgenic Mouse Model. Martinez MA, ed. *Microbiol Spectr*. 2021;9(1):e00536-21. doi:10.1128/Spectrum.00536-21

46. Chung J, Pierce J, Franklin C, Olson RM, Morrison AR, Amos-Landgraf J. Translating animal models of SARS-CoV-2 infection to vascular, neurological and gastrointestinal manifestations of COVID-19. *Disease Models & Mechanisms*. 2025;18(9):dmm052086. doi:10.1242/dmm.052086

47. Jordan S, Tung N, Casanova-Acebes M, et al. Dietary Intake Regulates the Circulating Inflammatory Monocyte Pool. *Cell*. 2019;178(5):1102-1114.e17. doi:10.1016/j.cell.2019.07.050

48. Heyde A, Rohde D, McAlpine CS, et al. Increased stem cell proliferation in atherosclerosis accelerates clonal hematopoiesis. *Cell*. 2021;184(5):1348-1361.e22. doi:10.1016/j.cell.2021.01.049

49. Robbins CS, Chudnovskiy A, Rauch PJ, et al. Extramedullary Hematopoiesis Generates Ly-6C(high) Monocytes That Infiltrate Atherosclerotic Lesions. *Circulation*. 2012;125(2):364-374. doi:10.1161/CIRCULATIONAHA.111.061986

50. Tyrrell DJ, Wragg KM, Chen J, et al. Clonally expanded memory CD8+ T cells accumulate in atherosclerotic plaques and are pro-atherogenic in aged mice. *Nat Aging*. 2023;3(12):1576-1590. doi:10.1038/s43587-023-00515-w

51. Maruggi G, Mallett CP, Westerbeck JW, et al. A self-amplifying mRNA SARS-CoV-2 vaccine candidate induces safe and robust protective immunity in preclinical models. *Molecular Therapy*. 2022;30(5):1897-1912. doi:10.1016/j.ymthe.2022.01.001

52. Winkler ES, Bailey AL, Kafai NM, et al. SARS-CoV-2 infection of human ACE2-transgenic mice causes severe lung inflammation and impaired function. *Nat Immunol*. 2020;21(11):1327-1335. doi:10.1038/s41590-020-0778-2

53. Rai P, Chuong C, LeRoith T, et al. Adenovirus transduction to express human ACE2 causes obesity-specific morbidity in mice, impeding studies on the effect of host nutritional status on SARS-CoV-2 pathogenesis. *Virology*. 2021;563:98-106. doi:10.1016/j.virol.2021.08.014

54. Kiernan K, MacIver NJ. The Role of the Adipokine Leptin in Immune Cell Function in Health and Disease. *Front Immunol*. 2021;11:622468. doi:10.3389/fimmu.2020.622468

55. Naylor C, Petri WA. Leptin Regulation of Immune Responses. *Trends in Molecular Medicine*. 2016;22(2):88-98. doi:10.1016/j.molmed.2015.12.001

CHAPTER 5: CONCLUSION

Summary

This dissertation had two primary objectives. The first objective was to answer fundamental questions regarding the impact of intermittent fasting (IF) on cardiovascular health **(Chapter 3).** Specifically, **Chapter 3** addressed the following questions: 1) What are the impacts of IF on arterial stiffness? 2) Are there differences in how acute IF (a single fasting-refeeding cycle) and chronic IF (recurrent fasting-refeeding bouts) impact arterial stiffness? 3) Do IF-induced cardiovascular benefits persist beyond the refeeding period and does persistence differ between acute and chronic IF? 4) Do IF-induced changes to the gut microbiota and immune system mediate potential improvements in arterial stiffness? The second objective was to investigate whether fasting-induced immune modifications impacted acute infection in a SARS-CoV-2 infection model **(Chapter 4)**.

The first major finding from **Chapter 3** was how differently acute versus chronic IF impacted arterial stiffness and the potential mechanisms governing these differences. We found that a single 24-hour fast acutely increased arterial stiffness in lean mice but had no effect on arterial stiffness in genetically obese mice. Additionally, gut microbial composition and circulating cytokines/chemokines, remained relatively stable throughout the single fasting-refeeding cycle in lean animals. This suggests that other factors not measured, such as blood pressure changes, might be implicated in the acute arterial stiffening. In contrast, once-weekly 24-hour IF (chronic IF) attenuated arterial stiffness in obese mice in as little as five weeks. Subsequent analyses found that these reductions were independent of weight loss, which can occur during IF and contribute to reduced arterial stiffness [1,2]. Instead, our findings align with the emerging hypothesis of weight-independent benefits of IF on cardiovascular health. [3] Chronic IF profoundly altered the gut microbiota, immune system, and aberrant interactions between the two, which may precede arterial de-stiffening. Ancillary analyses identified two distinct gut microbe-cytokine interactions in obese mice (*Clostridia*_186-CCL2/CXCL1 and *Lachnospiraceae*_436-CCL2/CXCL1) that were suppressed by IF to reduce arterial stiffness.

Taken together, **Chapter 3** convincingly shows that chronic IF is far more effective in reducing arterial stiffness in genetically obese mice than acute IF. We also discovered that IF's effects on the microbiota and immune system coincide with reduced arterial stiffness. This finding aligns with our previous research indicating that changes to the gut microbiota can reduce inflammation and impede arterial stiffness [4,5]. In addition, we identified CCL2 and CXCL1 as two pro-inflammatory cytokines that may mediate the detrimental effects of the obese gut microbiota on vascular health. Identifying these cytokines as mediators of arterial stiffness was crucial for three reasons: 1) few have addressed how IF regulates interactions between the gut microbiota, inflammation, and arterial stiffness; 2) the links between these cytokines and arterial stiffness are limited, but our findings incentivize further research to investigate the causal role of these cytokines in the development of arterial stiffness; 3) fasting-related reductions in CCL2 impede leukocyte egress from the bone marrow to the blood [6], further suggesting that immune cell redistribution could be a key biological process regulating vascular health.

The second major finding from this study was that the persistence of arterial effects differed between acute and chronic IF. We found that the increase in arterial stiffness in lean mice was only transient, as stiffness was diminished following 24 hours of refeeding and is thus unlikely to affect long-term cardiovascular health. However, chronic IF-induced arterial de-stiffening in obese mice persisted for at least 5 days following *ad libitum* refeeding. Since all gut microbiota and immune parameters were measured following a 24-hour refeeding period, arterial de-stiffening likely occurred through sustained alterations to the gut microbiota and immune system. When compared to acute IF, these results indicate a potential "training effect" that occurs with repeated fasting, resulting in prolonged vascular benefits in obese mice and stable pulse wave velocity measures in lean mice. These novel findings add to the existing data, as others have either measured the impacts of IF on cardiovascular health within one day after fasting [7–9] or do not explicitly state how long after the fasting period parameters were measured [10,11]. Most importantly, **Chapter 3** shows that chronic IF is a durable dietary strategy for long-term, sustained vascular health.

Despite the cardiovascular benefits of IF, its impact on the immune system could influence responses to infection. One particular pathogen of interest is SARS-CoV-2, since it is still a common pathogen that impacts multiple organs systems both acutely and longitudinally[12]. The gut microbiota and an active immune system are also critical determinants of SARS-COV-2 infection severity and symptom resolution [13–16]. Thus, the primary objective of **Chapter 4** was to assess whether chronic IF improved vascular health but altered responses to SARS-COV-2 infection in mice. Specifically, we hypothesized that IF-induced immune modulation would result in worsened outcomes in a SARS-COV-2 infection model. However, our results show that chronic IF simultaneously improved arterial stiffness in obese mice without impacting SARS-COV-2 severity or infection responses. Indeed, we show that 10-weeks of once-weekly 24-hour IF attenuated arterial stiffness in obese mice. However, IF did not predispose either lean or obese to worse SARS-COV-2 infection, as there were no substantial differences in lung SARS-CoV-2 viral titers, body weight, food intake, or SARS-COV-2 -specific antibody titers between infected *ad libitum* and IF mice. Furthermore, there were no profound differences in gut microbial composition or spleen and lung immune cell proportions between infected *ad libitum* and IF mice.

A particularly novel aspect of this chapter was that it was the first well-controlled pre-clinical study to directly evaluate the effects of IF on SARS-CoV-2 severity. Only a few other studies have investigated the impact of IF on SARS-CoV-2 infection, yet these were observational and case studies with many potential confounders [17–19]. Moreover, this chapter contributes significantly to the growing literature examining whether IF should be considered an overall healthy diet and suggests that chronic IF is probably the most net-beneficial in improving health without impacting infection responses.

Delimitations and Limitations

Chapters 3 and **4** possess methodological and experimental strengths and provide novel findings that make substantial contributions to the fields of cardiovascular health and infectious disease. In addition to the strengths discussed within each chapter, all experimental mice in **Chapters 3** and **4** were of the same age, sex, and genetic background. Controlling these factors allowed us to directly assess the effects of IF

on multiple physiological parameters, mainly arterial stiffness and gut microbe-immune interactions, in **Chapter 3**. This highlights the importance of including age- and sex-matched controls in prospective IF and arterial stiffness clinical trials. These delimitations also carry over to **Chapter 4**, and it was necessary to complete this chapter in a pre-clinical model. Additionally, the same personnel carried out all physiological parameters throughout **Chapters 3** and **4**. This reduced inter-researcher variability, human error, and the potential confounder of the mice being handled or experimented on by a new person in the middle of a study, which could induce unwanted stress. Furthermore, the names of all personnel who worked with the mice and their responsibilities were always written down. This ensured that we could statistically account for inter-researcher variability if ever needed.

Some limitations not mentioned in **Chapters 3 and 4** could have further confounded our results and interpretations. First, besides glucose tolerance testing which requires a 6-hour fast, all other primary outcomes were measured at least 24 hours after *ad libitum* feeding. Since mice were co-housed in both chapters, we could not accurately calculate how much food each mouse ate during the pre-measurement period (which varied from 24-hours to 5 days). This potential concern is highlighted by the fact that IF might lead to acute overconsumption on non-fasting days [20,21]. Furthermore, we did not precisely measure nutrient absorption (i.e., fecal bomb calorimetry) and thus, differences in food intake and nutrient absorption could have confounded some of our interpretations. Similarly, we did not measure water intake in either chapter, which may affect arterial stiffness by altering blood volume or osmolarity. However, we must reiterate that body weight and food intake throughout the entire dietary protocol were stable, and we did not observe a concerning amount of variability in our outcome measurements (PWV, gut microbiota data, circulating cytokines/chemokines, splenocyte populations, etc.). This suggests that *ad libitum* food and water intake before data collection likely had little effect on our data. Moreover, to identify the persistent rather than transient de-stiffening effects of IF, we purposefully wanted mice to eat *ad libitum* before measurements. This decision also made our data more translatable to human health, as humans tend to follow IF regimens that allow for *ad libitum* eating following fasting. Furthermore, employing a once-weekly 24-hour fasting protocol diminished the potential confound of altered light/dark

cycles and circadian misalignment that could arise with time-restricted feeding studies. Nevertheless, pre-measurement food intake, nutrient absorption, and water intake can and should be accounted for in future IF studies.

Secondly, we did not measure IF-related blood pressure changes in obese mice, which could have impacted arterial stiffness measurements. Blood pressure and arterial stiffness are bidirectionally related, as increased arterial stiffness leads to systemic peripheral resistance and augments blood pressure [22], while increased blood pressure causes vascular injury, arterial remodeling, and the transfer of load-bearing to collagen fibers, increasing arterial stiffness [23]. Since we measured arterial stiffness via the foot-to-foot method, any alterations in diastolic pressure could have impacted pulse wave velocity [24]. Intermittent fasting has been shown to reduce both systolic and diastolic blood pressure [25–27], and a potential mechanism for reduced blood pressure is alterations to the gut microbiota[7,25]. Thus, it is possible that changes in blood pressure may be contributing to the observed arterial de-stiffening. Leptin-deficient obese mice are unique in that they are typically normotensive and tightly regulate blood pressure [28–30]. Therefore, this limitation may not have substantially impacted our results. Nevertheless, to ensure that IF reduces arterial stiffness independent of blood pressure, it will be crucial to measure blood pressure in future clinical trials or pre-clinical studies that do not use leptin-deficient obese mice.

Finally, a specific limitation in **Chapter 4** was that we did not relocate the PBS-inoculated control mice to BSL3 laboratories. Therefore, these mice might not have experienced the same relocation stress as those randomized to SARS-CoV-2 infection, which could have acutely impacted eating behaviors. Our reasoning for this decision was that not enough people in the Gentile and Weir laboratories had access to the BSL3 facilities, and thus did not have the manpower to care for, infect, or euthanize these mice in the BSL3 laboratories.

Future Directions

The results from this dissertation provide several directions for further research. The first direction would uncover the mechanisms of how gut-immune interactions regulate obesity-related arterial

stiffness. The second direction would be to translate our findings to human health by running randomized clinical trials.

Regarding the first direction, future research should aim to determine a causal relationship between gut-immune signaling during obesity and arterial stiffness. A starting point for this research could be to inoculate germ-free or antibiotic-suppressed mice with either obese *ad libitum* or obese IF microbiotas. Following stabilization, we could quantify arterial stiffness, circulating cytokine levels, and perivascular adipose tissue lymphocytes. Ultimately, this preliminary study would indicate whether fasting-induced changes to the gut microbiota are sufficient to reduce arterial stiffness, and whether the gut microbiota drives the inflammation that provokes arterial stiffness in obese mice.

Chapter 3 identifies Clostridia_186 and *Lachnospiraceae*_436 as obesogenic microbes that augment arterial stiffness. We also provide evidence that the obese gut microbiota harbors "beneficial" microbes that were inversely associated with arterial stiffness. These data reveal a distinct possibility that specific microbes within the obese mouse gut, yet not the obese microbiota as a whole, determine arterial stiffness. To address whether *Clostridia*_186 and *Lachnospiraceae*_436 are independently impacting inflammation and arterial stiffness, we would need to more accurately identify both microbes. Next, to determine causality, we could isolate of *Clostridia*_186 from obese *ad libitum* mice, inoculate lean specific pathogen free (SPF) or germ-free mice, and measure changes in cytokines (CCL2, CXCL1) and arterial stiffness. In contrast, *Lachnospiraceae*_436 relative abundance was unchanged between obese *ad libitum* and IF mice even though its positive relationship with arterial stiffness was abolished, indicating that something other than its relative abundance regulates arterial stiffness (i.e., inflammatory metabolite production). Thus, transcriptomics on isolated *Lachnospiraceae*_436, as well as cecal and blood metabolomics in obese *ad libitum* and IF mice, would help determine whether *Lachnospiraceae*_436 metabolite production changes in response to IF in obese mice. A potential next step would be to collaborate with industry partners who specialize in developing drugs to alter the gut microbiota. Although technically challenging, these collaborations could help to develop drugs that either reduce the

relative abundance (bacteriophage) or alter the metabolism (plasmid that suppresses "obesogenic" gene expression identified via transcriptomics) of *Clostridia*_186 and *Lachnospiraceae*_436, respectively.

Additionally, **Chapter 3** reported striking reductions in the pro-inflammatory cytokines CCL2 and CXCL1. Studies determining the causal effects of these two cytokines on arterial stiffness would be valuable. Specifically, injecting increasing dosages of recombinant CCL2 and/or CXCL1 into lean SPF mice would validate their causality in increasing arterial stiffness. To control for the confounding effects of the already-established gut microbiota in SPF mice, we could inject these recombinant cytokines in antibiotic-suppressed or germ-free mice. This would allow us to define the role of CCL2 and CXCL1 in arterial stiffness independent of the gut microbiota. We could also inject anti-CCL2 or anti-CXCL1 antibodies into obese SPF or germ-free mice to corroborate that inhibiting CCL2 and CXCL1 is arterial de-stiffening. Finally, we show that CCL2 expression in adipose tissue, predominantly the subcutaneous adipose tissue, was reduced in obese IF mice. Identifying whether adipocytes or leukocytes within the subcutaneous adipose tissue produce CCL2 and/or CXCL1 could lead to enhanced inhibition of CCL2/CXCL1 during obesity.

To translate our findings to human health (direction 2), we could begin a randomized clinical trial to determine if once-weekly 24-hour IF reduces obesity-related arterial stiffness in humans. Blood and fecal samples could be obtained to determine whether similar gut microbiota and inflammation changes observed in mice during IF also occur in humans. Additionally, addressing the persistence of de-stiffening could be easily included in this clinical trial by following a similar protocol as in **Chapter 3**. It would be interesting to observe whether a training effect occurs in humans, whereby the rate of arterial de-stiffening is greater in those who have previously completed IF compared to those who have not. Indeed, high fat/high cholesterol yo-yo-like diets accelerate vascular inflammation and atherosclerosis compared to continuous eating in mice [31,32]. Thus, the opposite may also be true; restarting IF might lead to greater rates of arterial de-stiffening. Whether this phenomenon is from gut microbial or immune "training" or "memory" should be further explored.

Finally, regarding the clinical application for **Chapter 4**, arterial stiffness can remain elevated for up to a year after infection [12], while other post-COVID-19 cardiovascular sequelae (myocardial infarction, ischemic cardiomyopathy, atrial fibrillation, dysrhythmias, coagulation disorders) can remain elevated for up to two years after hospitalization from COVID-19 [12]. Consequently, it would be particularly intriguing to explore whether IF resolves post-COVID-19 cardiovascular sequelae in humans.

Overall, this dissertation provides many avenues of further exploration. Investigating these various avenues could result in a more comprehensive understanding of how IF leads to arterial de-stiffening. It could also lead to future clinical trials determining whether once-weekly 24-hour IF reduces arterial stiffness in humans with obesity or with post-COVID-19 cardiovascular sequelae.

REFERENCES

1. Varady KA, Cienfuegos S, Ezpeleta M, Gabel K. Clinical application of intermittent fasting for weight loss: progress and future directions. *Nat Rev Endocrinol*. 2022;18(5):309-321. doi:10.1038/s41574-022-00638-x

2. Dengo AL, Dennis EA, Orr JS, et al. Arterial Destiffening With Weight Loss in Overweight and Obese Middle-Aged and Older Adults. *Hypertension*. 2010;55(4):855-861. doi:10.1161/HYPERTENSIONAHA.109.147850

3. de Cabo R, Mattson MP. Effects of Intermittent Fasting on Health, Aging, and Disease. Longo DL, ed. *N Engl J Med*. 2019;381(26):2541-2551. doi:10.1056/NEJMra1905136

4. Battson ML, Lee DM, Jarrell DK, et al. Suppression of gut dysbiosis reverses Western diet-induced vascular dysfunction. *American Journal of Physiology-Endocrinology and Metabolism*. 2018;314(5):E468-E477. doi:10.1152/ajpendo.00187.2017

5. Battson ML, Lee DM, Li Puma LC, et al. Gut microbiota regulates cardiac ischemic tolerance and aortic stiffness in obesity. *American Journal of Physiology-Heart and Circulatory Physiology*. 2019;317(6):H1210-H1220. doi:10.1152/ajpheart.00346.2019

6. Jordan S, Tung N, Casanova-Acebes M, et al. Dietary Intake Regulates the Circulating Inflammatory Monocyte Pool. *Cell*. 2019;178(5):1102-1114.e17. doi:10.1016/j.cell.2019.07.050

7. Shi H, Zhang B, Abo-Hamzy T, et al. Restructuring the Gut Microbiota by Intermittent Fasting Lowers Blood Pressure. *Circ Res*. 2021;128(9):1240-1254. doi:10.1161/CIRCRESAHA.120.318155

8. Sutton EF, Beyl R, Early KS, Cefalu WT, Ravussin E, Peterson CM. Early Time-Restricted Feeding Improves Insulin Sensitivity, Blood Pressure, and Oxidative Stress Even without Weight Loss in Men with Prediabetes. *Cell Metabolism*. 2018;27(6):1212-1221.e3. doi:10.1016/j.cmet.2018.04.010

9. Azemi AK, Siti-Sarah AR, Mokhtar SS, Rasool AHG. Time-Restricted Feeding Improved Vascular Endothelial Function in a High-Fat Diet-Induced Obesity Rat Model. *Veterinary Sciences*. 2022;9(5):217. doi:10.3390/vetsci9050217

10. Razzak RLA, Abu-Hozaifa BM, Bamosa AO, Ali NM. Assessment of enhanced endothelium-dependent vasodilation by intermittent fasting in Wistar albino rats. *Indian J Physiol Pharmacol*. 2011;55(4):336-342.

11. Cui J, Lee S, Sun Y, et al. Alternate Day Fasting Improves Endothelial Function in Type 2 Diabetic Mice: Role of Adipose-Derived Hormones. *Front Cardiovasc Med*. 2022;9:925080. doi:10.3389/fcvm.2022.925080

12. Graham EL, D'Isabel S, Lofrano-Porto A, Smith DL. Musculoskeletal, Pulmonary, and Cardiovascular COVID-19 Sequelae in the Context of Firefighter Occupational Health: A Narrative Review. *IJERPH*. 2024;21(10):1383. doi:10.3390/ijerph21101383

13. Sencio V, Machelart A, Robil C, et al. Alteration of the gut microbiota following SARS-CoV-2 infection correlates with disease severity in hamsters. *Gut Microbes*. 2022;14(1):2018900. doi:10.1080/19490976.2021.2018900

14. Zuo T, Zhang F, Lui GCY, et al. Alterations in Gut Microbiota of Patients With COVID-19 During Time of Hospitalization. *Gastroenterology*. 2020;159(3):944-955.e8. doi:10.1053/j.gastro.2020.05.048

15. Yeoh YK, Zuo T, Lui GCY, et al. Gut microbiota composition reflects disease severity and dysfunctional immune responses in patients with COVID-19. *Gut*. 2021;70(4):698-706. doi:10.1136/gutjnl-2020-323020

16. Li Z, Chen J, Li Y, et al. Impact of SARS-CoV-2 infection on respiratory and gut microbiome stability: a metagenomic investigation in long-term-hospitalized COVID-19 patients. *npj Biofilms Microbiomes*. 2024;10(1):126. doi:10.1038/s41522-024-00596-4

17. Horne BD, May HT, Muhlestein JB, et al. Association of periodic fasting with lower severity of COVID-19 outcomes in the SARS-CoV-2 prevaccine era: an observational cohort from the INSPIRE registry. *BMJNPH*. Published online July 1, 2022:e000462. doi:10.1136/bmjnph-2022-000462

18. Horne BD, Anderson JL, Haddad F, et al. Periodic Fasting and Acute Cardiac Events in Patients Evaluated for COVID-19: An Observational Prospective Cohort Study. *Nutrients*. 2024;16(13):2075. doi:10.3390/nu16132075

19. Tewani GR, Sharma H, M.K. Nair P. Prolonged Intermittent Fasting As a Preventive Strategy Against COVID-19: A Case Report. *Integrative Medicine Reports*. 2022;1(1):38-42. doi:10.1089/imr.2021.0027

20. Zhang LN, Mitchell SE, Hambly C, Morgan DG, Clapham JC, Speakman JR. Physiological and behavioral responses to intermittent starvation in C57BL/6J mice. *Physiology & Behavior*. 2012;105(2):376-387. doi:10.1016/j.physbeh.2011.08.035

21. Cook F, Langdon-Daly J, Serpell L. Compliance of participants undergoing a '5-2' intermittent fasting diet and impact on body weight. *Clinical Nutrition ESPEN*. 2022;52:257-261. doi:10.1016/j.clnesp.2022.08.012

22. Boutouyrie P, Chowienczyk P, Humphrey JD, Mitchell GF. Arterial Stiffness and Cardiovascular Risk in Hypertension. *Circ Res*. 2021;128(7):864-886. doi:10.1161/CIRCRESAHA.121.318061

23. Pierce GL, Coutinho TA, DuBose LE, Donato AJ. Is It Good to Have a Stiff Aorta with Aging? Causes and Consequences. *Physiology*. 2022;37(3):154-173. doi:10.1152/physiol.00035.2021

24. Hartley CJ, Taffet GE, Michael LH, Pham TT, Entman ML. Noninvasive determination of pulse-wave velocity in mice. *American Journal of Physiology-Heart and Circulatory Physiology*. 1997;273(1):H494-H500. doi:10.1152/ajpheart.1997.273.1.H494

25. Camelo L, Marinho T de S, Águila MB, Souza-Mello V, Barbosa-da-Silva S. Intermittent fasting exerts beneficial metabolic effects on blood pressure and cardiac structure by modulating local renin-angiotensin system in the heart of mice fed high-fat or high-fructose diets. *Nutrition Research*. 2019;63:51-62. doi:10.1016/j.nutres.2018.12.005

26. Varady KA, Bhutani S, Church EC, Klempel MC. Short-term modified alternate-day fasting: a novel dietary strategy for weight loss and cardioprotection in obese adults. *The American Journal of Clinical Nutrition*. 2009;90(5):1138-1143. doi:10.3945/ajcn.2009.28380

27. Dutzmann J, Kefalianakis Z, Kahles F, et al. Intermittent Fasting After ST-Segment–Elevation Myocardial Infarction Improves Left Ventricular Function: The Randomized Controlled INTERFAST-MI Trial. *Circ: Heart Failure*. Published online May 2, 2024:e010936. doi:10.1161/CIRCHEARTFAILURE.123.010936

28. Morais RL, Hilzendeger AM, Visniauskas B, et al. High aminopeptidase A activity contributes to blood pressure control in *ob/ob* mice by AT_2 receptor-dependent mechanism. *American Journal of Physiology-Heart and Circulatory Physiology*. 2017;312(3):H437-H445. doi:10.1152/ajpheart.00485.2016

29. Aizawa-Abe M, Ogawa Y, Masuzaki H, et al. Pathophysiological role of leptin in obesity-related hypertension. *J Clin Invest*. 2000;105(9):1243-1252. doi:10.1172/JCI8341

30. Mark AL, Shaffer RA, Correia MLG, Morgan DA, Sigmund CD, Haynes WG. Contrasting blood pressure effects of obesity in leptin-deficient ob/ob mice and agouti yellow obese mice: *Journal of Hypertension*. 1999;17(Supplement):1949-1953. doi:10.1097/00004872-199917121-00026

31. Scolaro B, Brown EJ, Krautter F, et al. SHORT-TERM CALORIC RESTRICTION IN MICE PROMOTES RESOLUTION OF ATHEROSCLEROSIS, WHILE WEIGHT REGAIN ACCELERATES ITS PROGRESSION. Published online May 8, 2023. doi:10.1101/2023.05.07.539777

32. Lavillegrand JR, Al-Rifai R, Thietart S, et al. Alternating high-fat diet enhances atherosclerosis by neutrophil reprogramming. *Nature*. 2024;634(8033):447-456. doi:10.1038/s41586-024-07693-6

CHAPTER 3 SUPPLEMENTAL FIGURES

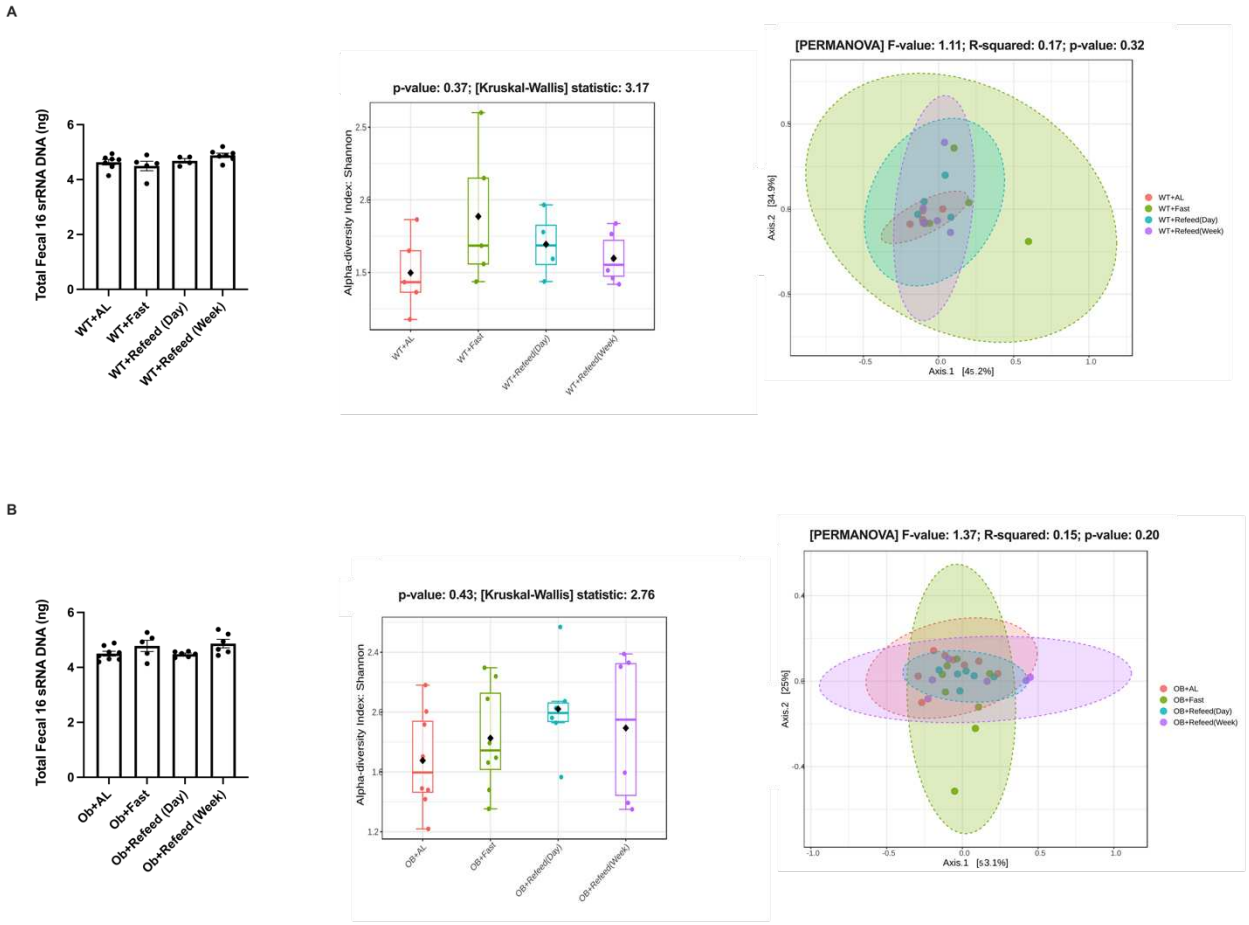

Figure 3.S1. A single fasting-refeeding cycle did not affect the gut microbiota in lean and obese mice. A-B) Total fecal 16s rRNA DNA **(left)**, gut microbial alpha diversity **(middle)** and gut microbiota beta diversity **(right)** diversity analyses at the genus level throughout a single fast-refeeding cycle in lean **A)** and obese **B)** mice. N=4-8 mice per group. WT=lean; OB=obese. AL=*ad libitum* fed; Fast=fasted for 24 hours; Refeed(Day)=mice that were fasted for 24 hours then refed for 24 hours; Refeed(Week)=mice that were fasted for 24 hours then refed for one week.

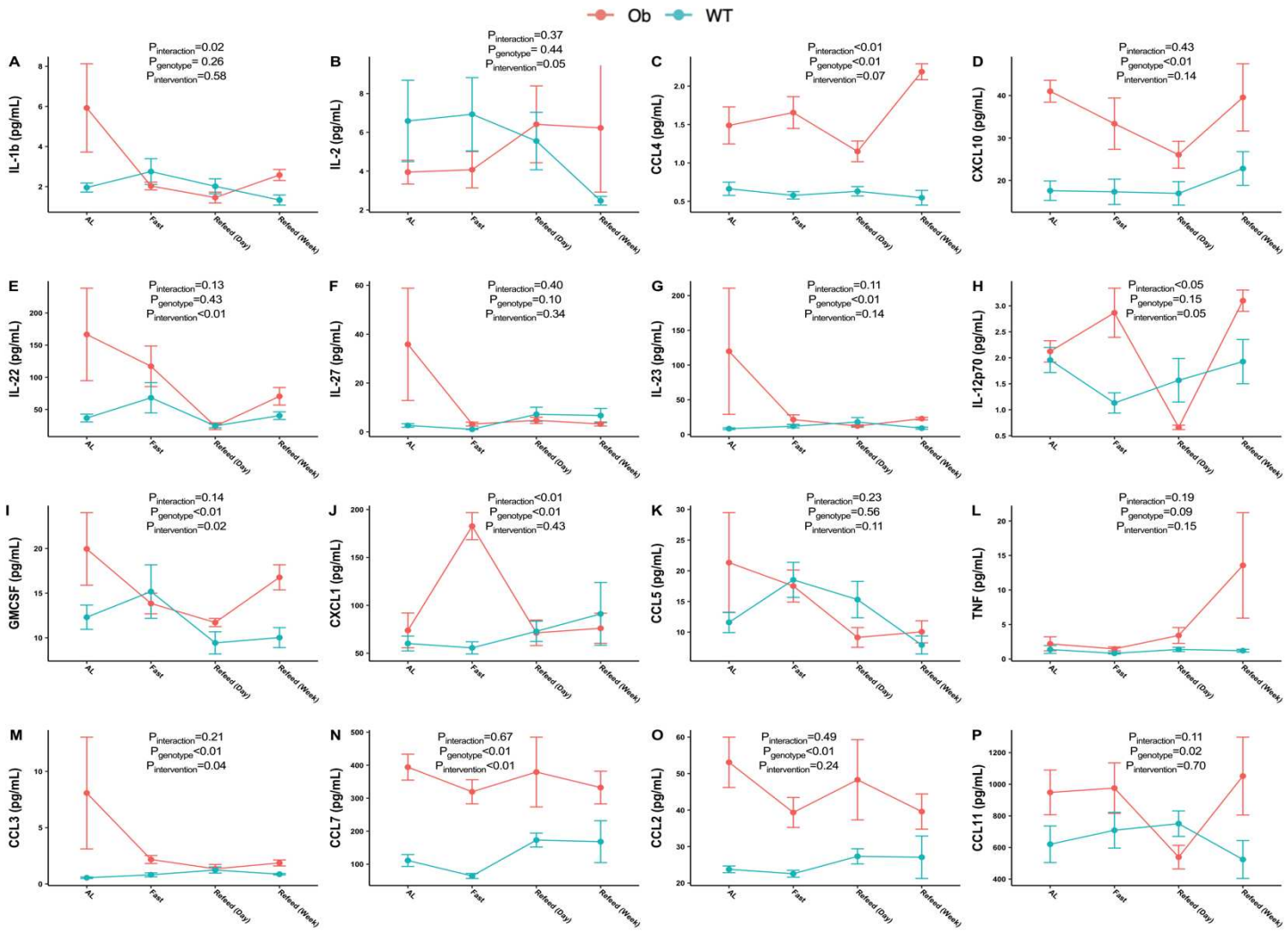

Figure 3.S2. Effects of a single fasting-refeeding cycle on plasma cytokine/chemokine levels in lean and obese mice. A-P) Changes in cytokine/chemokine levels between all respective time points in lean and obese mice. N=2-8 mice per group per cytokine/chemokine. WT=lean; Ob=obese; AL=*ad libitum* fed; Fast=fasted for 24 hours; Refeed(Day)=mice that were fasted for 24 hours then refed for 24 hours; Refeed(Week)=mice that were fasted for 24 hours then refed for one week.

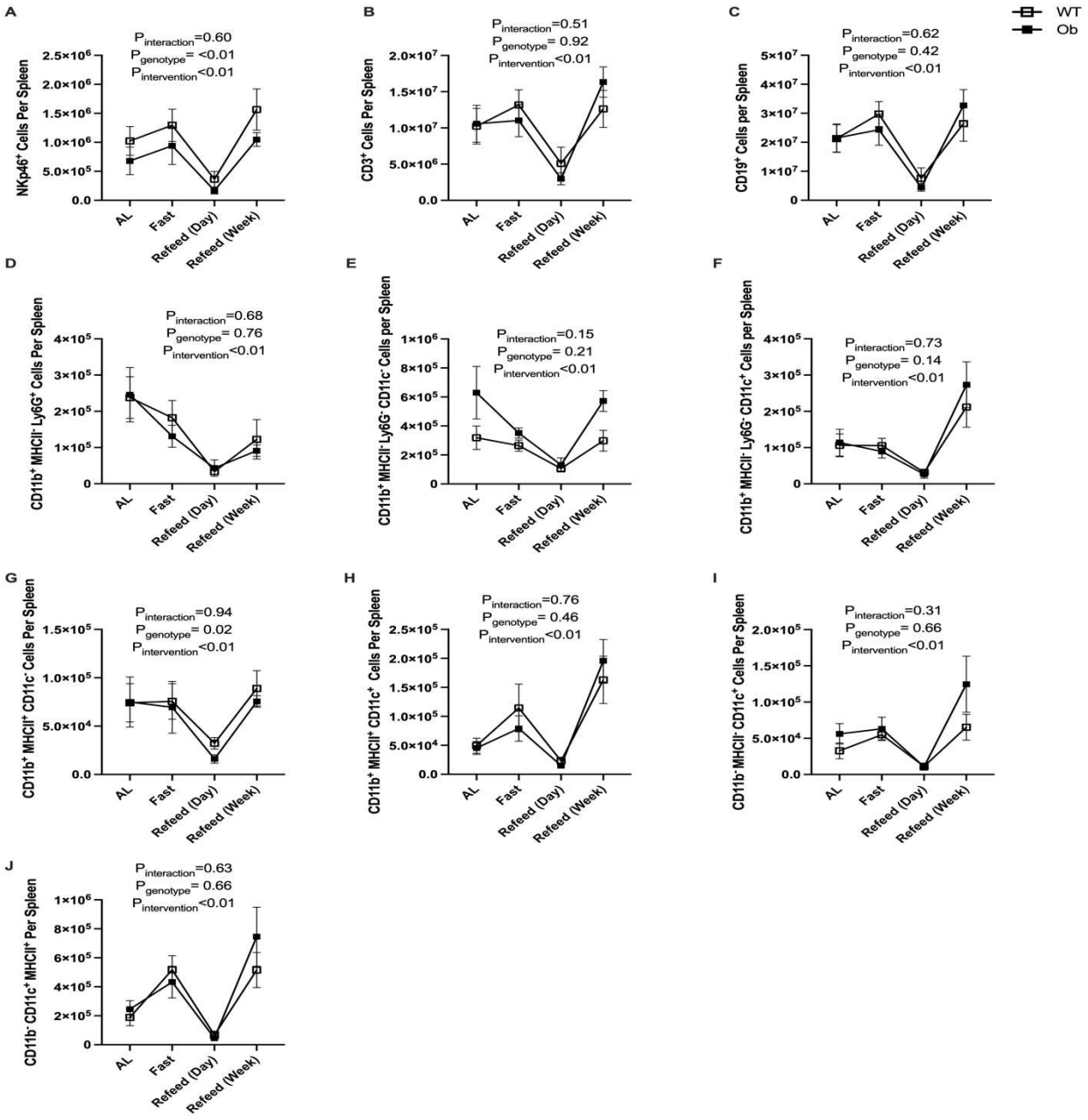

Figure 3.S3. A single fasting-refeeding cycle impacted splenocyte counts in lean and obese mice. A-J) Changes in absolute counts of spleen **A)** NKp46$^+$ (NK cell), **B)** CD3$^+$ (T cell), **C)** CD19$^+$ (B cell), **D)** Ly6G$^+$ (neutrophil), **E)** CD11b$^+$ MHCII$^-$ Ly6G$^-$ CD11c$^-$, **F)** CD11b$^+$ MHCII$^-$ Ly6G$^-$ CD11c$^+$, **G)** CD11b$^+$ MHCII$^+$ CD11c$^-$, **H)** CD11b$^+$ MHCII$^+$ CD11c$^+$, **I)** CD11b$^-$ MHCII$^-$ CD11c$^+$, and **J)** CD11b$^-$ MHCII$^+$ CD11c$^+$ populations between all respective time points in lean and obese mice. N=3-7 mice per group per subpopulation. WT=lean; Ob=obese; AL=*ad libitum* fed; Fast=fasted for 24 hours; Refeed(Day)=mice that were fasted for 24 hours then refed for 24 hours; Refeed(Week)=mice that were fasted for 24 hours then refed for one week.

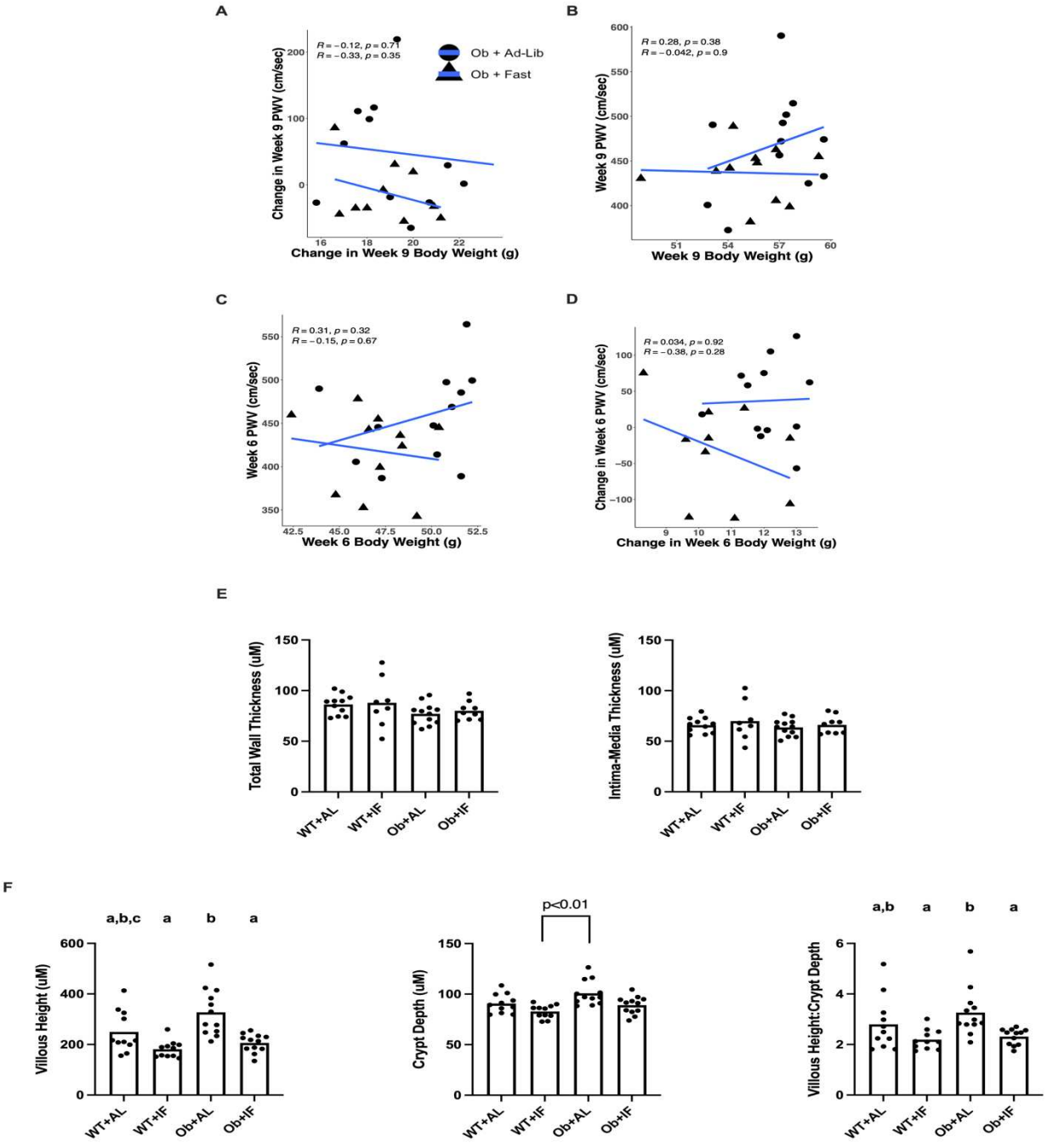

Figure 3.S4. Once-weekly 24-hour intermittent fasting reduced arterial stiffness in obese mice independent of changes in body weight and vascular remodeling. A-D) Scatterplot and Pearson correlations between pulse wave velocity and body weight changes from weeks 1-9 **A)**, week 9 pulse wave velocity and week 9 body weight **B)**, week 6 pulse wave velocity and week 6 body weight **C)**, and pulse wave velocity and body weight changes from weeks 1-6 **D)**. N=10-12 mice per group. **E)** Changes in thoracic aorta total wall thickness **(left)** and intima-media wall thickness **(right)** between groups. N=8-12 mice per group. **F)** Changes in small intestine villous height **(left)**, crypt depth **(middle)**, and the ratio between the two **(right)** between groups. N=11-12 mice per group. WT=lean; Ob=obese; AL=*ad libitum* feeding; IF=once-weekly 24-hour intermittent fasting; PWV=pulse wave velocity. Different letters indicate significant differences between groups.

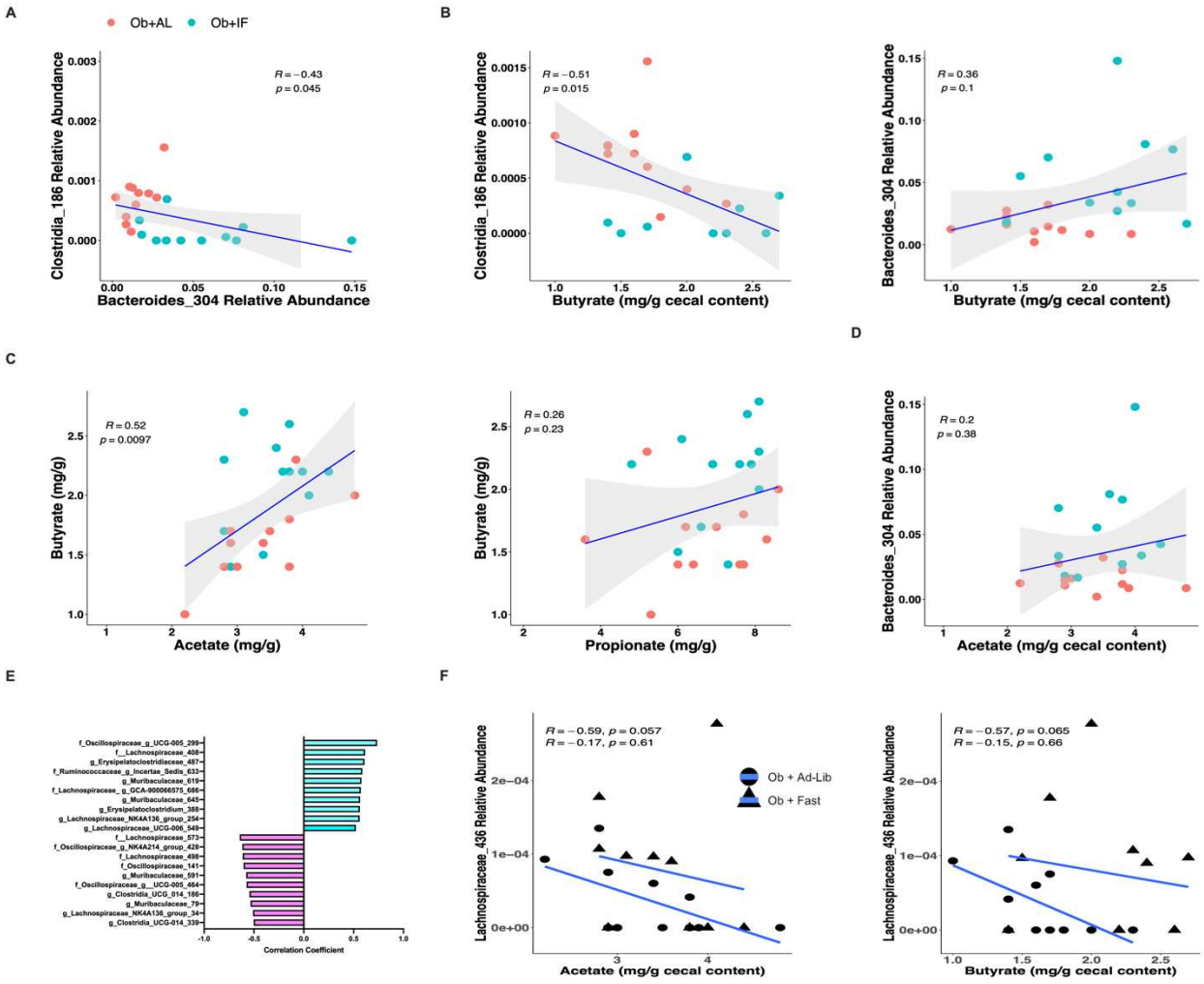

Figure 3.S5. Links Between *Clostridia*_186, *Bacteroides*_304, and *Lachnospiraceae*_436 relative abundances and cecal short chain fatty acid levels in obese mice. A) Scatterplot and Pearson correlations between *Clostridia*_186 and *Bacteroides*_304 in obese mice. N=11 mice per group. **B)** Scatterplot and Pearson correlations between cecal butyrate concentrations and *Clostridia*_186 **(left)** and *Bacteroides*_304 **(right)** relative abuncances. N=11 mice per group. **C)** Scatterplot and Pearson correlations between cecal butyrate concentrations and cecal acetate **(left)** and propionate **(right)** concentrations. N=12 mice per group. **D)** Scatterplot and Pearson correlations between cecal acetate ceoncentrations and *Bacteroides*_304 relative abundance. N=11 mice per group. **E)** The top 10 most positively (teal) and negatively (magenta) associated taxa with *Bacteroides*_304 in obese mice. Correlations were identified using the pattern search function in MicrobiomeAnalyst. All of the positively-associated microbes were elevated in Ob+IF mice compared to Ob+AL mice (FDR-adjusted p-value=0.16). **F)** Scatterplot and Pearson correlations between *Lachnospiraceae*_436 relative abundance and cecal acetate **(left)** and butyrate **(right)** concentrations. N=11 mice per group. Ob=obese; AL=*ad libitum* feeding; IF=once-weekly 24-hour intermittent fasting.

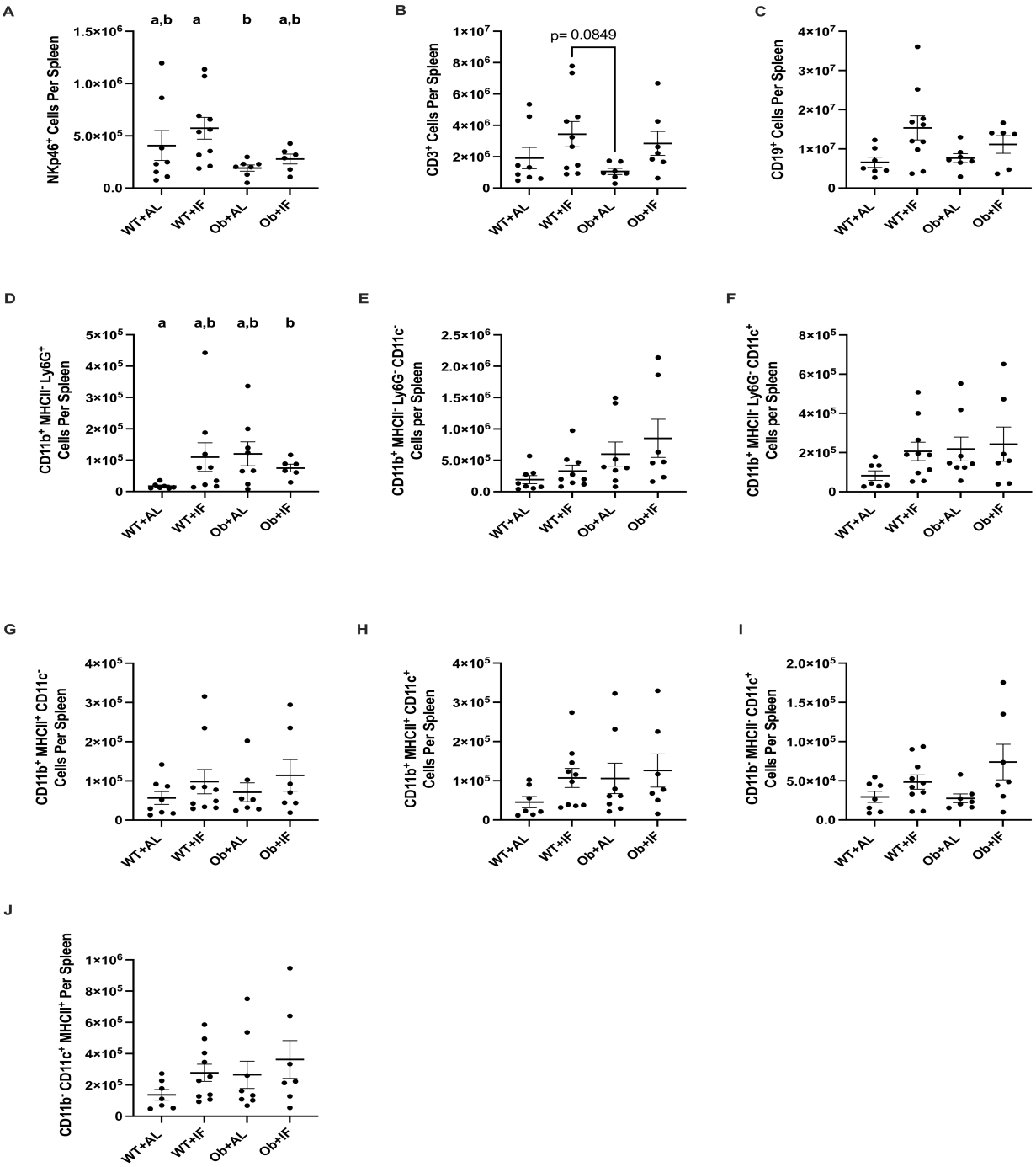

Figure 3.S6. Once-weekly 24-hour intermittent fasting did not affect splenocyte populations in lean and obese mice. A-J) Terminal differences in distinct splenocyte populations between groups. An identical gating strategy, as shown in Figure S2, was used to identify subpopulations. N=6-10 mice per group per subpopulation. WT=lean; Ob=obese; AL=*ad libitum* feeding; IF=once-weekly 24-hour intermittent fasting. Different letters indicate significant differences between groups.

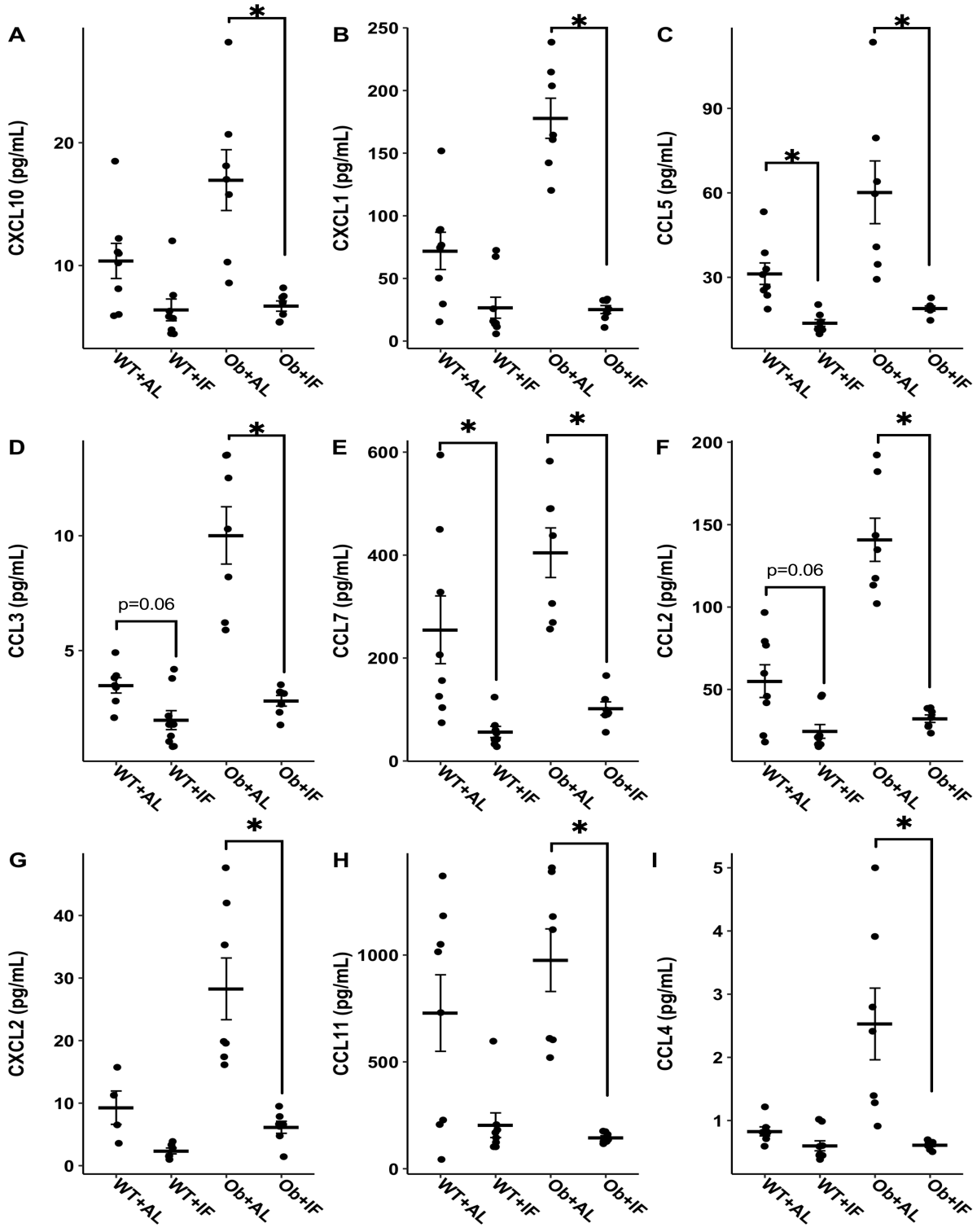

Figure 3.S7. Once-weekly 24-hour intermittent fasting reduced plasma cytokine/chemokine levels in obese mice. A-I) Differences in plasma cytokine/chemokines between groups. N=4-9 mice per group per cytokine/chemokine. WT=lean; Ob=obese; AL=*ad libitum* feeding; IF=once-weekly 24-hour intermittent fasting. Different letters indicate significant differences between groups.

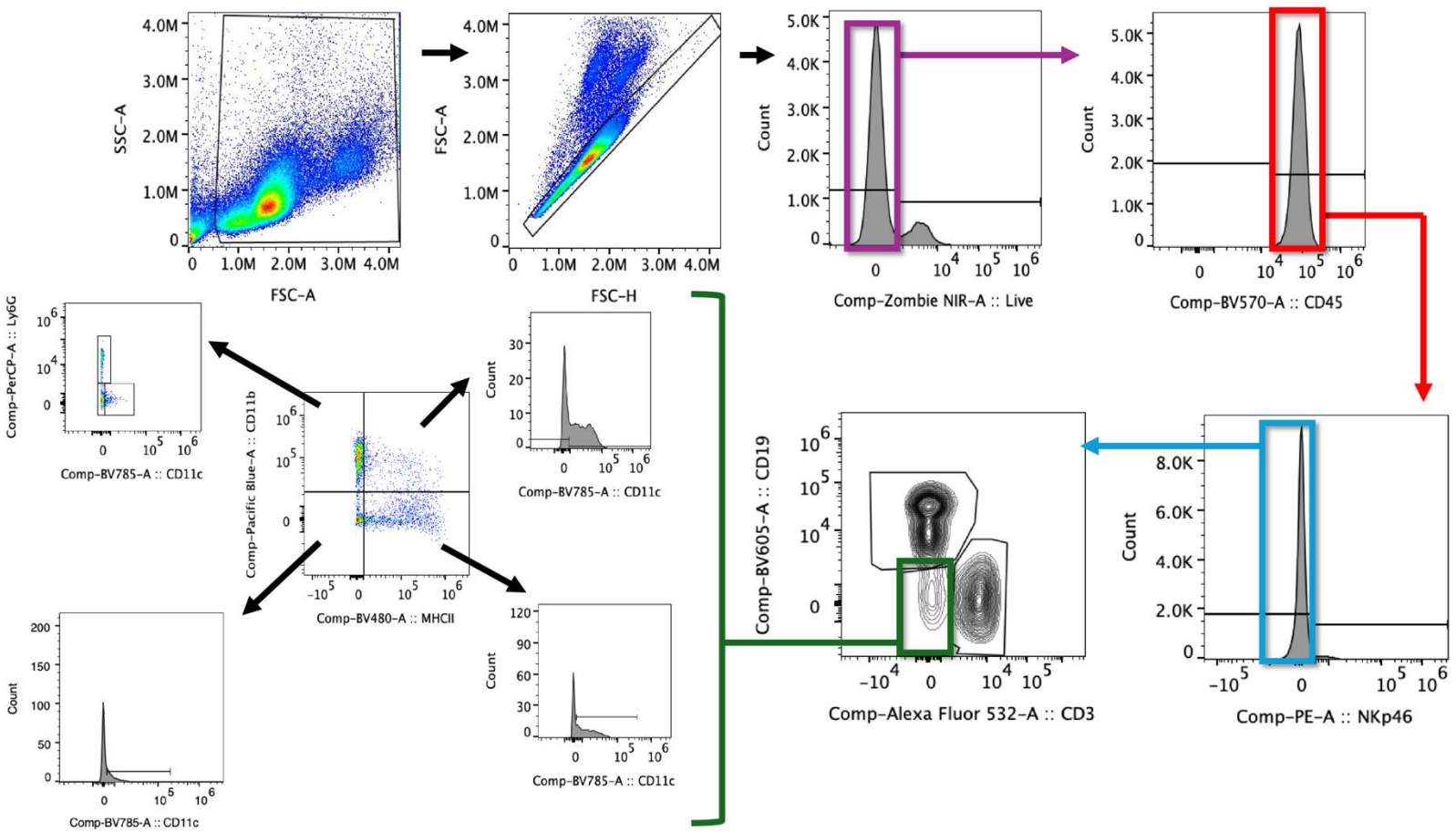

Figure 3.S8. Representative gating strategy for splenocyte populations. Intact, single, live, CD45^{+} cells were initially gated off of their expression of NKp46. NKp46^{-} cells were subsequentially gated for expression of CD3 or CD19. CD3^{-} CD19^{-} cells were then gated for MHCII and CD11b expression. CD11b^{+} MHCII^{+}, CD11b^{-} MHCII^{+}, and CD11b^{-} MHCII^{-} cells were then gated for CD11c expression. CD11b^{+} MHCII^{-} cells were gated for CD11c and Ly6G expression.

CHAPTER 3 SUPPLEMENTAL TABLES

Table 3.S1. Changes in Pulse Wave Velocity Over the Acute Fasting-Refeeding Cycle in Lean and Obese Mice.

	AL	Fast	Refeed (Day)	Refeed (Week)
WT	431.7 ± 11.9 [a]	508.5 ± 17.0 [b]	441.0 ± 25.6 [a, b]	455.6 ± 14.3 [a,b]
Ob	470.7 ± 12.0 [a]	460.2 ± 20.0 [a]	471.8 ± 25.6 [a]	482.7 ± 19.2 [a]

N=6-8 mice per group. Data are presented as mean ± SEM. Analysis was performed using one-way ANOVA with robust standard errors followed by Tukey's multiple comparisons test. Different letters indicate significant differences between groups ($p<0.05$). WT=lean; Ob=obese; AL=*ad libitum* fed; Fast=fasted for 24 hours; Refeed(Day)=mice that were fasted for 24 hours then refed for 24 hours; Refeed(Week)=mice that were fasted for 24 hours then refed for one week.

Table 3.S2. Termination Body- and Tissue Weights of Mice Subjected to Once-Weekly 24-Hour Intermittent Fasting Protocol.

	WT+AL	WT+IF	Ob+AL	Ob+IF
Body Weight (g)*	31.4 ± 0.9[a]	31.4 ± 0.8[a]	59.3 ± 0.8[b]	54.6 ± 1.4[c]
Liver Weight (mg)	1450.0 ± 86.7[a]	1523.0 ± 91.6[a]	4017.0 ± 93.9[b]	3212.0 ± 180.3[c]
Relative Liver Weight (mg/Termination BW)	45.8 ± 1.9[a]	48.3 ± 2.4[a]	67.1 ± 1.3[b]	58.5 ± 2.4[c]
Spleen Weight (mg)	83.0 ± 4.1[a,c]	80.3 ± 5.9[a,c]	90.5 ± 2.9 [a]	74.4 ± 4.3[c]
Relative Spleen Weight (mg/Termination BW)	2.6 ± 0.1[a]	2.5 ± 0.2[a]	1.5 ± 0.1[b]	1.4 ± 0.1[b]
Lung Weight (mg)	171.7 ± 8.7[a]	173.7 ± 8.3[a]	154.5 ± 3.3[a]	154.0 ± 4.7[a]
Relative Lung Weight (mg/Termination BW)	5.5 ± 0.4[a]	5.5 ± 0.2[a]	2.6 ± 0.1[b]	2.8 ± 0.1[b]
Heart Weight (mg)*	136.3 ± 4.5[a]	136.7 ± 4.9[a]	153.3 ± 3.2[b]	141.5 ± 3.8[a,b]
Relative Heart Weight (mg/Termination BW)	4.4 ± 0.2[a]	4.4 ± 0.1[a]	2.6 ± 0.1[b]	2.6 ± 0.1[b]
Cecum Weight (mg)	648.6 ± 33.6[a]	633.2 ± 33.3[a]	842.1 ± 82.7[a]	746.9 ± 48.9[a]
Relative Cecum Weight (mg/Termination BW)*	20.6 ± 0.8[a]	20.2 ± 0.9[a]	14.1 ± 1.4[b]	13.4 ± 0.8[b]
Colon Length (cm)*	5.7 ± 0.2[a,b]	5.5 ± 0.2[a]	6.4 ± 0.3[b]	6.2 ± 0.2[a,b]
Relative Colon Length (cm/Termination BW)*	0.18 ± 0.01[a]	0.17 ± 0.01[a]	0.11 ± 0.00[b]	0.11 ± 0.01[b]

N= 9-12 mice per group. Data is presented as mean ± SEM. Analysis was performed using Welch ANOVA followed by Dunnett's T3 multiple comparisons test. *Analysis was performed using one-way ANOVA followed by Tukey's multiple comparisons test. Different letters indicate significant differences between groups ($p<0.05$). WT=lean; Ob=obese.

Table 3.S3. Relative Abundance Differences in Gut Microbe Features Between *Ad libitum* and Once-Weekly 24-Hour Intermittent Fasting Obese Mice at Termination.

Comparison	Test	Microbe (Feature)	Score	FDR-Adjusted P-Value
Ob+IF vs. Ob+AL	Mann-Whitney		+/- Change	Threshold <0.05
		g__Bacteroides_304	+	<0.01
		g__Muribaculaceae_200	-	<0.01
		Clostridia_UCG_014_186	-	<0.01
Ob+IF vs. Ob+AL	Negative Binomial (EdgeR)		log2FC	Threshold <0.05
		g__Muribaculaceae_619	10.93	<0.01
		g__Muribaculaceae_22	9.88	<0.01
		g_Lachnospiraceae_NK4A136_group_156	-6.40	<0.01
		g_Lachnospiraceae_NK4A136_group_132	6.91	<0.01
		Clostridia_UCG_014_78	-5.01	<0.01
		g_Lachnospiraceae_NK4A136_group_1	5.65	<0.01
		g__Muribaculaceae_609	5.30	<0.01
		f_ Lachnospiraceae_280	3.36	<0.01
		g__Ruminococcus_52	-4.38	<0.01
		g__Lachnospiraceae_UCG-001_284	-4.19	<0.01
		f_ Lachnospiraceae_495	4.44	<0.01
		g__Blautia_477	3.88	<0.01
		Clostridia_UCG_014_168	4.03	<0.01
		f_ Lachnospiraceae_112	2.53	<0.01
		Clostridia_UCG_014_186	-2.25	<0.01
		g__[Eubacterium]_ventriosum_group_282	3.42	<0.01
		g__Muribaculaceae_375	-3.03	<0.01
		f__Oscillospiraceae_40	2.97	<0.01
		g__Erysipelatoclostridiaceae_487	3.21	<0.01
		Clostridia_UCG_014_306	3.14	<0.01
		g__Ruminococcus_719	-2.97	<0.01
		g__Erysipelatoclostridium_388	3.47	<0.01
		g__Romboutsia_726	-2.61	<0.01
		g_Monoglobus_149	-2.15	<0.01
		f__Lachnospiraceae_233	-2.05	0.01
		g_Lachnospiraceae_NK4A136_group_671	2.52	0.01
		f__Lachnospiraceae_451	2.81	0.02
		g_Akkermansia_690	-2.45	0.02
		g__Bacteroides_304	1.92	0.02
		g__Clostridia_UCG_014_553	-2.57	0.02
		f__Lachnospiraceae_612	2.10	0.03
		g__Roseburia_448	2.35	0.03
		f__Lachnospiraceae_4	2.12	0.03

		f__Lachnospiraceae_486	*-2.75*	0.03
		f__Oscillospiraceae_318	1.67	0.04
		f__Oscillospiraceae_511	2.23	0.04
		g__Tyzzerella_327	-1.99	0.04
		f__Lachnospiraceae_266	1.68	0.04
Ob+IF vs. Ob+AL	LEfSe		**LDAscore**	**Threshold <0.1**
		Clostridia_UCG_014_186	-2.47	0.04
		g__Bacteroides_304	4.31	0.04
		g__Muribaculaceae_200	-4.47	0.04
		g_Akkermansia_690	-4.52	0.07
		f__Lachnospiraceae_612	2.5	0.07
		f__Oscillospiraceae_245	3.14	0.07
		g__Muribaculaceae_619	4.72	0.07
		g__Parasutterella_311	-3.37	0.08
		g__Muribaculaceae_375	-4.27	0.09
		g_Monoglobus_149	-2.62	0.09
		g__Muribaculaceae_645	4.35	0.09
		f__Ruminococcaceae_228	1.91	0.09
		f__Lachnospiraceae_260	2.58	0.09

N=11 mice per group. EdgeR= R package that utilizes negative binomial models to analyze the differential analysis of sequence read count data; LEfSe= linear discriminant analysis effect size; Log2FC=log2 fold change; LDAscore=linear discriminant analysis score; FDR=false discovery rate. Underscore indicates the specific feature out of 733 distinct features. Red indicates the same bacteria in all three analyses. Blue indicates the same bacteria in two out of the three analyses.

Table 3.S4. Differences in Gut Microbe-PWV Relationships in Obese *Ad libitum* and Intermittent Fasting Mice.

Microbe	Arterial Stiffness Measure	Adjusted R^2	$pSLOPE_{AL}$ (Direction of Association)	$pSLOPE_{IF}$ (Direction of Association)	$pSLOPE_{IFzero}$
*Ruminococcaceae.g_Incertae_Sedis*_577	Week 9 PWV	0.39	<0.01(-)	0.05 (-)	0.98
*Peptococcales.f_Peptococcaceae*_618		0.31	0.01 (-)	0.05 (+)	0.33
*Lachnospirales.f_Lachnospiraceae*_414	Change in PWV (Week 1-9)	0.48	<0.01(-)	0.04 (-)	0.52
*Monoglobaceae.g_Monoglobus*_149		0.41	0.02 (-)	0.05 (+)	0.30
*Lactobacillaceae.g_Lactobacillus*_209		0.33	0.04 (-)	0.05 (+)	0.51
*Lachnospirales.f_Lachnospiraceae*_436		0.33	0.04 (+)	0.04 (-)	0.52

N=10-11 mice per group. $pSLOPE_{AL}$=p-value of default regression coefficient (is the slope in Ob+AL mice not equal to 0) with corresponding direction of association (positive (+) or negative (-)); $pSLOPE_{IF}$=p-value of default regression coefficient (is the slope in Ob+IF mice not equal to $pSLOPE_{AL}$) with corresponding direction of association (positive (+) or negative (-));$pSLOPE_{IFzero=}$ p-value of whether $pSLOPE_{IF}$ is significantly different than 0.

Table 3.S5. Significant Results from Mediation Analysis in Obese Mice.

Microbe	Chemokine (Mediator)	Outcome	p_{ACME}
Clostridia_UCG_014_186	CXCL1	Change in PWV (Week 1-9)	0.02
Muribaculaceae_200	CCL7		0.02
Clostridia_UCG_014_186	CCL2		0.04
Clostridia_UCG_014_186	CXCL1	Week 9 PWV	0.03
Muribaculaceae_200	CCL7		0.03

N=11 obese mice. 95% CI= 95 percent confidence interval; p-value=p-value of the average causal mediated effect (ACME); PWV= pulse wave velocity.

Table 3.S6. Flow Cytometry Panel Information.

Marker	Fluor	Dilution	Company	Catalog #
CD45	Brilliant Violet 570	1:200	Biolegend	103136
NKp46	PE	1:400	Biolegend	137604
CD3	Alexa Fluor 532	1:100	eBioscience	58-0032-82
CD19	Brilliant Violet 605	1:200	Biolegend	115539
CD11b	Pacific Blue	1:200	Biolegend	101224
CD11c	Brilliant Violet 785	1:400	Biolegend	117335
Ly6G	PerCP	1:100	Biolegend	127653
MHCII	Brilliant Violet 480	1:600	BD Biosciences	566088
Zombie NIR		1:2000	Biolegend	423105

CHAPTER 3 SUPPLEMENTAL RESULTS

The Observed Effects of a Single Fasting-Refeeding Cycle Are Transient

The single fasting-refeeding cycle did not affect total microbial load (16s rRNA DNA), Shannon's index (alpha diversity) or Bray-Curtis distances (beta diversity) diversity in WT or Ob mice **(Figure 3.S1A-3.S1B)**. We also saw no differences in community dispersion over the acute fasting-refeeding cycle in either genotype (WT PERMDISP p-value=0.11, Ob PERMDISP p-value=0.30).

Over the single cycle, there was considerable heterogeneity in plasma cytokine/chemokine levels **(Figure 3.S2).** Yet, the acute fasting-refeeding cycle seemed to most strongly affect plasma levels of CCL4 (MIP-1β), IL12p70 (IL-12), and CXCL1 in Ob mice compared to WT mice. Specifically, CCL4 (a mediator of leukocyte chemotaxis [74]) was increased in Ob+Refeed (Week) mice compared to Ob+AL ($p=0.01$) **(Figure 3.S2C)**. IL12p70, which aids in polarizing naïve CD4+ T cells into type 1 helper T cells (Th1) cells as well as activates natural killer (NK) cells [75], was significantly decreased in Ob+Refeed (Day) mice ($p<0.01$) and then rebounded to levels higher than Ob+AL in Ob+Refeed(Week) mice ($p=0.04$) **(Figure 3.S2H)**. Importantly, there were no significant differences in these two cytokines between AL and Fast time points, suggesting the refeeding period and not the 24-hour fast itself impacted the circulating levels of these cytokines. CXCL1 (a neutrophil chemoattractant shown to regulate vascular health through the CXCL1-CXCR2 pathway [76]) was significantly increased in Ob+Fast mice ($p<0.01$) but rebounded to normal levels upon refeeding (Ob+AL vs. Ob+Refeed(Day) p-value= 0.99; Ob+AL vs. Ob+Refeed(Week) p-value= 0.99) **(Figure 3.S2J)**. In contrast, when compared to WT+AL mice, concentrations for all three of these cytokines remained stable throughout the fasting-refeeding cycle in WT mice.

Acute fasting also affected immune responses in the spleen. After adjusting for genotype, $NKp46^+$ cells (natural killer cells) ($p<0.01$) **(Figure 3.S3A)**, $CD3^+$ cells (T cells) ($p<0.01$) **(Figure 3.S3B)**, $CD19^+$ cells (B cells) ($p<0.01$) **(Figure 3.S3C)**, $Ly6G^+$ cells (neutrophils) ($p<0.01$) **(Figure 3.S3D)**, $CD11b^+$ $MHCII^-$ $Ly6G^-$ $CD11c^-$ cells ($p<0.01$) **(Figure 3.S3E)**, $CD11b^+$ $MHCII^-$ $Ly6G^-$ $CD11c^+$ Cells ($p=0.01$) **(Figure 3.S3F)**, $CD11b^+$ $MHCII^+$ $CD11c^-$ ($p=0.02$) **(Figure 3.S3G),** $CD11b^+$ $MHCII^+$

$CD11c^+$ cells (p=0.01) **(Figure 3.S3H)**, $CD11b^-$ $MHCII^-$ $CD11c^+$ (p<0.01) **(Figure 3.S3I),** and $CD11b^-$ $MHCII^+$ $CD11c^+$ cells (p=0.01) **(Figure 3.S3J)** were decreased following the 24-hour refeed. These reductions were mostly temporary, as counts (except for neutrophils cells and $CD11b^+$ $MHCII^+$ $CD11c^+$ cells) reverted to values not significantly different from AL controls after a week of refeeding. Similarly, the 24-hour fast significantly reduced spleen weight in both WT and Ob mice, yet weight was stabilized after a day of refeeding (data not shown).

Next, we leveraged the VOLARE pipeline to observe whether the acute increase in PWV in WT+Fast mice was associated with changes in "Clinical Data", "Microbes", or "Splenocyte and Plasma Cytokines" analytes (see "bins" discussed in VOLARE Methods section for further clarification). This analysis revealed no linear relationships between PWV and other analytes that differed between WT+AL and WT+Fast mice. This finding suggests that the acute increase in PWV in WT+Fast animals is not associated with changes to the gut microbiota, immune system, or other measured physiological parameters.

We then investigated whether the acute fasting-refeeding cycle differentially impacted linear relationships between any two analytes within "Clinical Data", "Microbes", and/or "Splenocyte and Plasma Cytokines" bins in WT and Ob mice. Within WT and Ob mice, the VOLARE network revealed 13 and 56 analyte pairs, respectively, with a significant relationship at any time point during the fasting-refeeding cycle (AL, Fast, Refeed(Day), Refeed(Week). Of these significant analyte pairs, 6 in WT mice and 19 in Ob mice significantly differed between AL and Fast time points. This indicates that the 24-hour fast significantly altered several analyte relationships in both WT and Ob mice. Of the six altered relationships observed in WT+Fast Mice, 5/6 (83%) were not significantly different between WT+AL and WT+Refeed(Day). A similar trend was seen in Ob mice, as 12/19 (63%) relationships reverted to the relationship observed in Ob+AL mice after the 24-hour refeed (data not shown). Taken together, these results suggest that although the 24-hour fast differentially altered analyte relationships in WT and Ob mice, most of these relationships reverted to baseline after 24 hours of *ad libitum* feeding.

CHAPTER 4 SUPPLEMENTAL FIGURES

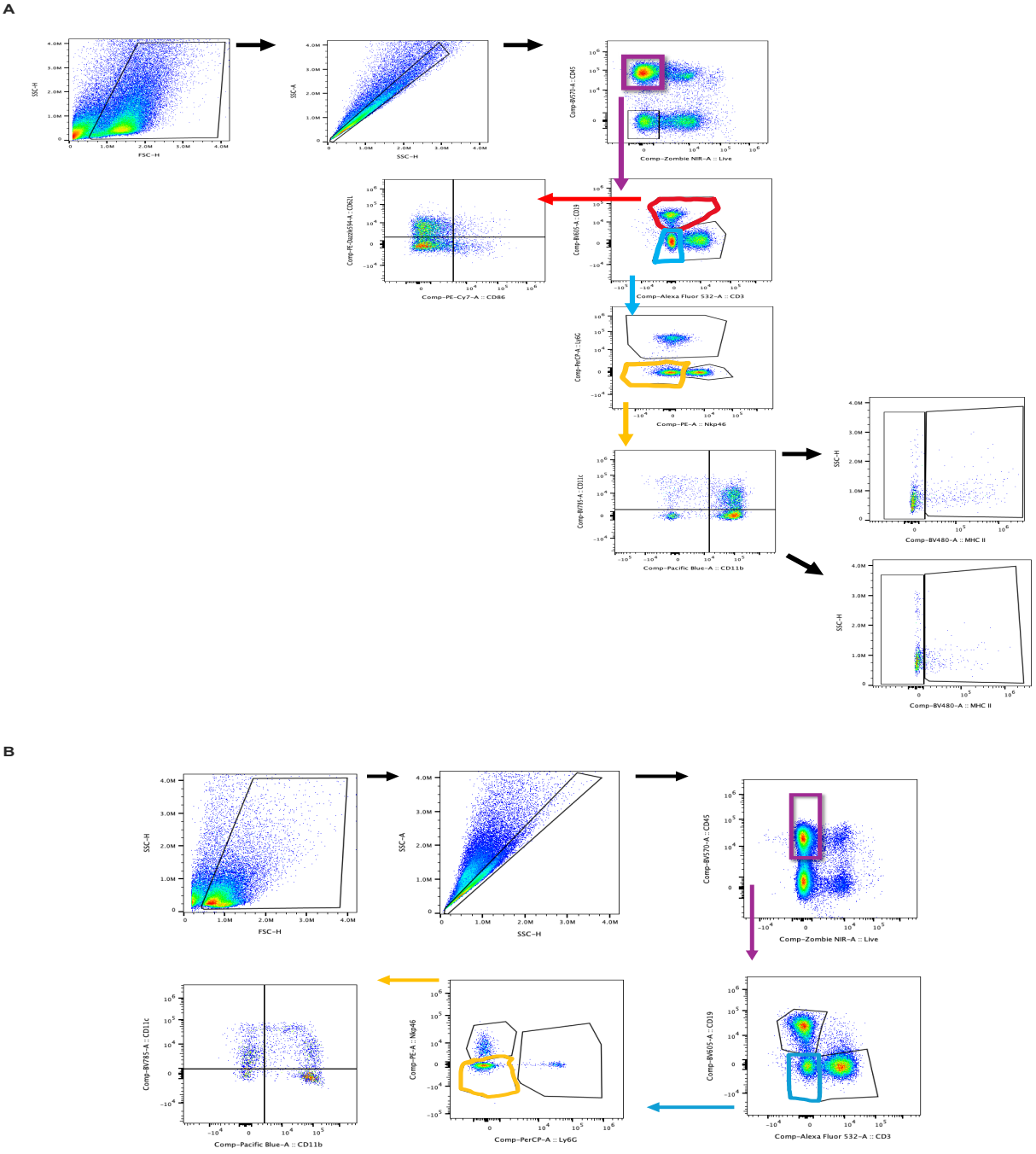

Figure 4.S1. Gating strategies to identify lung and spleen immune cell counts in lean and obese mice. A-B) Representative gating strategy for identifying lung **A)** and spleen **B)** immune cells during SC2 infection. Intact, single, live CD45^{+} cells were initially gated from their expression of CD3 or CD19. CD3^{-} CD19^{-} cells were gated for Ly6G or NKp46 expression. Ly6G^{-} NKp46^{-} cells were then gated for CD11b and CD11c expression. To further investigate changes in distinct B cell and innate immune cell populations in the lung, CD19^{+} cells were then gated for CD62L and CD86 expression, and CD11b/CD11c cells were gated for MHCII.

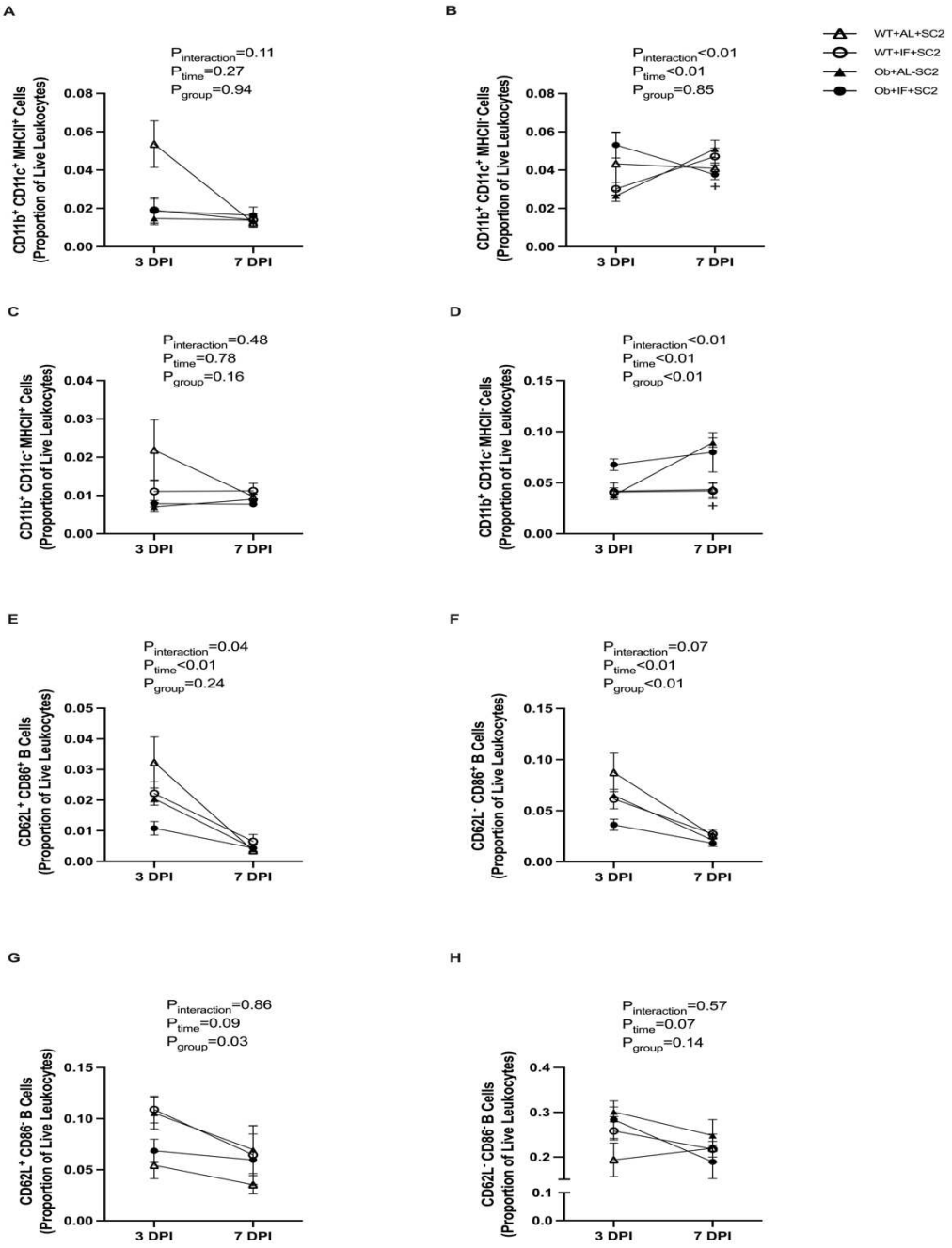

Figure 4.S2. Differences in lung innate immune cell and B cell populations following intermittent fasting and SARS-CoV-2 infection in lean and obese mice. Proportion of lung $CD11b^+$ $CD11c^+$ $MHCII^+$ **A)** $CD11b^+$ $CD11c^+$ $MHCII^-$ **B)** $CD11b^+$ $CD11c^-$ $MHCII^+$ **C)** $CD11b^+$ $CD11c^-$ $MHCII^-$ **D)** $CD62L^+$ $CD86^+$ B cells **E)** $CD62L^-$ $CD86^+$ B cells **F)** $CD62L^+$ $CD86^-$ B cells **G)** and $CD62L^-$ $CD86^-$ B cells **H)** during SARS-CoV-2 infection. N=3-5 mice per group per DPI. WT=lean; Ob=obese; AL=*ad libitum* feeding; IF=once-weekly 24-hour intermittent fasting; SC2=SARS-CoV-2 (MA10) infection; DPI= days post-inoculation. $^+$ indicates a p-value of less than 0.05 between 3- and 7 DPI in Ob+AL+SC2 mice.

CHAPTER 4 SUPPLEMENTAL TABLES

Table 4.S1. Pairwise PERMANOVA Analyses Between PBS- and SARS-CoV-2-Inoculated Lean and Obese Mice.

Comparison	Genotype	DPI	F-Value	FDR-Adjusted P-Value
	WT	3 vs. 7		**Threshold <0.05**
AL			1.19	0.30
AL+SC2			1.44	0.30
IF+SC2			1.60	0.29
		3		
AL vs. AL+SC2			3.62	0.12
AL vs. IF+SC2			2.50	0.21
AL+SC2 vs. IF+SC2			0.55	0.90
		7		
AL vs. AL+SC2			2.02	0.12
AL vs. IF+SC2			1.81	0.21
AL+SC2 vs. IF+SC2			0.41	0.94
	Ob	3 vs. 7		
AL			0.50	0.78
AL+SC2			0.93	0.62
IF+SC2			0.26	0.98
		3		
AL vs. AL+SC2			6.04	0.04
AL vs. IF+SC2			4.12	0.10
AL+SC2 vs. IF+SC2			1.25	0.48
		7		
AL vs. AL+SC2			0.91	0.64
AL vs. IF+SC2			3.74	0.04
AL+SC2 vs. IF+SC2			0.68	0.78

N=3-5 per group. FDR=false discovery rate. WT=lean; Ob=obese; AL=*ad libitum* feeding; SC2=SARS-CoV-2 (MA10) infection; DPI= days post-inoculation. Red indiicates significant FDR-adjusted p-value (<0.05).

Table 4.S2. Differences in Gut Microbe Relative Abundances Between PBS- and SARS-CoV-2-Inoculated *Ad libitum* Obese Mice at 3 Days Post-Inoculation

Comparison	Test	Microbe (Feature)	Score	FDR-Adjusted P-Value
Ob+AL+SC2 (3 DPI) vs. Ob+AL (3 DPI)	Mann-Whitney		**+/- Change**	**Threshold <0.05**
		NA	NA	NA
Ob+AL+SC2 (3 DPI) vs. Ob+AL (3 DPI)	Negative Binomial (EdgeR)		**log2FC**	**Threshold <0.05**
		g__Muribaculaceae_159	8.16	<0.01
		Monoglobus_170	-3.96	<0.01
		s__Dubosiella_newyorkensis_96	5.22	<0.01
		g__Marvinbryantia_34	-5.22	<0.01
		s__[Clostridium]_cocleatum_112	-3.41	0.02
Ob+AL+SC2 (3 DPI) vs. Ob+AL (3 DPI)	LEfSe		**LDAscore**	**Threshold <0.1**
		NA	NA	NA

N=3-5 per group. EdgeR= R package that utilizes negative binomial models to analyze the differential analysis of sequence read count data; LEfSe= linear discriminant analysis effect size; Log2FC=log2 fold change; LDAscore=linear discriminant analysis score; FDR=false discovery rate. Ob=obese; AL=*ad libitum* feeding; SC2=SARS-CoV-2 (MA10) infection; DPI= days post-inoculation. Underscore in Microbe (Feature) indicates the specific feature out of 198 distinct features.

Table 4.S3. Differences in Gut Microbe Relative Abundances Between PBS- Inoculated *Ad Libitum* Obese Mice and SARS-CoV-2-Inoculated Intermittent Fasted Obese Mice at 7 Days Post-Inoculation

Comparison	Test	Microbe (Feature)	Score	FDR-Adjusted P-Value
Ob+IF+SC2 (7 DPI) vs. Ob+AL (7 DPI)	Mann-Whitney		**+/- Change**	**Threshold <0.05**
		NA	NA	NA
Ob+IF+SC2 (7 DPI) vs. Ob+AL (7 DPI)	Negative Binomial (EdgeR)		**log2FC**	**Threshold <0.05**
		g__Coriobacteriaceae_UCG-002_179	-6.42	<0.01
		g__Lachnospiraceae_NK4A136_group_103	-7.55	<0.01
		g__Muribaculaceae_159	8.12	<0.01
		g__Marvinbryantia_34	-4.46	0.03
		g__Acetatifactor_144	4.02	0.04
Ob+IF+SC2 (7 DPI) vs. Ob+AL (7 DPI)	LEfSe		**LDAscore**	**Threshold <0.1**
		NA	NA	NA

N=4-5 per group. EdgeR= R package that utilizes negative binomial models to analyze the differential analysis of sequence read count data; LEfSe= linear discriminant analysis effect size; Log2FC=log2 fold change; LDAscore=linear discriminant analysis score; FDR=false discovery rate. Ob=obese; AL=*ad libitum* feeding; SC2=SARS-CoV-2 (MA10) infection; DPI= days post-inoculation. Underscore in Microbe (Feature) indicates the specific feature out of 198 distinct features.

Table 4.S4. Flow Cytometry Panel Information.

Marker	Fluor	Dilution	Company	Catalog #
CD45	Brilliant Violet 570	1:200	Biolegend	103136
NKp46	PE	1:400	Biolegend	137604
CD3	Alexa Fluor 532	1:100	eBioscience	58-0032-82
CD19	Brilliant Violet 605	1:200	Biolegend	115539
CD62L	PE/Dazzle 594	1:400	Biolegend	104447
CD86	PE/Cyanine7	1:200	Biolegend	105013
CD11b	Pacific Blue	1:200	Biolegend	101224
CD11c	Brilliant Violet 785	1:400	Biolegend	117335
Ly6G	PerCP	1:100	Biolegend	127653
MHCII	Brilliant Violet 480	1:600	BD Biosciences	566088
Zombie NIR		1:2000	Biolegend	423105